The Regulation of Endocytosis by Snf1-related Kinases in Yeast

By

Jessica M. Tumolo

Dissertation

Submitted to the Faculty of the

Graduate School of Vanderbilt University

in partial fulfillment of the requirements

for the degree of

DOCTOR OF PHILOSOPHY

in

Cell and Developmental Biology

June 30, 2019

Nashville, Tennessee

Approved:

Kathleen L. Gould, Ph.D.

William P. Tansey, Ph.D.

John D. York, Ph.D.

Maulik R. Patel, Ph.D.

Jason A. MacGurn, Ph.D.

Acknowledgements

I am grateful to my advisor, Dr. Jason MacGurn, for the enthusiasm and creativity he brings to the lab every day, and for granting me a lot of latitude to develop and push my studies forward, which helped to foster independence and self-confidence in my work. I am thankful to my lab-mates, who have created a fun and collegial atmosphere in which to conduct research. Additionally, I thank my committee members, including Dr. Kathy Gould, Dr. Bill Tansey, Dr. John York, and Dr. Maulik Patel, for insightful feedback and constructive criticism during committee meetings. Dr. Bill Tansey, especially, went above and beyond his duties as a committee member to advise me during my studies which I feel was instrumental in my success.

Finishing this degree would not have been possible without the constant strength and support of my parents, Tracy and Robert Tumolo, and my significant other, Gilbert "Gilligan" Rodriguez. My parents exude wisdom, confidence, and optimism, and always encourage me to reach for the stars. Gilligan is the smartest person I know; he stays one step ahead of the game with an aura of patience and love. He has shared in this journey with me since the very beginning, and has therefore been the foundation of my support system in graduate school. He has celebrated my successes, patiently listened to me vent my frustrations, and commiserated my failures. He is always in my corner, and for that I can't thank him enough. I also thank Pumpkin and Precious the cats, partners in crime and the homework companions I can always count on.

Table of Contents

List of Tables

List of Figures

CHAPTER 1

Introduction

1.1 Abstract

Cellular homeostasis, a fundamental requirement for all living organisms, is maintained in part through endocytic downregulation. Endocytosis of nutrient transporters is regulated in response to changing environmental conditions to adjust plasma membrane (PM) protein composition for optimal cell growth. Protein networks involved in cargo capture and sorting, membrane sculpting and deformation, and vesicle scission have been well-characterized, but less is known about the networks that sense extracellular cues and relay signals to trigger endocytosis of specific transporters. In Chapter 3 of this thesis, I establish that Hal kinases belong to a yeast kinase family that is orthologous with human AMPK/Snf1-related kinases, underscoring the importance of understanding the function and regulation of these evolutionarily conserved kinases. In Chapter 4, I demonstrate that loss of Hal4 and Hal5 leads to increased internalization of various nutrient transporters, including Art1-mediated endocytosis of the methionine transporter Mup1 and Art1-independent endocytosis of the uracil transporter Fur4. In Chapter 5, I find that acute inhibition of Hal5 in the absence of Hal4 triggers rapid endocytosis of these cargo, suggesting that Hal kinases function in the amino acid sensing relay upstream of the endocytic response. In Chapter 6, I report that Hal5 localizes to the cell surface, but relocalizes away from the cell surface in response to stimulation with specific nutrients, indicating that Hal5 responds to nutrient availability. Taken together, my research indicates that Hal5 contributes to cellular homeostasis by

functioning as a nutrient-responsive endocytic gatekeeper, antagonizing endocytosis and promoting stability of transporters at the PM in nutrient-limiting conditions. Broadly, my research sheds light on how signaling molecules regulate endocytic trafficking to coordinate an adaptive growth response.

1.2 Overview

Regulation of endocytic trafficking in response to changing environmental conditions is critical to human health and disease. Endocytic trafficking and signal transduction networks regulate each other to achieve a variety of biological outcomes, such as signaling attenuation by endocytic downregulation and plasma-membrane remodeling. Additionally, signals sensed at the plasma-membrane are integrated to elicit transcriptional program changes. Together, these processes coordinate an adaptive growth response. Therefore, there is a critical need to understand the cross-regulation of endocytic trafficking and signal transduction networks.

In this thesis, I present my study of two protein kinases Hal4 and Hal5, that maintain cellular homeostasis, at least in part, by acting as endocytic antagonists. In this Chapter, I introduce the concept of plasma-membrane homeostasis, and provide a review of the current understanding of how feedback mechanisms between signaling networks and trafficking machinery play a pivotal role in its regulation. Next, I describe how signaling proteins are poised to contribute to maintenance of cellular homeostasis not only through transcriptional regulation but also through endocytic downregulation, and I describe how the yeast AMP-sensing kinase Snf1 exemplifies this paradigm.

Then, I introduce the NPR/HAL5 kinase family in yeast as emerging endocytic regulators in nutrient-sensing relays. Finally, I discuss the known role for NPR/HAL5 family members Hal4 and Hal5 in cellular homeostasis, and the studies that position them as possible endocytic regulators.

1.3 Cellular homeostasis is a fundamental requirement for all living organisms

Complex homeostatic processes in humans, and the molecular mechanisms underlying their regulation, is a concept that unifies all of physiology. Originally described by French physiologist Claude Bernard as the *milieu interieur* or "internal environment," and later coined as "homeostasis" by Walter Bradford Cannon, homeostasis establishes a relationship between forces inside any given system that simultaneously interact with and protect from the forces outside of that system (Modell *et al.*, 2015). Homeostasis, the tendency to maintain health and function in the face of changing environmental conditions, is a fundamental requirement of all living organisms. Homeostatic processes coordinate to maintain function at every biological level of organization from complex ecosystems, to the individual organisms that comprise distinct populations within ecosystems. At the level of the organism, failure to maintain homeostatic balance contributes to development of many diseases including (but not limited to) diabetes (Röder *et al.*, 2016), heart failure (Azzam *et al.*, 2017; Vela, 2019), neurodegeneration (Galloway *et al.*, 2019), asthma (Vanoni *et al.*, 2019), atherosclerosis (Pennings *et al.*, 2006), inflammatory bowel disease (Maloy and Powrie, 2011; Röder *et al.*, 2016), and cancer (Panieri and Santoro, 2016). Homeostatic regulation also occurs within every

level of organization at the organismal level, including the organ systems, individual organs, tissues, cells, and subcellular compartments within cells.

At the cellular level, homeostasis is the tendency to maintain intracellular concentrations of ions and nutrients as well as energy and pH despite fluctuating extracellular conditions and stresses (Romero, 2004). As the physical barrier between the extracellular and intracellular environments, the plasma membrane (PM) is the interface through which the cell senses and samples nutrients and growth signals in the extracellular environment. Complex signaling networks integrate information detected at the PM to coordinate diverse biological processes as part of the adaptive growth response to maintain cellular homeostasis. Multiple classes of proteins mediate these complex transactions between the cell and its environment, including integral membrane proteins (the PM proteome) such as nutrient transporters, ion channels, and signaling receptors, as well as signal transduction molecules like protein kinases and phosphatases. Ultimately, the coordinated action of the PM proteome and signaling molecules dictates a cell's adaptive response, which is critical for regulation of cellular homeostasis in the face of changing environmental conditions.

The cell carefully manages the abundance of receptors, transporters, and channels at the PM in coordination with the concentration and availability of various input signals in order to maintain cellular homeostasis (Blazek *et al.*, 2015; Savir *et al.*, 2017). The steady-state abundance of plasma membrane proteins, then, is critical for cellular homeostasis. This plasma-membrane homeostasis is achieved through a delicate balance of protein synthesis and degradation, which is carefully coordinated by

membrane trafficking events including secretion, endocytosis, recycling, and trafficking to the vacuole (**Figure 1.1**).

1.3.1 Maintenance of cellular homeostasis by signal transducers

The PM detects information about the extracellular environment, while signaling networks integrate and propagate that information to the nucleus to regulate gene expression and therefore protein synthesis. A key relay mechanism in these signaling networks involves phosphorylation, a reversible post-translational modification that occurs through the competing actions of protein kinases and protein phosphatases (Graves and Krebs, 1999; Hunter, 2012). Phosphorylation often plays a central role in signal transduction by functioning as a type of molecular switch. For example, it can activate or deactivate specific enzymatic activities, affect protein stability, change protein interaction profiles, or impact subcellular localization in order to propagate a signal (Ardito *et al.*, 2017). Ultimately, protein kinases help to maintain cellular homeostasis by functioning as nutrient-sensing signal transducers that regulate gene expression (Wilson and Roach, 2002), and therefore protein synthesis, in response to changing environmental conditions.

Snf1 is perhaps the best-characterized example of a nutrient-sensing kinase in *Saccharomyces cerevisiae*. Snf1 and its human homolog, AMPK, are evolutionarily conserved kinases that sense insufficient ATP levels through detection of increased intracellular concentrations of AMP and ADP (Coccetti *et al.*, 2018). Snf1 and AMPK regulate downstream effector pathways that coordinate catabolic processes to control
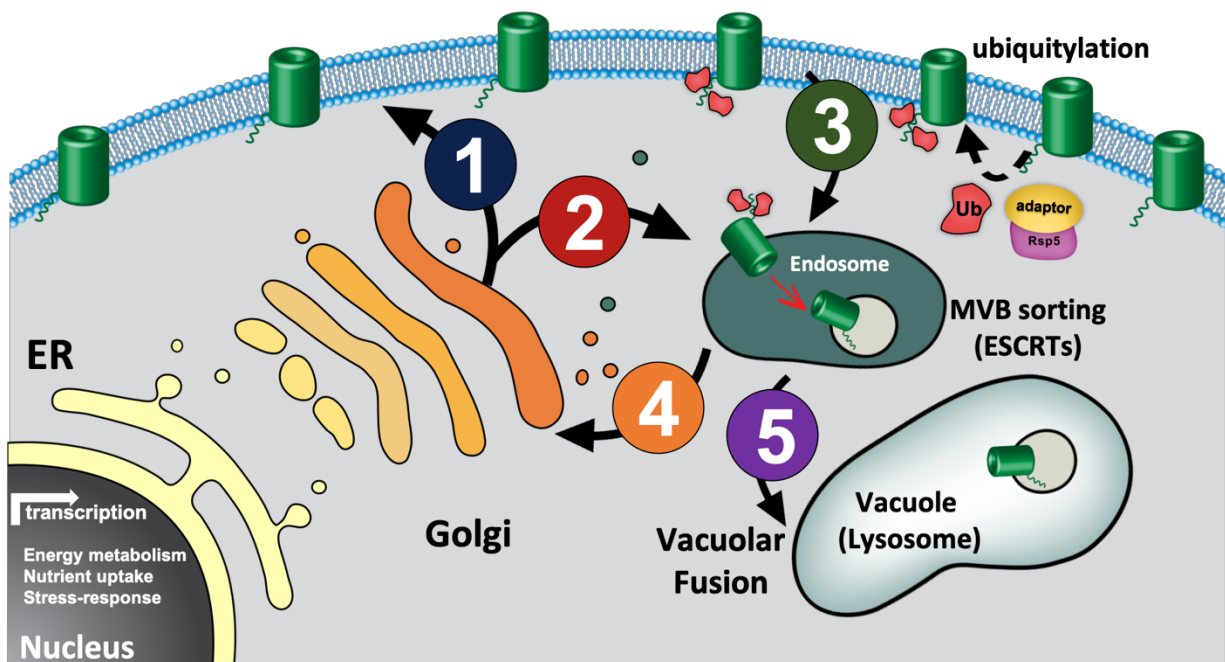
FIGURE 1.1 Membrane trafficking pathways coordinate protein synthesis and protein degradation. In the nucleus, genes are expressed as a function of interactions between transcription factors and promoter elements and translated to proteins at the ER. Integral membrane proteins, such as nutrient transporters (green cylinders) then undergo **1) secretion,** where they are trafficked from the Golgi to the PM in vesicles or **2) biosynthesis**, where they are trafficked to the endosome. At the PM, integral membrane proteins undergo **3) endocytosis**, where they are internalized in vesicles from the PM and trafficked to endosomes. At endosomes, PM proteins are subject to MVB sorting, where they then undergo **4) recycling** back out to the PM, either directly or through the Golgi, or **5) vacuolar trafficking** to the vacuole, where they are ultimately degraded. These major membrane trafficking pathways coordinate the balance of protein synthesis and protein degradation to achieve a steady-state abundance of plasma membrane proteins conducive to growth.

energy homeostasis in the cell and thus are required for eukaryotic cells to adapt to various nutrient restrictive conditions (Coccetti *et al.*, 2018). In yeast, Snf1 functions as the catalytic subunit of a multi-protein kinase complex that undergoes regulation by subcellular localization and nutrient availability (Vincent *et al.*, 2001; Hedbacker and Carlson, 2008). In low-glucose conditions, auto-inhibition of Snf1 catalytic activity by γ-subunit Snf4 is relieved (Leech *et al.*, 2003), permitting upstream activating kinases Tos3, Elm1, and Sak1 to interact with and phosphorylate Snf1 (Hong *et al.*, 2003). Active Snf1 then phosphorylates multiple transcription factors to regulate expression of more than 400 genes, allowing for adaptive growth in glucose-scarce conditions (Young *et al.*, 2012). This regulation includes relief of transcriptional repression to permit transcription of metabolic genes, including those that encode the metabolic enzymes for alternative carbon sources sucrose and galactose (*SUC2* and *GAL4*) as well those that control the expression of high-affinity glucose transporters such as *HXT2* and *HXT4* for glucose and hexose scavenging (Nicastro *et al.*, 2015). In glucose-replete conditions, active Snf1 is dephosphorylated by protein phosphatase Glc7 (Sanz *et al.*, 2000), allowing for auto-inhibition by γ-subunit Snf4 (Ludin *et al.*, 1998). The mammalian homolog of Snf1, AMPK, functions analogously through allosteric activation by AMP (Gowans *et al.*, 2013; Ahalawat and Murarka, 2017). While yeast Snf1 is not thought to be allosterically activated by AMP, it has been demonstrated that ADP molecules can bind the γ-subunit Snf4 to interfere with Glc7-mediated dephosphorylation of Snf1, stabilizing the active Snf1 complex (Mayer *et al.*, 2011).

This paradigm of transcriptional response mediated by signaling molecules is not limited to carbon metabolism. Nitrogen metabolism is maintained through at least two known nutrient-sensing pathways in yeast, including the target of rapamycin (TOR) pathway and the Ssy1-Ptr3-Ssy5 (SPS) sensor system (Ljungdahl, 2009; González and Hall, 2017). In the TOR pathway, nitrogen-rich conditions (amino acid sufficiency) inside the cell activate Tor1 protein kinase activity as part of a multi-protein complex (TORC1) at the limiting membrane of the vacuole (lysosome) (Hara *et al.*, 1998; Godard *et al.*, 2007; Stracka *et al.*, 2014). While the mechanism by which TORC1 senses amino acids in yeast is not clear, active TORC1 responds to amino acid sufficiency by multiple well-characterized effector pathways (Loewith and Hall, 2011), one of which involves sequestration of a transcription factor, Gln3, in the cytoplasm. In nitrogen-poor (starvation) conditions, TORC1 is inactive and Gln3 localization shifts to the nucleus to induce expression of genes required for scavenging poor nitrogen sources (Beck and Hall, 1999; Cox *et al.*, 2004). While Gln3 phosphorylation correlates with its nuclear localization, and TORC1 phosphorylates Gln3 *in vitro* (Bertram *et al.*, 2000)*,* it is not clear whether TORC1-mediated sequestration of Gln3 is due to a change in phosphorylation, a change in protein interactions, or some combination.

While the TOR pathway senses amino acid abundance inside the cell, the SPS sensor system detects amino acid abundance in the extracellular environment and integrates that information through the coordinated action of Ssy1, Ptr3, and Ssy5 (the SPS sensor) with two yeast casein kinases, Yck1 and Yck2 (Ljungdahl and Daignan-Fornier, 2012)}. Ssy1, a transporter-like integral membrane protein without transporter activity,

appears to sense amino acids by directly binding them, which stimulates a conformational change in the N-terminal cytoplasmic tail of Ssy1 (Wu *et al.*, 2006; Poulsen *et al.*, 2008). This signal is transduced by Ptr3, which then promotes the interaction of Yck1 and Yck2 with the SPS sensor (Liu *et al.*, 2008; Omnus *et al.*, 2011). Yck1 and Yck2 are PM-localized and constitutively active in nitrogen-poor conditions, but Ssy1 detection of excess amino acids brings them into close proximity of the SPS sensor, resulting in hyperphosphorylation and activation of the endoproteolytic enzyme Ssy5 (Omnus *et al.*, 2011). Ssy5 then activates two transcription factors, Stp1 and Stp2, releasing auto-inhibition and enabling nuclear translocation (Andréasson *et al.*, 2006; Pfirrmann *et al.*, 2010; Omnus *et al.*, 2011), resulting in the subsequent expression of amino acid and peptide transporter genes (Forsberg *et al.*, 2001). While Snf1/AMPK appears to directly sense nutrient status, Yck1/2 and Tor1 appear to sense nutrient status indirectly, through the action of the SPS sensor in the case of Yck1/2 and an unknown mechanism in the case of TORC1. In each pathway, cellular homeostasis is achieved, in part, through negative feedback mechanisms controlling transporter synthesis, thus lowering transporter abundance at the surface over time. These mechanisms regulate biosynthesis of new transporters, but other branches of these responses can also regulate the turnover of existing transporters at the surface.

1.3.2 Maintenance of cellular homeostasis by membrane trafficking
The major way the cell achieves acute clearance of receptors, transporters, and ion channels from the PM is through endocytic downregulation. Frequently, a substrate or ligand of a transporter or receptor selectively stimulates endocytic internalization and

trafficking along the endocytic route, culminating in sorting to the lysosome (or vacuole) for degradation. This type of endocytic downregulation has been described for many nutrient transporters in *Saccharomyces cerevisiae*, including Mup1 (a high-affinity methionine transporter) (Lin *et al.*, 2008; Guiney *et al.*, 2016), Can1 (a high-affinity arginine transporter) (Ghaddar *et al.*, 2014; Gournas *et al.*, 2017), and Fur4 (a high-affinity uracil transporter) (Marchal *et al.*, 2000; Moharir *et al.*, 2018). In each case, these proteins are stably expressed at the PM in the absence of their respective substrates, but are rapidly and selectively internalized and trafficked to the vacuole for degradation in the presence of specific substrates (**Figure 1.1**).

Endocytic downregulation of these transporters is selective and ubiquitin-dependent (Léon and Haguenauer-Tsapis, 2009; Lauwers *et al.*, 2010; MacGurn *et al.*, 2012). Rsp5, the lone Nedd4 family E3 ubiquitin ligase in yeast, mediates ubiquitylation of transporters via interaction with an extensive network of arrestin-related adaptor proteins (ARTs) which target Rsp5 substrate selection in a context-dependent manner (Léon and Haguenauer-Tsapis, 2009; Lauwers *et al.*, 2010; MacGurn *et al.*, 2012). Cargo ubiquitylation is sufficient for capture by ubiquitin-binding elements in the endocytic machinery, and therefore understanding how extracellular cues are sensed and signals are relayed to trigger ubiquitylation of specific transporters at the PM will be critical for understanding the molecular basis for specificity in endocytic responses (Goh *et al.*, 2010; Weinberg and Drubin, 2012; Schmid, 2017). Currently, the conventional wisdom is that the nutrient-sensing pathways relay signals to the ART-Rsp5 network to

regulate transporter ubiquitylation, as is the case for substrate-induced endocytic downregulation described above. In other cases, the signals are still not understood.

1.4 Kinase regulation of endocytosis in response to nutrient status

Clathrin-mediated endocytosis (CME) is a complex event, and how eukaryotic cells regulate endocytic site assembly and cargo selection for endocytosis remains poorly understood (Goh *et al.*, 2010; Weinberg and Drubin, 2012; Schmid, 2017). Multiple studies in yeast are beginning to shed light on phospho-regulation along the endocytic trafficking route, which can involve regulation of cargo selection (MacGurn *et al.*, 2011; Alvaro *et al.*, 2016; Lee *et al.*, 2019), endocytic site assembly (Chi *et al.*, 2012; Peng *et al.*, 2015), multi-vesicular body (MVB) sorting (Morvan *et al.*, 2012), or recycling from endosomes (Lee *et al.*, 2017). While there are many reported examples of phosphorylation regulating endocytic trafficking, here I will focus on summarizing the best reported examples of endocytic regulation by nutrient-sensing pathways (**Figure 1.2**).

1.4.1 Snf1/AMPK kinase regulates endocytosis of nutrient transporters

Snf1 is conventionally thought to contribute to maintenance of cellular homeostasis through transcriptional regulation in response to glucose availability, as described above. However, recent studies suggest that Snf1 signaling contributes to cellular homeostasis using multiple effector pathways that involve both control over the glucose-repression genes as well as glucose transporter abundance at the cell surface
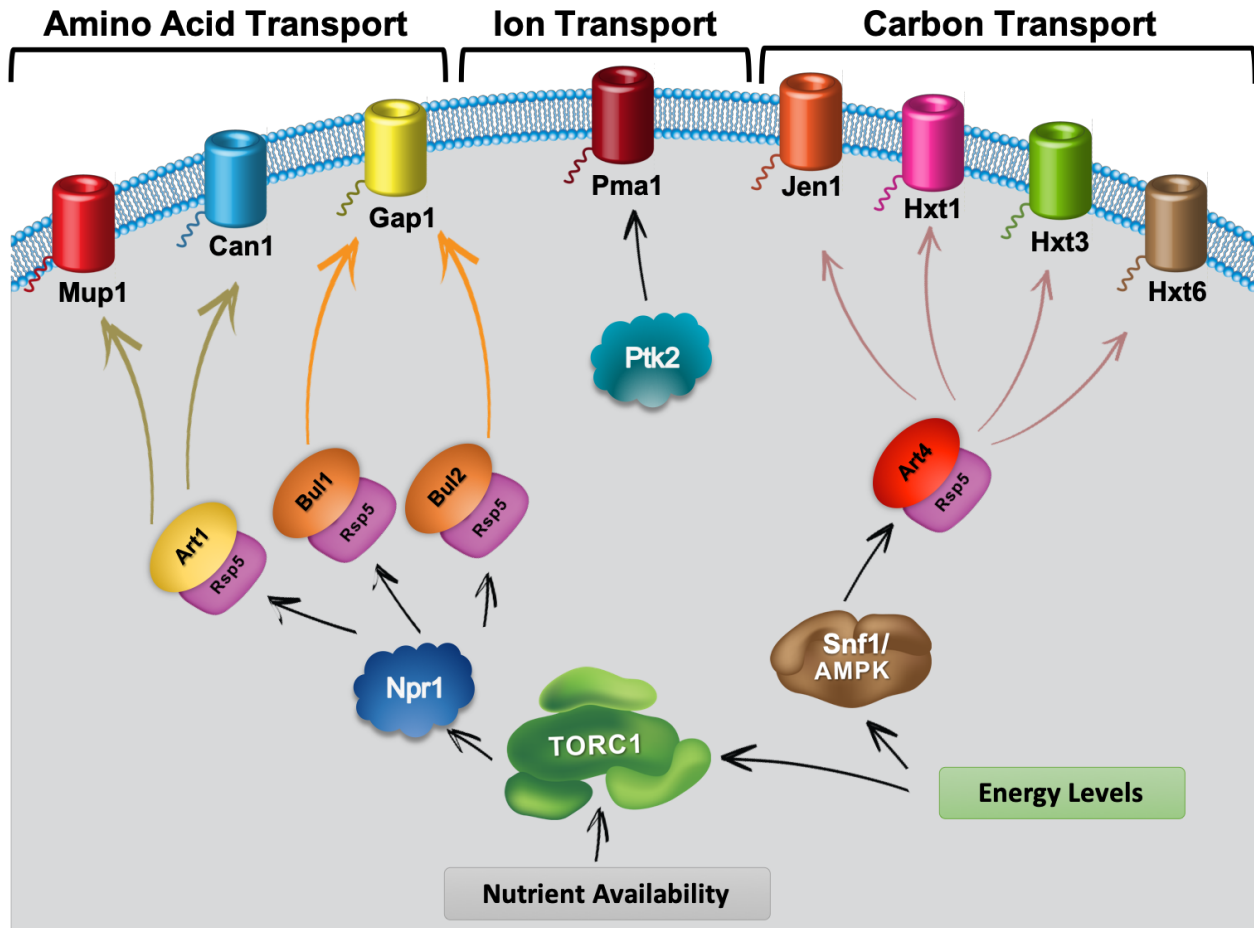
FIGURE 1.2 Kinase regulation of endocytosis in response to nutrient status. Snf1 regulates carbon transport in response to energy levels by inhibiting endocytosis of glucose transporters through regulation of Art4, an Rsp5 adaptor protein. Npr1 regulates amino acid uptake by acting as a TORC-effector kinase to inhibit endocytosis of amino acid transporters by regulating Rsp5 adaptors like Art1, Bul1, and Bul2. Ptk2 regulates ion transport by directly phosphorylating Pma1 to regulate its activity, although it is not clear whether this effects catalytic activity, abundance, or trafficking of Pma1.

(Becuwe *et al.*, 2012; O'Donnell *et al.*, 2015; Llopis-Torregrosa *et al.*, 2016).

Specifically, Snf1 phosphorylates the Rsp5 adaptor Art4 (Rod1) in response to glucose

availability to modulate endocytic downregulation of lactate transporter Jen1 (Becuwe *et*

al., 2012) as well as hexose transporters Hxt1, Hxt3, and Hxt6 (O'Donnell *et al.*, 2015;

Llopis-Torregrosa *et al.*, 2016). Thus, in a manner that is glucose-responsive, Snf1

regulates glucose transporter abundance at the cell surface (**Figure 1.2**). Importantly,

the activity of AMPK in human cells also regulates the stability and trafficking of the

GLUT1 and GLUT4 glucose transporters by regulating the activity of TXNIP, an arrestin

domain containing protein similar to the ART adaptors in yeast (Wu *et al.*, 2013;

Waldhart *et al.*, 2017). In each case, phosphorylation of Art4 and TXNIP by Snf1 and

AMPK, respectively, inhibits their endocytic activities, while dephosphorylation activates

or enhances endocytosis of nutrient transporters. Phosphorylation of Art4 by Snf1

appears to inhibit endocytosis by impeding ubiquitylation by Rsp5 (O'Donnell *et al.*,

2015), while AMPK-mediated phosphorylation of TXNIP appears to be destabilizing (Wu

et al., 2013). Thus, Snf1 and AMPK share similarities in regulation of nutrient

transporter endocytosis, but it is not clear if the effector mechanisms are precisely

analogous. Further studies elucidating the mechanism of endocytic regulation by Snf1

(in yeast) and AMPK (in humans) will be required to better understand how nutrient

signals are relayed to coordinate trafficking decisions in these two conserved signaling

systems.

1.4.2 NPR1/HAL5 family kinases are emerging as endocytic regulators

The NPR/HAL5 subgroup of kinases in yeast is emerging as a family of kinases that regulate nutrient transporter abundance at the PM. Npr1 kinase is known to be involved in nutrient-sensing, although this hasn't been established for Hal kinases. Here, I review what is known about Npr1 and Hal kinases, and how they regulate endocytic trafficking in response to changing nutrient availability.

Npr1, one of 11 NPR/HAL5 subgroup members, has a catalytic domain which comprises approximately half of the protein at the C-terminus, and similarly sized N-terminal domain that is heavily phosphorylated and regulated by the TORC1 kinase complex (Schmidt *et al.*, 1998; Bonenfant *et al.*, 2003; Gander *et al.*, 2008; Breitkreutz *et al.*, 2010; MacGurn *et al.*, 2011). In a manner that is TORC1-sensitive, Npr1 can phosphorylate and inhibit the Rsp5 adaptor protein Art1, specifically by antagonizing Art1 localization to the PM and therefore stabilizing the arginine transporter, Can1, at the cell surface (MacGurn *et al.*, 2011). Similarly, endocytic downregulation of the yeast general amino acid permease, Gap1, is stimulated by TORC1 signaling through release of Npr1-mediated phosphoinhibition of arrestin-related Rsp5 adaptors Bul1 and Bul2 (Merhi *et al.*, 2011; Merhi and André, 2012). Thus, the Npr1 kinase provides an effector mechanism for nutrient-sensing TORC1 to regulate endocytosis of specific nutrient transporters at the PM (**Figure 1.2**). Ptk2, another NPR/HAL5 family member, is reported to regulate the activity of the essential yeast proton pump Pma1 in response to glucose availability and pH stress, although it remains unclear if this regulation occurs at the level of catalysis, or stability and trafficking (Eraso *et al.*, 2006; Lecchi *et al.*, 2007;

Mason *et al.*, 2014; Mazón *et al.*, 2015) (**Figure 1.2**). These examples suggest that the broader NPR/HAL5 kinase family, like Snf1, may function in nutrient-sensing and the regulation of endocytosis.

In humans, two sub-families of kinases have been identified as sharing homology with AMPK called AMPK-related (Bright *et al.*, 2009) and Snf1-related (sometimes called Snf-related) (Jaleel *et al.*, 2005) which are also both poorly understood relative to AMPK. The evolutionary relationship between Snf1 and NPR/HAL5 kinases has not been analyzed. Given the similarities discussed, I propose that the NPR/HAL5 family of kinases in yeast, previously labeled as a yeast-specific kinase family, shares evolutionary conservation with Snf1, AMPK, and AMPK/Snf1-rleated kinases. I present this analysis in Chapter 3 of this dissertation.

1.4.3 Hal4 and Hal5 kinases regulate cellular homeostasis

Hal4 and Hal5, two closely related AMPK/Snf1-related kinases, have been best characterized for their redundant role in stabilizing two yeast potassium transporters, Trk1 and Trk2 (Mulet *et al.*, 1999; Casado *et al.*, 2010; Hirasaki *et al.*, 2011). SDS-PAGE mobility of Trk transporters shifts upon deletion of Hal kinases, prompting the hypothesis that Hal kinases phosphorylate Trk transporters directly to stabilize them at the PM, though direct phosphorylation has never been demonstrated. This hypothesis seems unlikely, as *hal* mutants exhibit decreased steady state abundance of a variety of nutrient transporters including Mup1, Gap1, Can1, Fur4, Hxt1, and Tat2 (Pérez-Valle *et al.*, 2007; Pérez-Valle *et al.*, 2010). Consistent with these findings, mutant cells

exhibited decreased nitrogen and carbon uptake, as well as dysregulated cytosolic pH
(Pérez-Valle *et al.*, 2010). Not surprisingly, a transcriptomic analysis in *Δhal4Δhal5* (or
hal) double mutant cells revealed changes consistent with starvation stress including (i)
genes associated with energy metabolism, carbohydrate metabolism, methionine
biosynthesis, and stress response and (ii) genes associated with nucleotide
metabolism, amino acid metabolism, iron assimilation, ribosome biogenesis, and
ergosterol biosynthesis (Pérez-Valle *et al.*, 2010).Taken together, these studies position
Hal kinases squarely as regulators of nitrogen, metabolism, and ion homeostasis.

Snf1, Npr1, and Hal mutants have all been reported to regulate the stability of nutrient
transporters at the PM. Snf1-mediated regulation in this capacity appears limited to the
stabilization of glucose transporters, while Npr1-mediated regulation appears limited to
the stabilization of amino acid transporters. Hal-mediated stabilization of nutrient
transporters does not appear to be limited to a particular class of nutrient, and spans
amino acid, ion, and glucose transport. While nutrient-sensing relays are involved in
Snf1-mediated and Npr1-mediated regulation of nutrient transporter stability, the ability
of Hal kinases to participate in nutrient-sensing remains unclear from these studies.

Consistent with the observed dysregulation of amino acid transporters, a recent study
has implicated Hal kinases in the nitrogen-sensing TOR pathway by demonstrating that
disruption of Hal kinases is associated with decreased Npr1 activity, and that
overexpression of Npr1 partially restores *hal* mutant phenotypes (Primo *et al.*, 2017).
These data suggest that Hal kinase function may overlap with Npr1, and that Hal

kinases, like Npr1, may be functioning within, or in parallel to, a TORC signaling

cascade. Interestingly, like Torc1, Hal4 and Hal5 appear to regulate the transcription

factor Gln3. Specifically, disruption of Hal kinases correlates with increased

phosphorylation and nuclear localization of the transcription factor Gln3 (Hirasaki *et al.*,

2011). Additionally, disruption of Hal kinases in a phosphatase mutant *ppz1* background

abolished Gln3-dependent gene expression of ENA1 (P-type ATPase/ sodium

transporter) (Hirasaki *et al.*, 2011). As Hal4 and Hal5 kinases were originally discovered

in an overexpression screen for their ability to confer resistance to salt stress (Mulet *et*

al., 1999), another possibility is that Hal kinases function in sensing ion concentrations,

which would be consistent with the observed dysregulation of ion transporters.

Transcriptomic data reveals that Hal5 expression is induced upon salt treatment ($CaCl_2$)

or alkaline pH stress in a calcineurin/Crz1-dependent manner (Casado *et al.*, 2010).

Consistent with these findings, Hal5 protein accumulates after salt treatment ($CaCl_2$ and

NaCl) and exhibits changes in SDS-PAGE mobility (Casado *et al.*, 2010), suggesting

nutrient-responsive changes in Hal5 phosphorylation that correlate with protein stability.

The phenotypes reported for *Δhal4Δhal5* double mutant cells (**Figure 1.3**) suggest that

Hal kinases stabilize nutrient transporters to achieve and maintain cellular homeostasis.

The process specifically regulated by Hal kinases, the mechanisms of action, and their
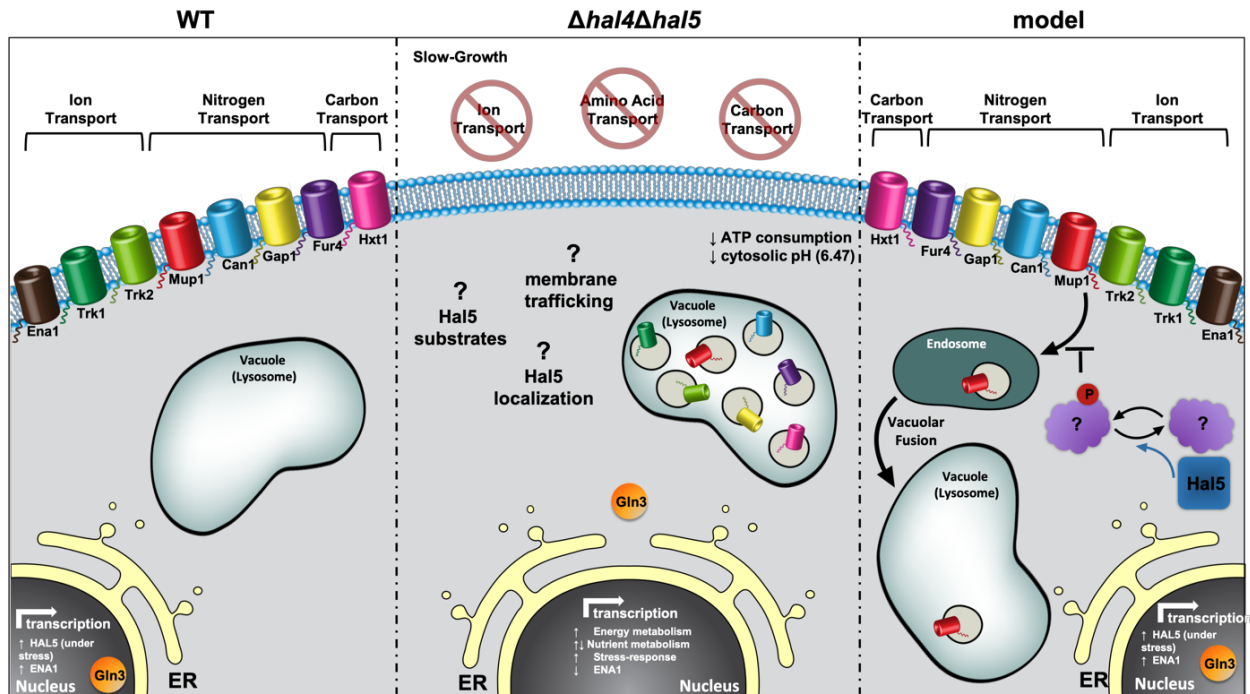
FIGURE 1.3 Hal-mediated stabilization of nutrient transporters A cartoon depicting the transcription-state and steady-state abundance of multiple nutrient transporters in WT cells in the left panel compared to *hal* mutant cells in the right panel.

relative contributions to transporter stabilization remain unknown. One possibility is that

Hal kinases regulate ART-Rsp5 regulated endocytosis in a manner similar to Npr1 and

Snf1. However, broad regulation of many different types of nutrient transporters by Hal

kinases suggests that they may play a more general role in endocytosis, perhaps

regulating a process upstream of cargo-specific ubiquitylation. Inspired by the parallels

observed for Snf1, Npr1, and Hal kinases, I examine the hypothesis that Hal kinases

regulate endocytosis in a manner similar to Npr1 and Snf1 kinases. Although my

research suggests that these kinases are all part of an evolutionarily related family, my

data indicates that Hal kinases regulate endocytic trafficking by a mechanism that is

distinct from that described for Npr1 and Snf1 (**Figure 1.2**).

1.5 Summary of thesis

My thesis research has been driven by understanding how Hal kinases coordinate

endocytic trafficking with nutrient response. Snf1 is a well-characterized example of how

the cell achieves this regulation, but the NPR/HAL5 kinases remain poorly understood.

In Chapter 2 of this thesis, I describe the materials and methods used to carry out my

studies. In Chapter 3, I establish that Snf1 and NPR/HAL5 kinases cluster together in an

original phylogenetic analysis, indicating evolutionary conservation. In Chapters 4-6 of

this thesis, I investigate the role of Snf1/AMPK-related protein kinases, Hal4 and Hal5,

in stabilizing nutrient transporters to maintain cellular homeostasis in yeast. In Chapter

4, I report that Hal kinases negatively regulate nutrient transporter endocytosis

upstream of the ART-Rsp5 network, and that in some cases Hal4 and Hal5 may exhibit

distinct functions. In Chapter 5, I report that Hal5 catalytic activity is required for its

negative regulation of nutrient transporter endocytosis. In Chapter 6, I find that the previously uncharacterized N-terminal region of Hal5 is critical for regulation of endocytosis as well as localization of Hal5 to the PM. Parallel to Snf1, Hal5 localization to the PM is responsive to nutrient stimulation, as addition of specific nutrients triggered Hal5 ejection from the PM. In Chapter 7, I discuss how these results, taken together, indicate that Hal5 maintains cellular homeostasis, in part, by coordinating upstream nutrient-sensing events with the stability of nutrient transporters at the cell surface. These results improve our understanding of how endocytic trafficking and signaling networks regulate each other to coordinate an adaptive growth response.

CHAPTER 2

Materials and Methods

2.1 Plasmids, yeast strains and culturing conditions

Unless otherwise indicated, all genes were cloned with native promoter sequence from genomic yeast DNA using standard PCR methods, restriction digest and ligation into centromeric (pRS) vector backbones. Constructs with point mutations were generated using PCR site-directed mutagenesis. All constructs generated by PCR in this study were verified by sequencing. See **Table 2.1** for a list of plasmids used in this study.

The *SEY6210* strain background (*MATα leu2-3,112 ura3-52 his3-Δ200 trp1-Δ901 lys2-801 suc2-Δ9)* was used for most experiments. Genomic tagging and deletion of genes was performed using standard PCR-based homologous recombination, as described previously (Lin *et al.*, 2008). Strains with multiple genomic modifications (genomic tags, deletions, or some combination) were generated by mating, sporulation (potassium acetate raffinose media), and subsequent tetrad dissection using a tetrad dissection microscope (MSM System 400, Singer Instruments). For determination of growth phenotypes, yeast cells were cultured in indicated media (SC or YP + dextrose liquid media) overnight at 26°C. 1 OD_{600} equivalent was harvested, serially diluted into sterile water, and plated onto indicated media (SC or YP + dextrose solid media, either control of treated) using a 48-well metal replica plater (Sigma). Sensitivity to thialysine (toxic lysine analogue; 0.8 or 2.0 µg/ml on SC + dextrose solid media) was tested in the

plasmid designation	plasmid backbone	genotype	source
pCHL642	pRS416	MUP1-GFP	(Lin *et al.*, 2008)
pSR21	pRS416	FUR4-GFP	(Lin *et al.*, 2008)
pCHL571	pRS416	CAN1-GFP	(Lin *et al.*, 2008)
pSR25	pRS416	PMA1-GFP	(Lin *et al.*, 2008)
Pil1-GFP	pRS416	PIL1-GFP	This study
Snc1-GFP	pRS416	SNC1-GFP	(Lewis *et al.*, 2000)
Cps-GFP	pRS416	CPS-GFP	This study
pJAM1292	pRS415	native Hal5	This study
pJAM1368	pRS415	HAL5-adh1terminator-HTF	This study
pJMT4	pRS415	*hal5K546R*-adh1 terminator-HTF	This study
pJMT5	pRS415	*hal5D688A*-adh1 terminator-HTF	This study
pJMT6	pRS415	*hal5M620G*-adh1 terminator-HTF	This study
pJMT10	pRS415	*hal5Δ1-493*	This study
pJMT11	pRS415	*hal5Δ1-493*-adh1 terminator-HTF	This study
pJAM1583	pRS415	HAL5-mNG	This study
pJAM1585	pRS415	*hal5Δ494-855*-mNG	This study
pJMT13	pRS415	*hal5Δ1-493*-mNG	This study
pJMT14	pRS415	*hal5M620G*-mNG	This study
pJAM1621	pRS415	*hal5Δ1-339*	This study
pJAM1622	pRS415	*hal5Δ1-248*	This study
pJAM1623	pRS415	*hal5Δ1-99*	This study
pJMT18	pRS415	*hal5Δ1-339-mNG*	This study
pJMT19	pRS415	*hal5Δ1-339*-adh1 terminator-HTF	This study
pJMT21	pRS415	*hal5Δ1-248-mNG*	This study
pJMT23	pRS415	*hal5Δ1-99-mNG*	This study
pJAM1547	pRS415	ART1-mNG	This study

Table 2.1 List of plasmids Plasmids generated and/or used in this study including: plasmid designation, backbone, genotype, and source.

BY4741 strain background (*MATa his3Δ1 leu2Δ0 met15Δ0 ura3Δ0)* since *SEY6210* is a

lysine auxotroph. See **Table 2.2** for a list of strains used in this study.

2.2 Fluorescence microscopy analysis of cargo trafficking and Hal localization

Protein trafficking and localization analyses were performed by growing yeast cells

expressing fluorescent fusion proteins (GFP, mNG, MARS, or mCherry) to mid-log

phase in indicated synthetic liquid media at 26°C and imaged live in synthetic liquid

media using a DeltaVision Elite Imaging system (Olympus IX-71 inverted microscope;

Olympus 100× oil objective (1.4 NA); DV Elite sCMOS camera, GE Healthcare). In

experiments using FM 4-64 as a PM label, cells were incubated on ice for 5 minutes,

then spotted onto a slide and mixed with FM 4-64 (final concentration of 12.5x or 125

μg/mL) and imaged within 10 minutes. In experiments examining cargo-GFP trafficking

in response to treatment with 1-NA-PP1 (Adooq Bioscience, Irvine, CA), cells were

treated for 1 hour and imaged in the same media. In experiments examining Hal5-mNG

localization in response to 1-NA-PP1 treatment, cells were treated for 10 minutes, and

placed on ice for 5 minutes prior to imaging. In experiments examining Hal5-mNG

localization in response to nutrients, cells were either resuspended in a starvation media

(potassium-acetate raffinose media), or excess nutrients were added to the media

(10μg/mL uracil, leucine, methionine, histidine, or tryptophan, 500mM NaCl, or 300mM

KCl). After 10 minutes of treatment, cultures were placed on ice for 5 minutes prior to

imaging. Images were collected and deconvolved, then quantified. The PM:Vac ratio

analysis was performed as previously described (Lee *et al.*, 2019). Specifically,

Softworx image analysis software was used to measure the fluorescence

strain designation	strain background	genotype	source
WT	BY4741	*MATa his3Δ0 leu2Δ0 met15Δ0 ura3Δ0*	ResGen™ Collection
WT	SEY6210	*MATα leu2-3,112 ura3-52 his3-Δ200 trp1-Δ901 lys2-801 suc2-Δ9*	(Robinson *et al.*, 1988)
NHY101.1	BY4741	*Δhal4::clonNATR*	This study
NHY102.1	BY4741	*Δhal5::clonNATR*	This study
NHY107.1	SEY6210	*Δhal4::KanMx*	This study
NHY108.1	SEY6210	*Δhal5::KanMx*	This study
CLY461	SEY6210	*Δart1::HIS3*	(Lin *et al.*, 2008)
JMY1811	SEY6210	*MUP1-pHlourin::KanMx*	(Lee *et al.*, 2019)
JMY909	SEY6210	*VPH1-MARS::TRP1*	(Lee *et al.*, 2017)
JTY220	SEY6210	*HAL5-mNG::KanMx*	This study
JTY195	SEY6210	*Δhal4::KanMx VPH1-MARS::TRP1*	This study
JTY150	SEY6210	*Δhal5::KanMx VPH1-MARS::TRP1*	This study
JTY158	SEY6210	*Δart1::HIS3 VPH1-MARS::TRP1*	This study
NHY134	SEY6210	*Δhal4::KanMx MUP1-pHlourin::KanMx*	This study
NHY136	SEY6210	*Δhal5::KanMx MUP1-pHlourin::KanMx*	This study
JTY245	SEY6210	*Δart1::HIS3 MUP1-pHlourin::KanMx*	(Lee *et al.*, 2019)
JTY167	SEY6210	*Δhal4::KanMxΔhal5::KanMx*	This study
JTY229	SEY6210	*Δhal4::KanMxΔhal5::KanMx VPH1-MARS::TRP*	This study
JTY154	SEY6210	*Δhal4::KanMx Δhal5::KanMx MUP1-pHlourin::KanMx*	This study
JTY247	SEY6210	*Δart1::HISΔhal4::KanMxΔhal5::KanMx*	This study
JTY314	SEY6210	*Δart1::HISΔhal4::KanMx Δhal5::KanMx VPH1-MARS::TRP1*	This study
JTY306	SEY6210	*Δart1::HIS3Δhal4::KanMxΔhal5::KanMx MUP1-pHlourin::KanMx*	This study
JTY285	SEY6210	*HAL5-mNG::KanMx ART1-mCherry::TRP1*	This study
JTY287	SEY6210	*HAL5-mNG::KanMx EDE1-mCherry::TRP1*	This study
JTY290	SEY6210	*HAL5-mNG::KanMx SLA2-mCherry::TRP1*	This study
JTY292	SEY6210	*HAL5-mNG::KanMx ENT1-mCherry::TRP1*	This study
JTY294	SEY6210	*HAL5-mNG::KanMx PIL1-mCherry::TRP1*	This study
JTY295	SEY6210	*HAL5-mNG::KanMx ABP1-mCherry::TRP1*	This study
JTY308	SEY6210	*HAL5-mNG::KanMx MUP1-MARS::TRP1*	This study
JTY283	SEY6210	*Δhal4::KanMxΔhal5::KanMxΔarg4::KanMx ART1-HTF::TRP*	This study
JTY255	SEY6210	*Δarg4::KanMx ART1-HTF::TRP*	This study
JTY254	SEY6210	*Δhal4::KanMxΔhal5::KanMxΔarg4::KanMx*	This study
JTY259	SEY6210	*Δhal4::KanMx Δarg4::KanMx*	This study
JTY260	SEY6210	*Δhal5::KanMxΔarg4::KanMx*	This study

Table 2.2 List of strains Strains used in this study including strain designation, background, genotype, and source.

signal intensity at the PM and in the vacuole and PM:Vac ratios were computed for a large number of cells (n=50). In cases where some cells contained no detectable localization to the PM, binning analysis was performed. Specifically, cells were counted and grouped (binned) into categories defined by the localization of Mup1-GFP, Can1-GFP, or Fur4-GFP. If cargo was localized exclusively to the PM with no detectable signal in the vacuole above background, cells were binned into a category called "PM". If cargo was localized with signal detectable above background at both the PM and vacuole, cells were binned into a category called "PM + Vac". If cargo was localized exclusively to the vacuole with no detectable signal at the PM, cells were binned into a category called "Vac". Pearson correlation coefficients were determined by drawing a region of interest around each cell and using the Pearson correlation coefficient function using Softworx software (GE Healthcare). Images were pseudo-colored using the free open-source program Fiji.

2.3 Analysis of endocytic recycling by measurement of FM4-64 efflux

FM 4-64 efflux was measured by growing yeast cells were grown to mid-log phase in liquid media (YP + dextrose) at 30°C then shifted to 22°C for 10 minutes. Cells were pulsed with FM 4-64 (1x or 10μg/mL) for 8 minutes at 22°C then placed on ice for 10 minutes. Cells were washed with ice-cold liquid media (SM + dextrose) three times. Cells were distributed into a 96-well plate in 250 μl aliquots while on ice, and then warmed to room temperature for 3 minutes prior to analysis by flow cytometry using a BD Accuri C6 Plus benchtop flow cytometer (BD Biosciences). Over 10,000 cells per

time point were detected and analyzed per condition based on gating in the PE channel, which detects signal from FM 4-64.

2.4 Analysis of Mup1-pHluorin trafficking

Analysis of Mup1-pHluorin trafficking and steady state surface abundance was performed as previously described (Lee *et al.*, 2019). Briefly, Mup1-pHluorin trafficking was examined at steady-state or over time in response to stimulus (either 2μg/mL methionine or 26.3μM 1-NA-PP1) by growing yeast cells to mid-log phase in indicated synthetic liquid media at 26$°$C. Cells were distributed into a 96-well plate in 250 μl aliquots prior to analysis by flow cytometry using a Guava easyCyte benchtop flow cytometer (Millipore). Over 10,000 cells per time point were detected and analyzed per condition based on gating in the FITC channel, which detects signal from pHluorin.

2.5 Analysis of protein expression in cultured yeast cells

Yeast lysates were prepared from mid-log phase cultures grown in the indicated selective synthetic liquid media at 26$°$C. 5 OD_{600} equivalents were precipitated in 10% trichloroacetic acid (TCA) in TE (10 mM Tris-HCl, 1mM EDTA, pH 8.0) and subsequently washed with acetone, aspirated, dried under vacuum, solubilized in lysis buffer (150 mM NaCl, 50 mM Tris pH7.5, 1 mM EDTA, 1% SDS) and disrupted by vortex with 100 µL of acid-washed glass beads. Urea-sample buffer (150 mM Tris pH 6.8, 6 M Urea, 6% SDS, 10% β-mercaptoethanol, 20% glycerol) was added and samples were heated to 65$°$C prior to analysis by SDS-PAGE and subsequent immunoblotting. SDS-PAGE gels were transferred to a polyvinylidene fluoride (PVDF)

membrane (Immobilon-FL; 0.45μM pore-size; MilliporeSigma), and blocked using 5%

milk in TBST (tris buffered saline with tween-20; 10mM tris-HCl, 150 mM NaCl, 0.05%

tween-20, pH 7.5). Membranes were incubated with primary antibodies α-FLAG (M2;

mouse monoclonal; Sigma; used at 1:2000 dilution) and/or α-G6PDH (rabbit polyclonal;

Sigma; used at 1:20,000 dilution), washed using TBST, and incubated with fluorescently

labeled secondary antibodies (LI-COR Biosciences; IRDye® 680RD Goat anti-Mouse

IgG and IRDye® 800CW Goat anti-Rabbit IgG; used at 1:10,000 dilution). Fluorescent

imaging of immunoblots was performed using an Odyssey infrared imaging system (LI-

COR Biosciences) and quantified using the proprietary Odyssey software LI-COR

Image Studio (LI-COR Biosciences).

2.6 Analysis of Art1 and Hal5 by SILAC-MS

Quantitative mass spectrometry analysis of Art1-FLAG and Hal5-FLAG by SILAC-MS

was performed as previously described (Lee *et al.*, 2019). Briefly, lysates were

generated from yeast cultures labelled with heavy or light arginine and lysine and

FLAG-tagged bait proteins (Art1-FLAG or Hal5-FLAG) were purified using EZView M2

FLAG agarose beads (Sigma). After washing, baits were eluted from beads by boiling in

10% SDS and eluates were collected and precipitated by addition of 50% ethanol,

49.9% acetone and 0.1% acetic acid. Protein pellets were resuspended in 20μL of 8M

urea/50mM Tris (pH 8.0) and the suspension was diluted by addition of 50μL of water

and digested overnight with 1μg trypsin (Gold, Promega). To analyze Art1 and Hal5

phosphorylation, resulting phosphopeptides were enriched using immobilized metal

affinity chromatography (MacGurn *et al.*, 2011) and analyzed on a Q Exactive mass

spectrometer (Thermo). To analyze Hal5 interactions, resulting peptides were (insert description here) Resulting spectra were searched using MaxQuant software (ver. 1.5.3.30) and chromatography was analyzed using Skyline software (MacCoss Lab).

2.7 Bioinformatic analysis

Protein kinase sequences were retrieved from *Saccharomyces* Genome Database (SGD, https://www.yeastgenome.org) and aligned using Clustal Omega (EMBL-EBI, multiple sequence alignment) or EMBOSS Water (EMBL-EBI, pairwise sequence alignment) (Madeira *et al.*, 2019). Sequence alignments were visualized using iTOL (https://itol.ebl.de.itol.cgi) (Letunic and Bork, 2019), EvolView v3 (www.evolgenius.info/evolview.html) (Subramanian *et al.*, 2019), or JalView (www.jalview.org) (Waterhouse *et al.*, 2009). SGD YeastMine (https://yeastmine.yeastgenome.org/yeastmine) was used to search and retrieve *S. cerevisiae* data, populated by SGD based on a curated list of protein kinases. Data retrieved through YeastMine for this study includes the number of publications annotated for each protein kinase (as of April 29, 2019) and orthologous across several model organisms. Information about protein kinase domains and architecture was retrieved automatically through the EvolView interface from UniProt (EMBL-EBI, https://www.uniprot.org). Secondary structure prediction of Hal5 was performed using JPred (Drozdetskiy *et al.*, 2015). A pairwise sequence alignment of Hal5 and Snf1 catalytic domains was used to generate a structural model for the Hal5 catalytic domain using MODELLER (https://salilab.org/modeller/) (Sali and Blundell, 1993) through the Chimera interface (UCSF, https://www.cgi.ucsf.edu/chimera/) (Pettersen *et al.*, 2004).

CHAPTER 3

The Evolution of NPR1/HAL5 family of Kinases and their Relationship to AMPK/Snf1

3.1 Introduction

Protein kinases represent a significant portion of all genomes, specifically about 2-3% of both the human and yeast genomes (Krupa *et al.*, 2004). These enzymes catalyze the transfer of the γ-phosphate group from ATP to a protein target (usually at serine, threonine, and tyrosine residues), forming a reversible post-translational modification that serves to increase the functional complexity of the genome. The vast majority of protein kinases are defined by a eukaryotic protein kinase (ePK) catalytic domain, and therefore belong to a single superfamily of kinases known as the ePKs. In these kinases, there is generally a lysine residue critical for coordinating ATP in the ATP-binding pocket, and a catalytic aspartate residue in the active site. In spite of high conservation within the ATP-binding pockets and active sites across most protein kinases, sequence divergences within the catalytic domains and outside of the catalytic domains, as well as known biological functions, have led to further classification of ePKs into distinct groups, many of which are conserved across evolution. These groups fall into two divisions, the tyrosine kinases and the serine/threonine kinases. The serine/threonine kinase subdivision of ePKs includes the AGC Group (containing PKAs, PKGs, and PKCs, or protein kinase A, protein kinase G, and protein kinase C subfamilies), the CMGC Group (containing CDKs and MAPKs, or cyclin-dependent kinase and mitogen-activated protein kinase families), the STE group (containing

MEKs, or mitogen-activated protein kinase kinases), the CK1 group (containing casein

kinases). and finally, the CAMK group (encompassing CAMKs, or calcium and

calmodulin-regulated kinase subfamilies, as well as several other related families)

(Manning *et al.*, 2002). Most of what we know about each of these kinase groups, and

our conventional wisdom about how these kinases function, is rooted in the

characterization of just a few flagship kinases in each group.

Nearly 40% of protein kinases identified in yeast failed to be classified into a classical

ePK group, and were instead grouped into catch-all categories such as "Other" and

"Atypical" (Hunter and Plowman, 1997). One such yeast-specific subfamily lacking

classification into the classical ePK groupings is the NPR1/HAL5 family of kinases,

which hasn't garnered a lot of attention because it is not thought to be conserved in

humans. This is in contrast to protein kinases with clear human homologs, such as

TORC1 or Snf1, which have been intensely characterized. Npr1, one of the better-

characterized kinases of the NPR1/HAL5 family, shares striking similarities to Snf1-

mediated regulation of glucose transporter abundance. For example, as an effector

molecule for TORC1 in intracellular nitrogen sensing, Npr1 regulates amino acid

transporter abundance (reviewed in Chapter 1). Similar to Npr1 and Snf1, Hal4 and

Hal5 kinases of the NPR1/HAL5 family regulate nutrient transporter abundance,

although the mechanism of this regulation is poorly characterized relative to Snf1 and

Npr1. Thus, Npr1 and Hal kinases appear to function similarly to Snf1 in this capacity, a

hallmark of defining and refining functional protein kinase families. However, the

evolutionary relationship between NPR1/HAL5 kinases with Snf1 in yeast or AMPK in

humans has not been explored. Defining this evolutionary relationship, and re-classifying NPR1/HAL5 kinases into ePK groups based on phylogenetic analysis presented in this chapter, and the functional data reviewed in Chapter 1 and presented in Chapters 4-6, will inform us broadly about the functions of an otherwise understudied group of kinases, including their human counterparts.

3.2 Results

3.2.1 Kinases clustering with Snf1 are understudied

To better understand the evolutionary relationship of Snf1 with other protein kinases in yeast, I first examined the history of protein kinase classification. The first classical protein kinase groups (AGC, CMGC, CAMK, CK1, and protein tyrosine kinases or PTKs) were established in 1995 using about 400 kinases across evolution that had been previously characterized and/or sequenced (Hanks and Hunter, 1995). A combination of available functional data, and sequence conservation with the catalytic domains, ultimately informed the classical protein kinase groupings in yeast in 1997, shortly after the yeast genome was sequenced (Hunter and Plowman, 1997). In a cutting-edge bioinformatic approach at the time, the majority of kinases in yeast (encompassing metabolic, lipid, and protein kinases) were identified and classified into families based on gene sequence similarity with a known ePK catalytic domain. In 2002, a similar analysis was carried out in humans shortly after the human genome was sequenced, which expanded the classical kinase groupings (Manning *et al.*, 2002). These studies were pioneering and powerful, because gene sequence analysis enabled

comprehensive identification of the yeast and human protein kinase complements.

Establishing protein kinase groups and subfamilies for newly discovered kinase domain

sequences was important because it allowed us to hypothesize function based on the

physiology of known protein kinases, and to then study them *in vivo.* Since these

pioneering studies that established protein kinase classification, additional kinases with

divergent sequences have been identified, and others were revealed not to be kinases

at all. For the most part, these classic family groupings remain, with revisions being

made as we learn more about the physiological function of uncharacterized protein

kinases.

In contrast to the analysis carried out in 1997 to predict ePK domains in yeast, I used a

widely-accessible and modern multiple sequence alignment algorithm to perform a

multiple sequence alignment of full protein sequences for the 130 known protein

kinases in yeast, which reveals 6 distinct kinase clades (**Figure 3.1** and **3.2**).

Surprisingly, these clades don't divide exactly into the classical ePK groupings, which

may be a result of several factors, including (i) using full-length sequences as opposed

to only catalytic domains, (ii) excluding all metabolic and lipid kinases, or (iii) improved

algorithm performance compared to 1997. The NPR1/HAL5 kinases, among others

lacking classical group classification, cluster into the clade that contains the well-studied

CAMK kinase Snf1, implying that these protein kinases have undergone relatively

recent evolutionary separation from a common ancestor, and may be part of the

broader CAMK group which includes a variety of subfamilies. To gain a better sense of
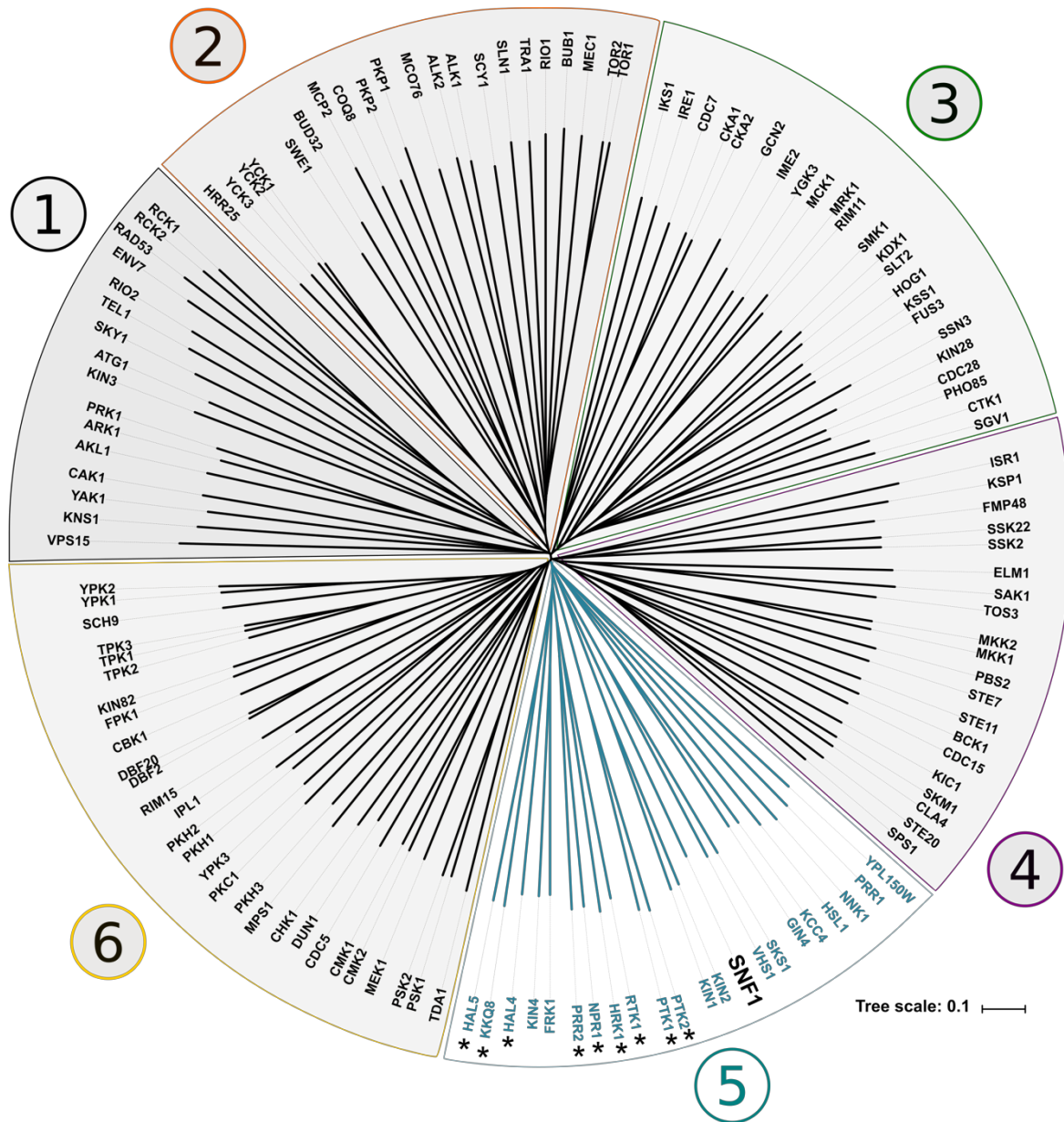
FIGURE 3.1 Protein kinases in yeast cluster into 6 major clades that share evolutionary conservation. A multiple sequence alignment of all 130 known protein kinases in yeast was performed using Clusal Omega and visualized as a scaled, unrooted phylogenetic tree using iTOL. The protein kinases cluster into 6 major clades, which have been arbitrarily numbered and color-coded for simplicity and ease of viewing across different figures. The 5th clade in teal contains Snf1. Kinases clustering with Snf1 include many kinases originally described as the NPR/HAL5 family, denoted by black asterisks (PTK1, PTK2, NPR1, PRR2, RTK1, HRK1, HAL5, KKQ8, and HAL4) GCN2 and CHK1, also originally described as NPR/HAL5 family members, are clustering with groups 3 and 6, respectively.

Figure 3.2 Kinases clustering with Snf1 are relatively understudied. A multiple sequence alignment of all 130 known protein kinases in yeast was performed using Clusal Omega and visualized as a scaled, rooted phylogenetic tree using iTOL. The protein kinases cluster into 6 major clades, which have been arbitrarily numbered and color-coded for simplicity and ease of viewing across different figures. A heat-map to the right of the phylogenetic tree conveys the number of publications annotated in SGD per kinase. Dots to the right of the heat map indicate the classical family assignment for each kinase.

how much research interest the 130 protein kinases in yeast, and each of the 6 kinase

clades, have garnered, I determined how many publications have mentioned each

kinase (as annotated in SGD as of April 29, 2019) (**Figure 3.2**). I found that the majority

of protein kinases appear understudied relative to a select few, namely Rad53 and Snf1

of the CAMK group and Cdc28 of the CMGC group, based on number of publications

annotated in the *Saccharomyces* Genome Database (SGD).

3.2.2 *Kinases clustering with Snf1 are orthologous to human AMPK/Snf1-related kinases*

Hunter and Plowman speculated in their 1997 review of protein kinases in yeast that

many of the unique kinases grouped into a category called "Other", such as the

NPR/HAL5 kinase family, would have homologs in other species. To identify related

kinases across evolution, I used SGD YeastMine to search and retrieve *S. cerevisiae*

data from SGD, specifically orthologs of the kinases clustering with Snf1 across

evolution (**Table 3.1**). Of the orthologs identified in this approach, 82% are either the

Snf1 homolog AMPK, or part of the CAMK subfamily CAMK-like kinases, including the

AMPK-related and Snf1-related kinases (**Figure 3.3**).

The AMPK/Snf1-related kinases in humans were first identified in the 2002 analysis

based on sequence homology with the AMPK catalytic domain (Manning *et al.*, 2002),

and have since been split into two subfamilies based on functional data: the AMPK-

related kinases (BRSKs, NUAKs, QIKs, SIKs, MARKs, and MELK) and the Snf1-related

Saccharomyces cerevisiae (budding yeast)	Caenorhabditis elegans (worm)		Drosophila melanogaster (fly)		Danio rerio (zebrafish)		Mus musculus (mouse)		Homo sapiens (human)	
PRR2	aak-2 (human PRKAA1, PRKAA2) (AMP-Activated Kinase) [WBGene00020142]	ortholog	Dmel/AMPKα (human PRKAA2, PRKAA1) [FBgn0023169]	ortholog	hunk (human HUNK) [ZDB-GENE-050309-240]	ortholog	Prkaa2 (human PRKAA2) [MGI:1336173]	ortholog	HUNK [30811]	ortholog
			Dmel/CG10177 (human STK33) [FBgn0039083]	ortholog	prkaa2 (human PRKAA2) [ZDB-GENE-081120-5]	ortholog	Hunk (human HUNK) [MGI:1347352]	ortholog	PRKAA2 [5563]	ortholog
NPR1	aak-2 (human PRKAA1, PRKAA2) (AMP-Activated Kinase) [WBGene00020142]	ortholog	Dmel/AMPKα (human PRKAA2, PRKAA1) [FBgn0023169]	ortholog	hunk (human HUNK) [ZDB-GENE-050309-240]	ortholog	Prkaa2 (human PRKAA2) [MGI:1336173]	ortholog	HUNK [30811]	ortholog
			Dmel/CG10177 (human STK33) [FBgn0039083]	ortholog	prkaa2 (human PRKAA2) [ZDB-GENE-081120-5]	ortholog	Hunk (human HUNK) [MGI:1347352]	ortholog		
HRK1	aak-2 (human PRKAA1, PRKAA2) (AMP-Activated Kinase) [WBGene00020142]	ortholog	Dmel/AMPKα (human PRKAA2, PRKAA1) [FBgn0023169]	ortholog	hunk (human HUNK) [ZDB-GENE-050309-240]	ortholog	Prkaa2 (human PRKAA2) [MGI:1336173]	ortholog	none	
			Dmel/CG10177 (human STK33) [FBgn0039083]	ortholog	prkaa2 (human PRKAA2) [ZDB-GENE-081120-5]	ortholog	Hunk (human HUNK) [MGI:1347352]	ortholog		
RTK1	aak-2 (human PRKAA1, PRKAA2) (AMP-Activated Kinase) [WBGene00020142]	ortholog	Dmel/AMPKα (human PRKAA2, PRKAA1) [FBgn0023169]	ortholog	hunk (human HUNK) [ZDB-GENE-050309-240]	ortholog	Prkaa2 (human PRKAA2) [MGI:1336173]	ortholog	HUNK [30811]	ortholog
			Dmel/CG10177 (human STK33) [FBgn0039083]	ortholog	prkaa2 (human PRKAA2) [ZDB-GENE-081120-5]	ortholog	Hunk (human HUNK) [MGI:1347352]	ortholog	PRKAA2 [5563]	ortholog
HAL4	aak-2 (human PRKAA1, PRKAA2) (AMP-Activated Kinase) [WBGene00020142]	ortholog	Dmel/AMPKα (human PRKAA2, PRKAA1) [FBgn0023169]	ortholog	hunk (human HUNK) [ZDB-GENE-050309-240]	ortholog	Prkaa2 (human PRKAA2) [MGI:1336173]	ortholog	HUNK [30811]	ortholog
			Dmel/CG10177 (human STK33) [FBgn0039083]	ortholog	prkaa2 (human PRKAA2) [ZDB-GENE-081120-5]	ortholog	Hunk (human HUNK) [MGI:1347352]	ortholog	PRKAA2 [5563]	ortholog
HAL5	aak-2 (human PRKAA1, PRKAA2) (AMP-Activated Kinase) [WBGene00020142]	ortholog	Dmel/AMPKα (human PRKAA2, PRKAA1) [FBgn0023169]	ortholog	hunk (human HUNK) [ZDB-GENE-050309-240]	ortholog	Prkaa2 (human PRKAA2) [MGI:1336173]	ortholog	HUNK [30811]	ortholog
			Dmel/CG10177 (human STK33) [FBgn0039083]	ortholog	prkaa2 (human PRKAA2) [ZDB-GENE-081120-5]	ortholog	Hunk (human HUNK) [MGI:1347352]	ortholog	PRKAA2 [5563]	ortholog
KKQ8	aak-2 (human PRKAA1, PRKAA2) (AMP-Activated Kinase) [WBGene00020142]	ortholog	Dmel/AMPKα (human PRKAA2, PRKAA1) [FBgn0023169]	ortholog	hunk (human HUNK) [ZDB-GENE-050309-240]	ortholog	Prkaa2 (human PRKAA2) [MGI:1336173]	ortholog	HUNK [30811]	ortholog
			Dmel/CG10177 (human STK33) [FBgn0039083]	ortholog	prkaa2 (human PRKAA2) [ZDB-GENE-081120-5]	ortholog	Hunk (human HUNK) [MGI:1347352]	ortholog	PRKAA2 [5563]	ortholog
PTK1	W02B12.12 (human TSSK6) [WBGene00012207],	ortholog	Dmel/CG9222 (human TSSK4) [FBgn0031784]	ortholog	tssk6 (human TSSK6) [ZDB-GENE-060216-3]	ortholog	Tssk1 (human TSSK1A) [MGI:1347557]	ortholog	TSSK2 [23617]	ortholog
	Y38H8A.4 (human TSSK1B, TSSK2, TSSK6) [WBGene00012638]	ortholog	Dmel/CG14305 (human TSSK1B) [FBgn0038630]	ortholog			Tssk2 (human TSSK2) [MGI:1347559]	ortholog	TSSK4 [283629]	ortholog
	tag-344 (human TSSK1B, TSSK2, TSSK6) [WBGene00015230]	ortholog					Tssk4 (human TSSK4) [MGI:1918349]	ortholog	TSSK3 [81629]	ortholog
	F23C8.8 [WBGene00017737]	ortholog					Tssk3 (human TSSK3) [MGI:1929914]	ortholog	TSSK1B [83942]	ortholog
	C27D6.11 (human TSSK1B, TSSK2, TSSK6) [WBGene00044388]	ortholog					Tssk6 (human TSSK6) [MGI:2148775]	ortholog	TSSK6 [83983]	ortholog
PTK2	W02B12.12 (human TSSK6) [WBGene00012207],	ortholog	Dmel/CG9222 (human TSSK4) [FBgn0031784]	ortholog	tssk6 (human TSSK6) [ZDB-GENE-060216-3]	ortholog	Tssk1 (human TSSK1A) [MGI:1347557]	ortholog	TSSK2 [23617]	ortholog
	Y38H8A.4 (human TSSK1B, TSSK2, TSSK6) [WBGene00012638]	ortholog	Dmel/CG14305 (human TSSK1B) [FBgn0038630]	ortholog			Tssk2 (human TSSK2) [MGI:1347559]	ortholog	TSSK4 [283629]	ortholog
	tag-344 (human TSSK1B, TSSK2, TSSK6) [WBGene00015230]	ortholog					Tssk4 (human TSSK4) [MGI:1918349]	ortholog	TSSK3 [81629]	ortholog
	F23C8.8 [WBGene00017737]	ortholog					Tssk3 (human TSSK3) [MGI:1929914]	ortholog	TSSK1B [83942]	ortholog
	C27D6.11 (human TSSK1B, TSSK2, TSSK6) [WBGene00044388]	ortholog					Tssk6 (human TSSK6) [MGI:2148775]	ortholog	TSSK6 [83983]	ortholog

Table 3.1 Orthologs of yeast AMPK/Snf1-related kinase across evolution. SGD YeastMine was used to search and retrieve *S. cerevisiae* data, populated by SGD and powered by InterMine by using a gene list of 130 protein kinases in yeast to identify orthologs across evolution. For brevity, this table displays orthologs of the NPR/HAL5 subgroup of kinases. Red text = AMPK ortholog, blue text = Snf1-related ortholog, and orange text = AMPK-related ortholog.

Saccharomyces cerevisiae (budding yeast)	Caenorhabditis elegans (worm)		Drosophila melanogaster (fly)		Danio rerio (zebrafish)		Mus musculus (mouse)		Homo sapiens (human)	
VHS1	ZK524.4 (human SNRK) [WBGene00013994]	ortholog	Dmel/CG8485 (human SNRK) [FBgn0033915]	ortholog	snrkb (human SNRK) [ZDB-GENE-040426-1724]	ortholog	Snrk (human SNRK) [MGI:108104]	ortholog	SNRK [54861]	ortholog
					snrka (human SNRK) [ZDB-GENE-040718-84]	ortholog				
SKS1	ZK524.4 (human SNRK) [WBGene00013994]	ortholog	Dmel/CG8485 (human SNRK) [FBgn0033915]	ortholog	snrkb (human SNRK) [ZDB-GENE-040426-1724]	ortholog	Snrk (human SNRK) [MGI:108104]	ortholog	none	
					snrka (human SNRK) [ZDB-GENE-040718-84]	ortholog				
FRK1	W02B12.12 (human TSSK6) [WBGene00012207]	homolog	Dmel/CG9222 (human TSSK4) [FBgn0031784]	ortholog	tssk6 (human TSSK6) [ZDB-GENE-060216-3]	ortholog	Tssk2 (human Tssk2) [MGI:1347559]	homolog	none	
	Y38H8A.4 (human TSSK1B, TSSK2, TSSK6) [WBGene00012638]	homolog	Dmel/CG14305 (human TSSK1B) [FBgn0038630]	ortholog			Tssk4 (human Tssk4) [MGI:1918349]	homolog		
	tag-344 (human TSSK1B, TSSK2, TSSK6) [WBGene00015230]	homolog, least diverged ortholog, ortholog					Tssk5 (human Tssk5) [MGI:1920792]	homolog		
	F23C8.8 [WBGene00017737]	homolog					Tssk6 (human Tssk6) [MGI:2148775]	homolog		
	C27D6.11 (human TSSK1B, TSSK2, TSSK6)[WBGene00044388]	homolog								
KIN4	W02B12.12 (human TSSK6) [WBGene00012207]	homolog	Dmel/CG9222 (human TSSK4) [FBgn0031784]	ortholog	tssk6 (human TSSK6) [ZDB-GENE-060216-3]	ortholog	Tssk2 (human Tssk2) [MGI:1347559]	homolog	none	
	Y38H8A.4 (human TSSK1B, TSSK2, TSSK6) [WBGene00012638]	homolog	Dmel/CG14305 (human TSSK1B) [FBgn0038630]	ortholog			Tssk4 (human Tssk4) [MGI:1918349]	homolog		
	tag-344 (human TSSK1B, TSSK2, TSSK6) [WBGene00015230]	homolog					Tssk5 (human Tssk5) [MGI:1920792]	homolog		
	F23C8.8 [WBGene00017737]	homolog					Tssk6 (human Tssk6) [MGI:2148775]	homolog		
	C27D6.11 (human TSSK1B, TSSK2, TSSK6)[WBGene00044388]	homolog								
HSL1	kin-29 (human SIK1, SIK2) [WBGene00002210]	homolog	Dmel/Sik2 (human SIK2) [FBgn0025625]	homolog	mark2a (human MARK2) [ZDB-GENE-030131-4145]	homolog	Sik1 (human SIK1) [MGI:104754]	homolog	[102724428]	
	par-1 (human MARK1) [WBGene00003916]	homolog	Dmel/KP78b (human MARK1) [FBgn0026063]	homolog	mark3a (human MARK3) [ZDB-GENE-030131-6232]	homolog	Snrk (human SNRK) [MGI:108104]	homolog	SIK1 [150094]	homolog
	sad-1 (human BRSK1, BRSK2) [WBGene00004719]	homolog, least diverged ortholog	Dmel/KP78a (human MARK1) [FBgn0026064]	homolog	sik1 (human SIK1) [ZDB-GENE-030131-9446]	homolog	Mark3 (human MARK3) [MGI:1341865]	homolog	NIM1K [167359]	homolog
	F49C5.4 (human NIM1K) [WBGene00009867]	homolog	Dmel/CG4629 (human NIM1K) [FBgn0031299]	homolog	snrkb (human SNRK) [ZDB-GENE-040426-1724]	homolog	Mark4 (human MARK4) [MGI:1920955]	homolog	MARK2 [2011]	homolog
	ZK524.2 (human SNRK)[WBGene00013994]	homolog	Dmel/CG8485 (human SNRK) [FBgn0033915]	ortholog	snrka (human SNRK) [ZDB-GENE-040718-84]	homolog	Brsk2 (human BRSK2) [MGI:1923020]	homolog, ortholog	SIK3 [23387]	homolog
			Dmel/sff (human BRSK1) [FBgn0036544]	homolog, least diverged ortholog	mark4a (human MARK4) [ZDB-GENE-060531-156]	homolog	Nim1k (human NIM1K) [MGI:2442399]	homolog	MARK1 [4139]	homolog
			Dmel/par-1 (human MARK3) [FBgn0260934]	homolog	mark3b (human MARK3) [ZDB-GENE-060929-80]	homolog	Sik2 (human SIK2) [MGI:2445031]	homolog	MARK3 [4140]	homolog
			Dmel/Sik3 (human SIK3) [FBgn0262103]	homolog	sik2a (human SIK2) [ZDB-GENE-070705-451]	homolog	Sik3 (human SIK3) [MGI:2446296]	homolog	SNRK [54861]	homolog
					sik2b (human SIK2) [ZDB-GENE-071012-1]	homolog	Mark1 (human MARK1) [MGI:2664902]	homolog	MARK4 [57787]	homolog
					si:ch211-22d5.2 [ZDB-GENE-091204-283]	homolog	Brsk1 (human BRSK1) [MGI:2685946]	homolog, least diverged ortholog	BRSK1 [84446]	homolog, least diverged ortholog
					si:ch211-255p10.4 [ZDB-GENE-121214-354]	homolog, least diverged ortholog	Mark2 (human MARK2) [MGI:99638]	homolog	BRSK2 [9024]	homolog, ortholog
					si:dkey-31m14.7 [ZDB-GENE-121214-92]	homolog				
					nim1k (human NIM1k) [ZDB-GENE-130530-744]	homolog				
					si:dkey-16p21.7 [ZDB-GENE-131122-54]	homolog, ortholog				

Table 3.1 continued

Saccharomyces cerevisiae (budding yeast)	Caenorhabditis elegans (worm)		Drosophila melanogaster (fly)		Danio rerio (zebrafish)		Mus musculus (mouse)		Homo sapiens (human)	
GIN4	kin-29 (human SIK1, SIK2) [WBGene00002210]	homolog	Dmel/Sik2 (human SIK2) [FBgn0025625]	homolog	mark2a (human MARK2) [ZDB-GENE-030131-4145]	homolog	Sik1 (human SIK1) [MGI:104754]	homolog	none	
	par-1 (human MARK1) [WBGene00003916]	homolog	Dmel/KP78b (human MARK1) [FBgn0026063]	homolog	mark3a (human MARK3) [ZDB-GENE-030131-6232]	homolog	Snrk (human SNRK) [MGI:108104]	homolog, ortholog		
	sad-1 (human BRSK1, BRSK2) [WBGene00004719]	homolog	Dmel/KP78a (human MARK1) [FBgn0026064]	homolog	sik1 (human SIK1) [ZDB-GENE-030131-9446]	homolog	Mark3 (human MARK3) [MGI:1341865]	homolog		
	F49C5.4 (human NIM1K) [WBGene00009867]	homolog	Dmel/CG4629 (human NIM1K) [FBgn0031299]	homolog	snrkb (human SNRK) [ZDB-GENE-040426-1724]	homolog, least diverged ortholog	Mark4 (human MARK4) [MGI:1920955]	homolog		
	ZK524.2 (human SNRK)[WBGene00013994]	homolog, least diverged ortholog	Dmel/CG8485 (human SNRK) [FBgn0033915]	homolog, least diverged ortholog	snrka (human SNRK) [ZDB-GENE-040718-84]	homolog, ortholog	Brsk2 (human BRSK2) [MGI:1923020]	homolog		
			Dmel/sff (human BRSK1) [FBgn0036544]	homolog	mark4a (human MARK4) [ZDB-GENE-060531-156]	homolog	Nim1k (human NIM1K) [MGI:2442399]	homolog		
			Dmel/par-1 (human MARK3) [FBgn0260934]	homolog	mark3b (human MARK3) [ZDB-GENE-060929-80]	homolog	Sik2 (human SIK2) [MGI:2445031]	homolog		
			Dmel/Sik3 (human SIK3) [FBgn0262103]	homolog	sik2a (human SIK2) [ZDB-GENE-070705-451]	homolog	Sik3 (human SIK3) [MGI:2446296]	homolog		
					sik2b (human SIK2) [ZDB-GENE-071012-1]	homolog	Mark1 (human MARK1) [MGI:2664902]	homolog		
					si:ch211-22d5.2 [ZDB-GENE-091204-283]	homolog	Brsk1 (human BRSK1) [MGI:2685946]	homolog		
					si:ch211-255p10.4 [ZDB-GENE-121214-354]	homolog	Mark2 (human MARK2) [MGI:99638]	homolog		
					si:dkey-31m14.7 [ZDB-GENE-121214-92]	homolog				
					nim1k (human NIM1k) [ZDB-GENE-130530-744]	homolog				
					si:dkey-16p21.7 [ZDB-GENE-131122-54]	homolog				
KCC4	kin-29 (human SIK1, SIK2) [WBGene00002210]	homolog	Dmel/Sik2 (human SIK2) [FBgn0025625]	homolog	mark2a (human MARK2) [ZDB-GENE-030131-4145]	homolog	Sik1 (human SIK1) [MGI:104754]	homolog	[102724428]	homolog
	par-1 (human MARK1) [WBGene00003916]	homolog	Dmel/KP78b (human MARK1) [FBgn0026063]	homolog	mark3a (human MARK3) [ZDB-GENE-030131-6232]	homolog	Snrk (human SNRK) [MGI:108104]	homolog, ortholog	SIK1 [150094]	homolog
	sad-1 (human BRSK1, BRSK2) [WBGene00004719]	homolog	Dmel/KP78a (human MARK1) [FBgn0026064]	homolog	sik1 (human SIK1) [ZDB-GENE-030131-9446]	homolog	Mark3 (human MARK3) [MGI:1341865]	homolog	NIM1K [167359]	homolog
	F49C5.4 (human NIM1K) [WBGene00009867]	homolog	Dmel/CG4629 (human NIM1K) [FBgn0031299]	homolog	snrkb (human SNRK) [ZDB-GENE-040426-1724]	homolog, ortholog	Mark4 (human MARK4) [MGI:1920955]	homolog	MARK2 [2011]	homolog
	ZK524.2 (human SNRK)[WBGene00013994]	homolog, ortholog	Dmel/CG8485 (human SNRK) [FBgn0033915]	homolog, ortholog	snrka (human SNRK) [ZDB-GENE-040718-84]	homolog, ortholog	Brsk2 (human BRSK2) [MGI:1923020]	homolog	SIK3 [23387]	homolog
			Dmel/sff (human BRSK1) [FBgn0036544]	homolog	mark4a (human MARK4) [ZDB-GENE-060531-156]	homolog	Nim1k (human NIM1K) [MGI:2442399]	homolog	MARK1 [4139]	homolog
			Dmel/par-1 (human MARK3) [FBgn0260934]	homolog	mark3b (human MARK3) [ZDB-GENE-060929-80]	homolog	Sik2 (human SIK2) [MGI:2445031]	homolog	MARK3 [4140]	homolog
			Dmel/Sik3 (human SIK3) [FBgn0262103]	homolog	sik2a (human SIK2) [ZDB-GENE-070705-451]	homolog	Sik3 (human SIK3) [MGI:2446296]	homolog	SNRK [54861]	homolog, ortholog
					sik2b (human SIK2) [ZDB-GENE-071012-1]	homolog	Mark1 (human MARK1) [MGI:2664902]	homolog	MARK4 [57787]	homolog
					si:ch211-22d5.2 [ZDB-GENE-091204-283]	homolog	Brsk1 (human BRSK1) [MGI:2685946]	homolog	BRSK1 [84446]	homolog
					si:ch211-255p10.4 [ZDB-GENE-121214-354]	homolog	Mark2 (human MARK2) [MGI:99638]	homolog	BRSK2 [9024]	homolog
					si:dkey-31m14.7 [ZDB-GENE-121214-92]	homolog				
					nim1k (human NIM1k) [ZDB-GENE-130530-744]	homolog				
					si:dkey-16p21.7 [ZDB-GENE-131122-54]	homolog				

Table 3.1 continued

| Saccharomyces cerevisiae (budding yeast)	Caenorhabditis elegans (worm)		Drosophila melanogaster (fly)		Danio rerio (zebrafish)		Mus musculus (mouse)		Homo sapiens (human)	
SNF1	aak-2 (AMP-Activated Kinase) [WBGene00020142]	homolog, least diverged ortholog, ortholog	Dmel/AMPKα (human PRKAA2, PRKAA1) [FBgn0023169]	homolog, least diverged ortholog, ortholog	trib3 (human TRIB3) [ZDB-GENE-040426-2609]	homolog	Melk (human MELK) [MGI:106924]	homolog	TRIB1 [10221]	homolog
	nipi-3 (human TRIB1, TRIB2, TRIB3) [WBGene00010700]	homolog	Dmel/trbl (human TRIB2) [FBgn0028978]	homolog	hunk (human HUNK) [ZDB-GENE-050309-240]	homolog, ortholog	Prkaa2 (human PRKAA2) [MGI:1336173]	homolog, least diverged ortholog, ortholog	TRIB2 [28951]	homolog
	aak-1 (human PRKAA1, PRKAA2) (AMP-Activated Kinase)[WBGene00019801]	homolog, ortholog	Dmel/CG10177 (human STK33) [FBgn0039083]	ortholog	prkaa2 (human PRKAA2) [ZDB-GENE-081120-5]	ortholog, least diverged ortholog	Trib3 (human TRIB3) [MGI:1345675]	homolog	HUNK [30811]	homolog, orhtolog
					trib2 (human TRIB2) [ZDB-GENE-091207-3]	homolog	Hunk (human HUNK) [MGI:1347352]	homolog, ortholog	PRKAA1 [5562]	homolog, ortholog
					trib1 (human TRIB1)[ZDB-GENE-091207-4]	homolog	Stk40 (human STK40) [MGI:1921428]	homolog	PRKAA2 [5563]	homolog, least diverged ortholog, ortholog
					melk (human MELK) [ZDB-GENE-990603-5]	homolog	Trib2 (human TRIB2) [MGI:2145021]	homolog	TRIB3 [57761]	homolog
							Prkaa1 (human PRKAA1) [MGI:2145955]	homolog, ortholog	STK40 [83931]	homolog
							Trib1 (human TRIB1) [MGI:2443397]	homolog	MELK [9833]	homolog
PRR1	W02B12.12 (human TSSK6) [WBGene00012207]	ortholog	Dmel/CG9222 (human TSSK4) [FBgn0031784]	ortholog	tssk6 (human TSSK6) [ZDB-GENE-060216-3]	ortholog	Tssk4 (human Tssk4) [MGI:1918349]	ortholog	ULK3 [25989]	ortholog
	Y38H8A.4 (human TSSK1B, TSSK2, TSSK6) [WBGene00012638]	ortholog	Dmel/CG14305 (human TSSK1B) [FBgn0038630]	ortholog			Tssk5 (human Tssk5) [MGI:1920792]	ortholog	TSSK4 [283629]	ortholog
	tag-344 (human TSSK1B, TSSK2, TSSK6) [WBGene00015230]	ortholog					Tssk6 (human Tssk6) [MGI:2148775]	ortholog	TSSK6 [83983]	ortholog
	C27D6.11 (human TSSK1B, TSSK2, TSSK6)[WBGene00044388]	ortholog								
YPL150W	aak-2 (AMP-Activated Kinase) [WBGene00020142]	ortholog	Dmel/AMPKα (human PRKAA2, PRKAA1) [FBgn0023169]	ortholog	hunk (human HUNK) [ZDB-GENE-050309-240]	ortholog	Prkaa2 (human PRKAA2) [MGI:1336173]	ortholog	none	
			Dmel/CG10177 (human STK33) [FBgn0039083]	ortholog	prkaa2 (human PRKAA2) [ZDB-GENE-081120-5]	ortholog	Hunk (human HUNK) [MGI:1347352]	ortholog		
							Smok2a [MGI:1351487]	homolog, ortholog		
							1810024B03Rik [MGI:1925560]	homolog		
							4921509C19R [MGI:2685851]	homolog, ortholog		
							[MGI:3036233]	ortholog		
							Smok2b [MGI:3037705]	homolog, ortholog		
							4932414J04Rik [MGI:3605619]	ortholog		
							4932415M13Rik [MGI:3608328]	orhtolog		
							Smok3b [MGI:3615348]	homolog, ortholog		
							Gm10668 [MGI:3642587]	ortholog		
							Gm10662 [MGI:3642760]	ortholog		
							Gm7168 [MGI:3643198]	ortholog		
							[MGI:3643324]	ortholog		
							Gm4922 [MGI:3644318]	ortholog		
							Gm6176 [MGI:3644439]	ortholog		
							[MGI:3647238]	ortholog		
							Smok3c [MGI:3647925]	homolog, ortholog		
							[MGI:3648804]	ortholog		
							Gm5891 [MGI:3649014]	ortholog		
							Gm14151 [MGI:3651016]	ortholog		
							Smok3a [MGI:3693943]	homolog		
							Gm4567 [MGI:3809658]	homolog, ortholog		

Table 3.1 continued

Saccharomyces cerevisiae (budding yeast)	Caenorhabditis elegans (worm)		Drosophila melanogaster (fly)		Danio rerio (zebrafish)		Mus musculus (mouse)		Homo sapiens (human)	
KIN1	aak-2 (AMP-Activated Kinase) [WBGene00020142]	ortholog	Dmel/AMPKα (human PRKAA2, PRKAA1) [FBgn0023169]	ortholog	nuak1a (human NUAK1) [ZDB-GENE-041210-122]	homolog	Prkaa2 (human PRKAA2) [MGI:1336173]	ortholog	none	
			Dmel/CG10177 (human STK33) [FBgn0039083]	ortholog	nuak2 (human NUAK2) [ZDB-GENE-050208-563]	homolog	Hunk (human HUNK) [MGI:1347352]	ortholog		
			Dmel/Nuak1 (human NUAK1) [FBgn0262617]	homolog	hunk (human HUNK) [ZDB-GENE-050309-240]	ortholog	Nuak2 (human NUAK2) [MGI:1921387]	homolog		
					prkaa2 (human PRKAA2) [ZDB-GENE-081120-5]	homolog	Nuak1 (human NUAK1) [MGI:1925226]	homolog		
					nuak1b (human NUAK1)[ZDB-GENE-131120-18]	homolog				
KIN2	aak-2 (AMP-Activated Kinase) [WBGene00020142]	ortholog	Dmel/AMPKα (human PRKAA2, PRKAA1) [FBgn0023169]	ortholog	nuak1a (human NUAK1) [ZDB-GENE-041210-122]	homolog	Prkaa2 (human PRKAA2) [MGI:1336173]	ortholog	none	
			Dmel/CG10177 (human STK33) [FBgn0039083]	ortholog	nuak2 (human NUAK2) [ZDB-GENE-050208-563]	homolog	Hunk (human HUNK) [MGI:1347352]	ortholog		
			Dmel/Nuak1 (human NUAK1) [FBgn0262617]	homolog	hunk (human HUNK) [ZDB-GENE-050309-240]	ortholog	Nuak2 (human NUAK2) [MGI:1921387]	homolog		
					prkaa2 (human PRKAA2) [ZDB-GENE-081120-5]	ortholog	Nuak1 (human NUAK1) [MGI:1925226]	homolog		

Table 3.1 continued
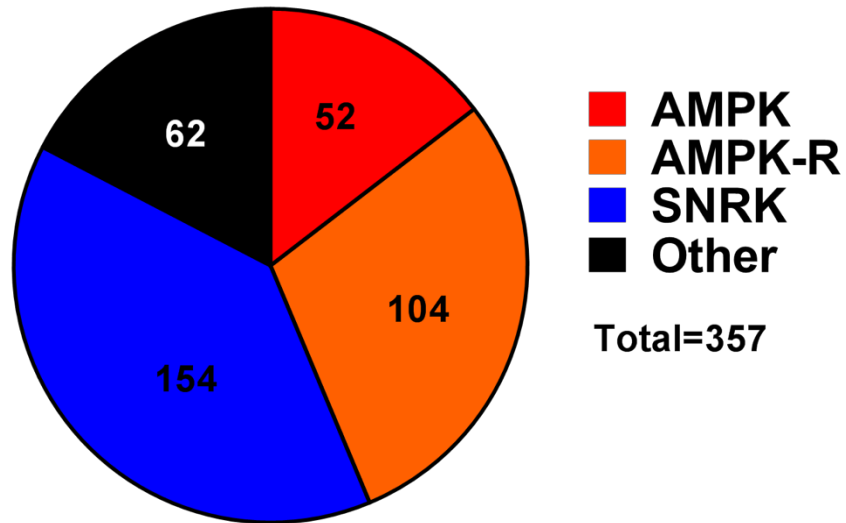
FIGURE 3.3 Kinases clustering with Snf1 are orthologous to human AMPK/Snf1-related kinases. Every identified ortholog for kinases clustering with Snf1 by multiple sequence alignment was tallied and identified as AMPK (red), AMPK-related (AMPK-R, orange), Snf1-related (SNRK, blue), or Other (black).

kinases (NIMs, SNRKs, TSSKs, SSTKs, and HUNK). While the AMPK-related kinases were identified through sequence homology with the protein kinase domain of AMPK, they differ from AMPK in protein architecture and regulation. These kinases, like AMPK, are activated by phosphorylation at a conserved threonine residue within the activation loop (Bright *et al.*, 2009). Broadly, they appear to participate in signaling cascades that respond to nutrient availability, and to regulate cell polarization in epithelial and neuronal cell types (Bright *et al.*, 2009). Importantly, appropriate regulation of membrane trafficking events underlies the diverse functions described for AMPK-related kinases.

The Snf1-related kinases have been grouped together due to their similarity to AMPK and AMPK-related kinases in sequence (Jaleel *et al.*, 2005), but are distinct from AMPK-related kinases due to the fact that they either do not require activation at the conserved threonine in the activation loop, or do not contain a conserved threonine in the activation loop (Bright *et al.*, 2009). While the function of AMPK is understood better than either AMPK-related or Snf1-related kinases, considerably less is known about the function of Snf1-related kinases compared to the AMPK-related subfamily.

3.2.3 Kinases clustering with Snf1 appear to subdivide into two distinct groups
A multiple sequence alignment of full protein sequences for kinases clustering with Snf1 by phylogenetic analysis reveals that this group is characterized by high conservation restricted to the catalytic domains, and divergent sequences outside of the catalytic
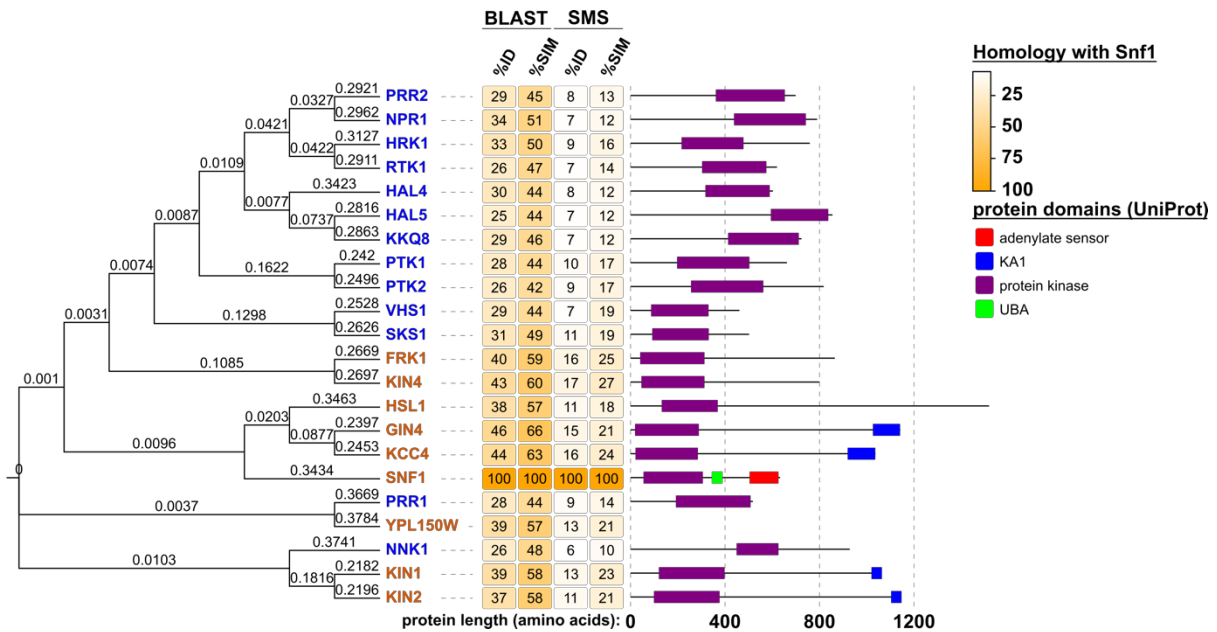
FIGURE 3.4 Kinases clustering with Snf1 are characterized by homology within the catalytic domains and divergent sequences outside of the catalytic domains. A multiple sequence alignment of the kinases that clustered with Snf1 yeast was performed using Clusal Omega and visualized as a scaled, rooted phylogenetic tree using EvolView. To the right of the phylogenetic tree, sequence homology for each kinase with Snf1 is displayed as a 4-column heat-map divided into two sections. In the first section labeled BLAST, percent identity (%ID) or percent similarity (%SIM) was calculated by aligning the two sequences using NCBI-BLAST. In the second section labeled SMS percent identity (%ID) or percent similarity (%SIM) was calculated by aligning the two sequences using Sequence Manipulation Suite (Stothard, 2000). Both programs were used due to having different methods for calculating homology. BLAST calculates homology based on only the aligned region, which in every case is restricted to mostly the catalytic domains. While SMS also aligns sequences, its calculation accounts for the entirety of the protein sequences, demonstrating lower sequence homology outside of the catalytic domains. To the right of the sequence homology heat-map are protein architecture maps for each kinase drawn to scale. These were automatically generated in EvolView from data available for each kinase in UniProt. YPL150W is not annotated in UniProt, and therefore does not have a protein architecture map. Kinases with a conserved threonine in the activation loop are colored in orange, and kinases without a conserved threonine in the activation loop are colored in blue (See **Table 3.2** and **Figure 3.5** for more information).

43

kinase name	kinase domain	ATP-coordinating Lysine	Catalytic Asapartate	Amino acid that aligns with Snf1 T210 (activation loop)	Amino acid that aligns with Snf1 I132 (gatekeeper residue)	non-catalytic domains
PRR2	361-653	K390	D484	G522	L440	unknown
NPR1	438-742	K467	D561	G599	M517	unknown
HRK1	215-722	K244	D340	G378	M296	unknown
RTK1	302-575	K330	D430	G468	M386	unknown
HAL4	316-590	K353	D449	G487	M403	unknown
HAL5	503-837	K546	D688	G726	M620	unknown
KKQ8	412-712	K455	D563	G601	M513	unknown
PRR1	192-508	K225	D354	A403	M307	unknown
NNK1	449-912	K478	D580	L738	T525	unknown
PTK1	196-503	K226	D329	G370	M282	unknown
PTK2	255-562	K285	D388	G429	M341	unknown
VHS1	12-237	K41	D185	V217	M138	unknown
SKS1	10-338	K39	D186	V218	M139	unknown
FRK1	41-313	K80	D175	T209	L129	unknown
KIN4	46-313	K80	D175	T209	L129	unknown
YPL150W	41-287	K70	D157	T190	L111	unknown
KIN1	120-398	K149	D269	T302	F223	KA1 (1015-1064)
KIN2	99-377	K128	D248	T281	F202	KA1 (1098-1147)
HSL1	81-369	K110	D239	T273	L193	KA1 (1379-1518)
SNF1	55-306	K84	D177	T210	I132	UBA (348-389), Adenylate Sensor (493-629)
GIN4	19-289	K48	D156	T189	L110	KA1 (1007-1142)
KCC4	21-285	K50	D152	T185	L106	KA1 (901-1037)

TABLE 3.2 Important features of kinases clustering with Snf1 Most kinase domain boundaries, ATP-coordinating lysine residues, and catalytic aspartate residues were annotated in UniProt. These features corresponding to YPL150W were annotated here for the first time using the multiple sequence alignment. Activation loops and gatekeeper residues were annotated for the first time here using the multiple sequence alignment. Accessory domains identified here were retrieved from UniProt and include KA1, UBA, and adenylate sensor domains.

FIGURE 3.5 MSA of activation Loops in kinases clustering with Snf1 A multiple sequence alignment, performed using Clustal Omega and visualized in JalView, of the activation loops (DFG…APE) in kinases clustering with Snf1 by phylogenetic analysis. The amino acid position aligning with T210, critical threonine of the Snf1 activation loop (McCartney *et al.*, 2016), is denoted by the black indicator.

```
              ▼
PTK1     281  VMELGLR-DLFAMIQKSG---WRSVALAEKF----CIFKQVACGVKFCH 321
PTK2     340  IMELGVK-DLFQLMERTG---WKNVPFNEKY----CLFKQVAQGIKFCH 380
VHS1     137  VMDYYPT-DLFTSIVDNR-------HFVTNGLLVKKVFLQICSALNYCH 177
SKS1     138  VMDYYDR-DLFTSIVDDK-------HFVNHGILIKKVFLQLCSALDHCH 178
NNK1     524  LTERINDGTLYDLVISWDEFKRSKIPFAERCRLTIFLSLQLLSALKYMH 572
HAL5     619  VMEFCASGDLYSLLTRNNI------SNE-SN----NGSSRLIQTVKEGS 656
PRR1     306  IMSYCPAGDLLAAVMARN---G-RLEAWLIQ----RIFTEVVLAVKYLH 346
RTK1     385  VMEYAPY-DFFNLVMS-N----LMTQDEVN----CYFKQLCHGVNYLH 422
HRK1     295  VMEYCPI-DFFAVVMT-G----KMSRGEIN----CCLKQLTEGVKYLH 332
PRR2     439  ILEYCEY-DLFSLVMS-E----KMHYEEIC----CLFKQLINGVKYLH 476
NPR1     516  VMEYCEY-DLFAIVMS-N----KMSYEEIC----CCFKQILTGVQYLH 553
KIN1     222  LFEYVSGGQLLDYIIQHG----SIREHQAR----KFARGIASALIYLH 261
KIN2     201  LFEYVSGGQLLDYIIQHG----SLKEHHAR----KFARGIASALQYLH 240
YPL150W  110  ALEYCPGKELYDHLLSLR-----RISLLECG----ELFAQISGAVYYAH 149
KKQ8     502  VMEFCPAGDLYGMLVGKSKLKG-RLHPLEAD----CFMKQLLHGVKF-- 553
FRK1     128  VLEYACGGEFYKYIQKKR-----RLKEMNAC----RLFSQLISGVHYIH 167
KIN4     128  VLEFVSGGEFYKYIQRKR-----RLKESSAC----RLFAQLISGVNYMH 167
SNF1     131  VIEY-AGNELFDYIVQRD-----KMSEQEAR----RFFQQIISAVEY-- 167
HAL4     402  VMEYCAGGDLFTLVVAAG-----KLEYMEAD----CFFKQLIRGVVYMH 441
HSL1     192  VLEYVDGGELFDYLVSKG-----KLPEREAI----HYFKQIVEGVSYCH 231
GIN4     109  VLEYAEKGELFNLLVERG-----PLPEHEAI----RFFRQIIIGVSYCH 148
KCC4     105  ILEYAEKGELFNLLVDHG-----PLPEREAI----NCFRQIIIGISYCH 144
```

FIGURE 3.6 MSA of ATP-binding pockets in kinases clustering with Snf1 A multiple sequence alignment of a portion of the ATP-binding pockets to identify the gatekeeper residues (denoted by black indicator) conserved with the Snf1 gatekeeper reside, I132 (Young *et al.*, 2012).

46

domains (**Figure 3.4**). Next, using a combination of information available on UniProt

and conservation with Snf1, I identified and annotated the kinase domain boundaries,

and conserved residues such as the catalytic aspartate, the ATP-coordinating lysine

residues, the gatekeeper residues which govern access to the ATP-binding pockets, as

well as the activation loops and the presence or absence of a conserved threonine

residue (**Table 3.2**, and **Figures 3.5** and **3.6**). I found that the kinases clustering with

Snf1 subdivide into roughly two groups, those with and those without a conserved

threonine residue in the activation loop (**Figure 3.4**). This analysis suggests that

kinases clustering with Snf1 may divide into two subfamilies, reminiscent of human

AMPK/Snf1-related kinases.

3.3 Discussion

While it is clear that these kinases clustering with Snf1 are orthologous to subfamilies

within the broader CAMK group, it is not immediately clear how to classify them. Like

the AMPK-related and Snf1-related subfamilies delineated in humans, I propose to

classify these protein kinases into two subfamilies based on three sets of criteria

including (i) domain architecture, (ii) classification of orthologous kinases across

evolution, and (iii) the presence of a conserved threonine residue within the activation

loop. I classify FRK1, KIN4, HSL1, GIN4, KCC4, YPL150W, KIN1, and KIN2 into one

subfamily called the yeast AMPK-related kinases (yAMPK-RKs). These kinases are

characterized by C-terminal kinase domains, conserved threonine residues within their

activation loops, and are orthologous with AMPK-related kinases across evolution (with

the exception of FRK1 and KIN4, which are orthologous with Snf1-related kinases). I

Yeast AMPK/Snf1-related kinases

Snf1
(AMPK)

yAMPK-RKs		ySnf1-RKs
	Frk1	Prr2
	Kin4	Npr1
	Hsl1	Hrk1
	Kcc4	Rtk1
	YPL150W	Hal4
	Kin1	Hal5
	Kin2	Kkq8
		Ptk1
		Ptk2
		Vhs1
		Sks1
		Prr1
		Nnk1
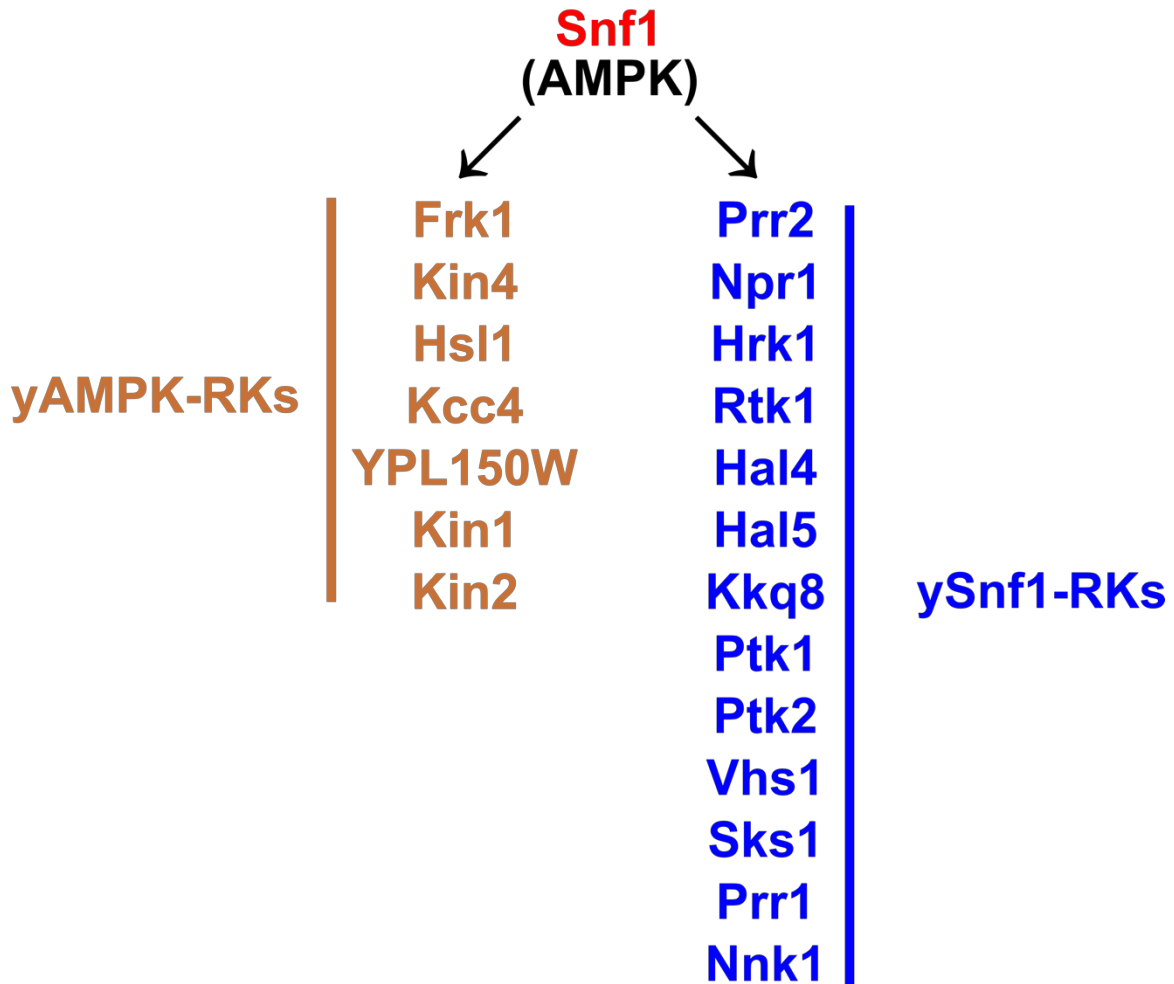
FIGURE 3.7 Kinases clustering with Snf1 are the yeast AMPK/Snf1-related kinases
A schematic depicting the division of the broader yeast AMPK/Snf1-related kinase family into yeast AMPK-related kinases (yAMPK-RKs) and yeast Snf1-related kinases (ySnf1-RKs) based on protein domain architecture, kinase orthologs across evolution, and activation loops.

classify PRR2, NPR1, HRK1, RTK1, HAL4, HAL5, KKQ8, PTK1, PTK2, VHS1, SKS1, PRR1, and NNK1 into a second subfamily called the yeast Snf1-related kinases (ySnf1-RKs). These kinases are characterized by mid-to-N-terminal kinase domains, they lack conserved threonine residues in the activation loop, and are orthologous with Snf1-related kinases across evolution. Together, these subfamilies comprise the broader AMPK/Snf1-related kinase family in yeast (**Figure 3.7**).

In this Chapter, I have demonstrated the evolutionary relationship between NPR/HAL5 kinases and Snf1/AMPK, which is significant because it lays the foundation to study a group of kinases in yeast that has been historically ignored due to lack of true human homologs. In the next Chapter, I will begin to examine the mechanism by which NPR/HAL5 kinases regulate nutrient transporter abundance, which is not currently known.

CHAPTER 4

Hal Kinases Inhibit Endocytosis of Nutrient Transporters

4.1 Introduction

Plasma-membrane protein abundance at steady-state results from a balance between protein synthesis and protein degradation, and a multitude of membrane trafficking pathways that bridge these processes including secretion, endocytosis, and recycling. Previous studies identified a role for Hal kinases in stabilizing a variety of APC-type superfamily nutrient transporters at the PM, however the mechanism remains unknown. Often, kinases impact nutrient transporter abundance by regulating transporter gene expression, and therefore protein synthesis. A limited number of nutrient-sensing kinases, such as Snf1 and Npr1, have been characterized in regulating transporter abundance through endocytic downregulation. The phenotypic similarities observed so far for Snf1, Npr1, and Hal kinases, and the evolutionary relationship demonstrated between these kinases in Chapter 3, have led me to hypothesize that Hal kinases regulate nutrient transporter abundance through negative regulation of membrane trafficking events.

In this chapter, I test this hypothesis and present evidence that dysregulation of endocytic trafficking appears to be the primary mechanism by which the steady state-abundance of nutrient transporters is altered in *hal* mutant cells, although this does not exclude a role for Hal kinases in the regulation of transporter transcription. This is

significant because it places Hal kinases as regulators of a specific membrane trafficking pathway for the first time.

4.2 Results

4.2.1 Hal4 and Hal5 regulate endocytosis but not endosomal recycling

To better understand the role of Hal kinases in plasma membrane protein stability, I first analyzed the subcellular location of various GFP-tagged integral membrane proteins that are normally stably localized at the PM in wildtype cells. I found that Mup1-GFP (high-affinity methionine transporter), Can1-GFP (arginine transporter) and Fur4-GFP (high-affinity uracil transporter) localized to the PM in wildtype cells but exclusively to the vacuole lumen in *Δhal4Δhal5* (or *hal*) mutant cells (**Figures 4.1A-B, 4.2A-B,** and **4.3A-B**), consistent with previous reports (Pérez-Valle *et al.*, 2007; Pérez-Valle *et al.*, 2010). Surprisingly, Pma1-GFP, an essential proton pump in yeast, also localized exclusively to the vacuole in *hal* mutant cells (**Figure 4.4A-B**). I next examined the localization of the peripheral plasma membrane protein Pil1 - a BAR domain protein and a core structural component of eisosomes (Karotki *et al.*, 2011; Olivera-Couto *et al.*, 2011). This analysis revealed no defects in Pil1-GFP localization or morphology in *hal* mutant cells (**Figure 4.5**). Consistent with previous studies double *hal* mutants, but not single mutants, also exhibit a growth defect (**Figure 4.6A-B**). However, the relationship between the observed instability of nutrient transporters and the growth defects exhibited by *hal* mutant cells remains unclear. This data, combined with previous studies, suggests that PM protein instability observed is limited to nutrient transporters,
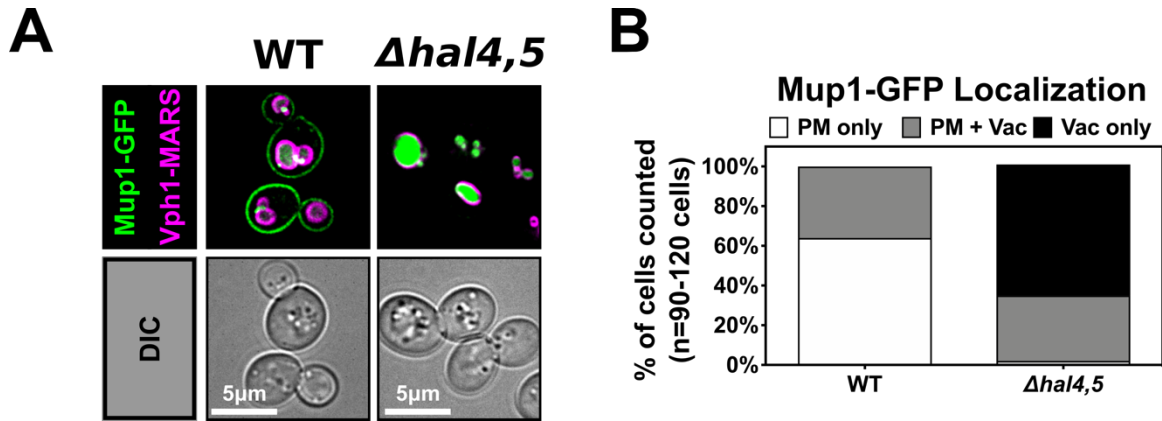
FIGURE 4.1 Mup1 aberrantly localizes to the vacuole in *hal* mutants (A)
Representative images of Mup1-GFP expressed from a centromeric plasmid under
native promoter control in the presence of endogenously-tagged Vph1-MARS, a marker
for the limiting membrane of the vacuole. WT and *Δhal4,5* mutant cells were imaged
after being cultured to mid-log phase in selective media. **(B)** Quantification of Mup1-
GFP localization in (A) performed by binning ells into localization categories as
indicated.
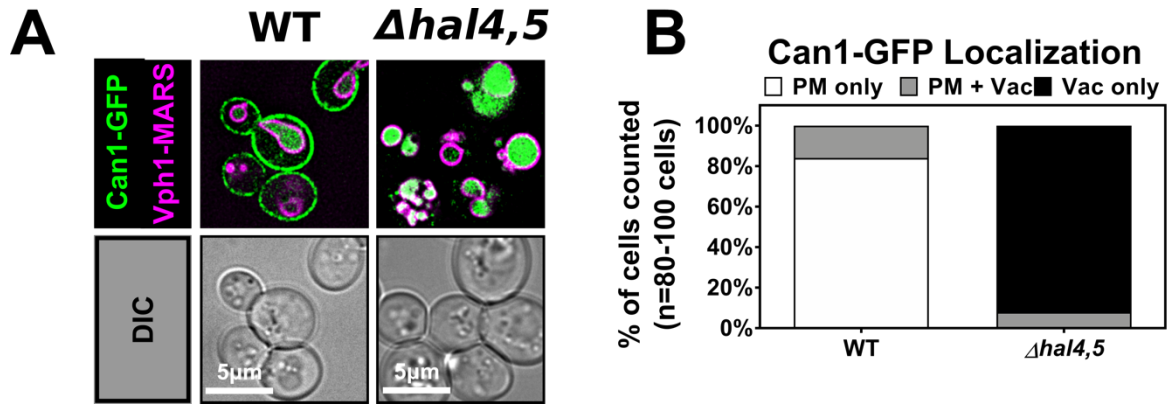
FIGURE 4.2 Can1 aberrantly localizes to the vacuole in *hal* mutants (A)
Representative images of Can1-GFP expressed from a centromeric plasmid under
native promoter control in the presence of endogenously-tagged Vph1-MARS, a marker
for the limiting membrane of the vacuole. WT and *Δhal4,5* mutant cells were imaged
after being cultured to mid-log phase in selective media. **(B)** Quantification of Can1-GFP
localization in (A) performed by binning ells into localization categories as indicated.

FIGURE 4.3 Fur4 aberrantly localizes to the vacuole in *hal* mutants (A) Representative images of Fur4-GFP expressed from a centromeric plasmid under native promoter control in the presence of endogenously-tagged Vph1-MARS, a marker for the limiting membrane of the vacuole. WT and *Δhal4,5* mutant cells were imaged after being cultured to mid-log phase in selective media. **(B)** Quantification of Fur4-GFP localization in (A) performed by binning ells into localization categories as indicated.

FIGURE 4.4 Pma1 aberrantly localizes to the vacuole in *hal* mutants (A)
Representative images of Pma1-GFP expressed from a centromeric plasmid under native promoter control in the presence of endogenously-tagged Vph1-MARS, a marker for the limiting membrane of the vacuole. WT and *Δhal4,5* mutant cells were imaged after being cultured to mid-log phase in selective media. **(B)** Quantification of Pma1-GFP localization in (A) performed by binning ells into localization categories as indicated.

FIGURE 4.5 Pil1 localizes to the PM in *hal* mutants Representative images of Pil1-GFP expressed from a centromeric plasmid under native promoter control in the presence of endogenously-tagged Vph1-MARS, a marker for the limiting membrane of the vacuole. WT and *Δhal4,5* mutant cells were imaged after being cultured to mid-log phase in selective media.

A SCD (complete media)

WT	
Δhal4	
Δhal5	
Δhal4,5	

cell number

B SCD (complete media)

◄ WT
◄ Δhal4
◄ Δhal5

◄ Δhal4,5

OD_{600nm} vs time (hours)

FIGURE 4.6 Disruption of *hal4* and *hal5* results in a growth defect (A)
Representative image of cells serially diluted on synthetic complete media and grown
for 3 days to assess growth of various *hal* mutants. **(B)** Growth of cells seeded at 0.05
OD from mid-log phase and monitored over time for OD_{600nm} in synthetic complete liquid
media.

although the nutrient transporters involve multiple nutrient classes, including amino acids, uracil, glucose, and ions.

Given the broad destabilization of integral PM proteins, I considered the possibility that *hal* mutants are defective for endosomal recycling. To test this, I analyzed the localization of Snc1-GFP, a v-SNARE which normally cycles between the PM and endosomes but exhibits aberrant endosomal localization in mutants defective for endosomal recycling (Rossi *et al.*, 1997; Lewis *et al.*, 2000; Robinson *et al.*, 2006). Importantly, I found that Snc1-GFP is not mislocalized upon loss of Hal4 and Hal5 kinases (**Figure 4.7**), suggesting that Hal kinases do not regulate endocytic recycling. To explore this further, I assayed endosome-to-PM lipid recycling by measuring efflux of a lipophilic tracer dye (FM 4-64) into the media (Vida and Emr, 1995; Galan *et al.*, 2001; Carroll *et al.*, 2012). I detected no difference in lipid recycling upon loss of Hal kinases compared to WT cells, in contrast to *Δrcy1* mutant cells which are known to exhibit lipid recycling defects (**Figure 4.8)** (Lewis *et al.*, 2000; Galan *et al.*, 2001). Additionally, I found that GFP-tagged carboxypeptidase S (CPS-GFP) (Spormann *et al.*, 1992; Katzmann *et al.*, 2001) exhibited normal vacuolar localization in *hal* mutant cells, indicating that Hal kinases are not required for the transport of proteases to the lumen of the vacuole (**Figure 4.9**). This analysis suggests *hal* mutant yeast cells exhibit broadly aberrant endocytic downregulation of multiple PM transporters while endosomal recycling and vacuolar transport are unaffected.
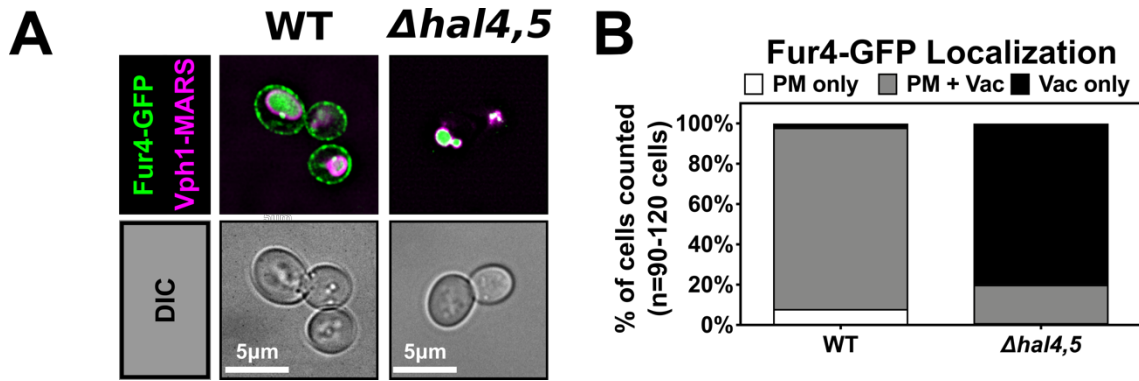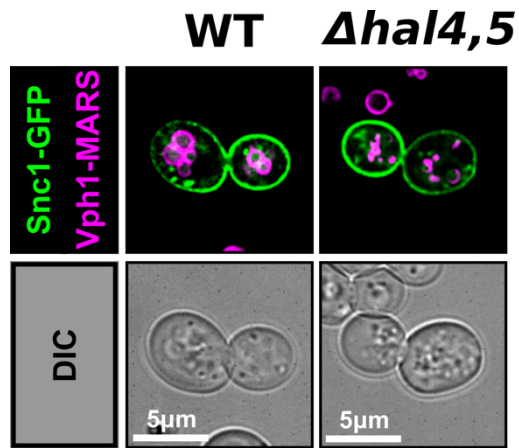
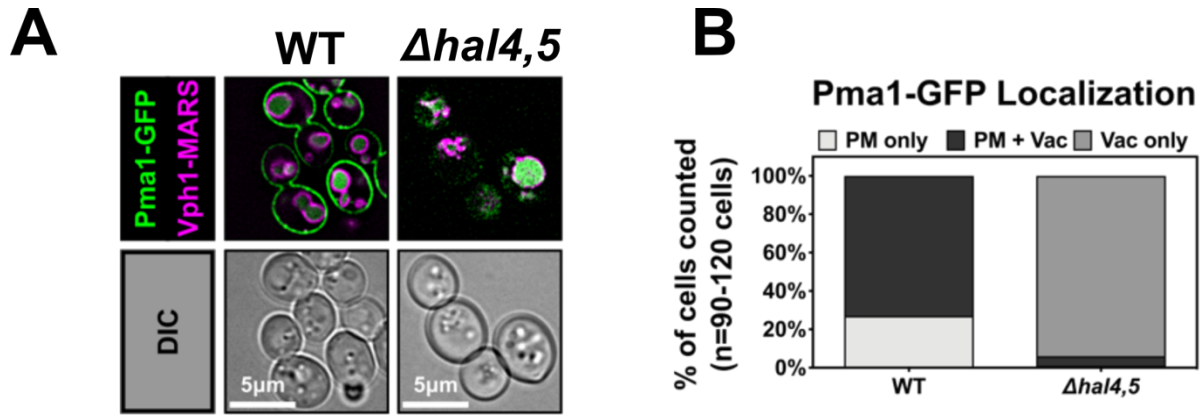**FIGURE 4.7 Snc1 localizes to the PM in *hal* mutants** Representative images of Snc1-GFP expressed from a centromeric plasmid under native promoter control in the presence of endogenously-tagged Vph1-MARS, a marker for the limiting membrane of the vacuole. WT and *Δhal4,5* mutant cells were imaged after being cultured to mid-log phase in selective media.

FM 4-64 Efflux
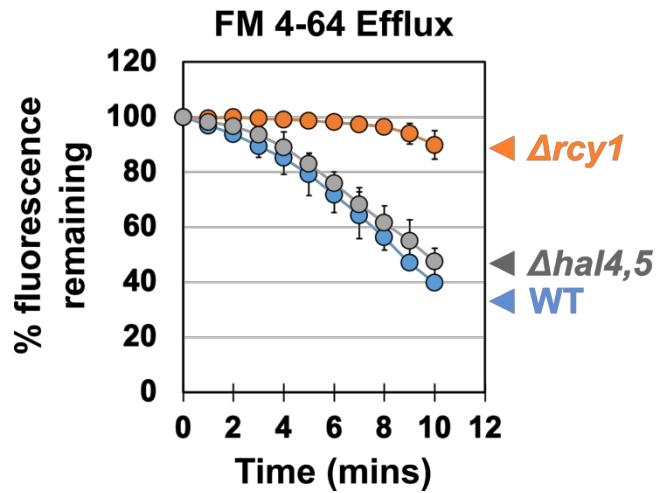
FIGURE 4.8 Lipid recycling is not affected in *hal* mutants Percentage of cell population positive for FM 4-64 fluorescence as measured by cells that fall within a defined PE gate as measured by flow cytometry (10,000 cells counted per condition per time point, n=3 biological replicates graphed as an average $\pm$ standard deviation) in WT, *Δhal4,5* or *Δrcy1* cells.

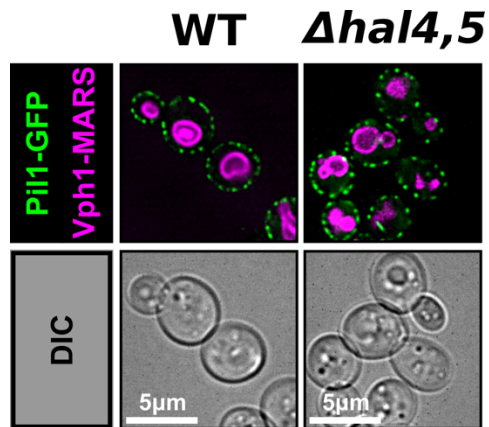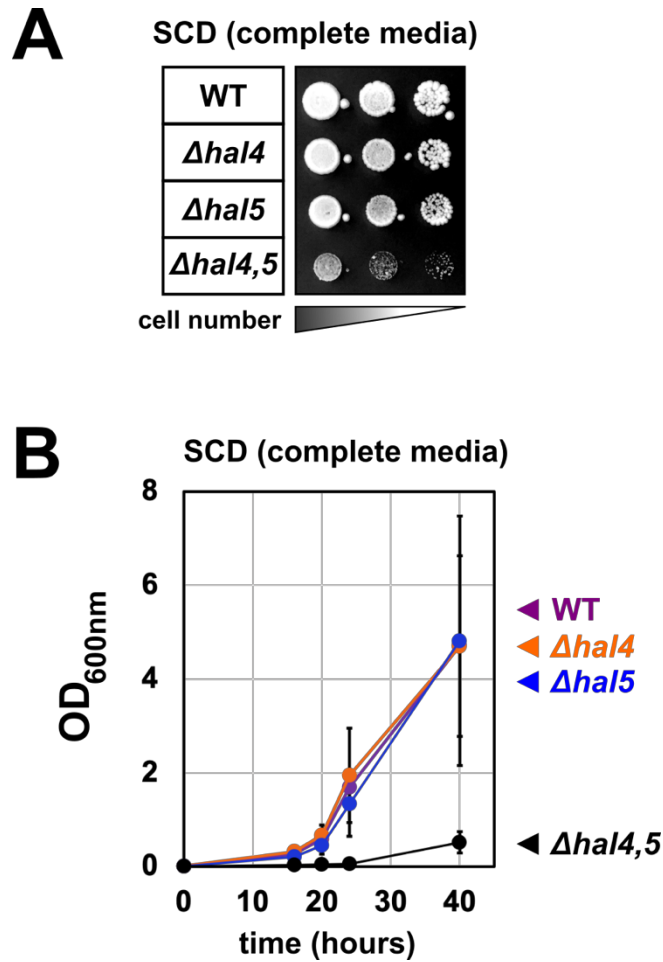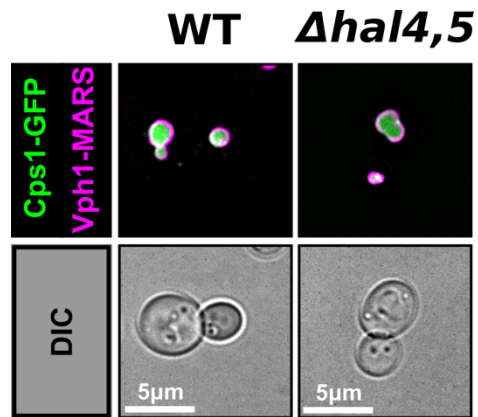**FIGURE 4.9 Cps1 localizes to the PM in *hal* mutants** Representative images of Cps1-GFP expressed from a centromeric plasmid under native promoter control in the presence of endogenously-tagged Vph1-MARS, a marker for the limiting membrane of the vacuole. WT and *Δhal4,5* mutant cells were imaged after being cultured to mid-log phase in selective media.

4.2.2 Hal4 and Hal5 exhibit partially redundant roles with respect to transporter

trafficking

Although the destabilization of PM transporters has been previously reported for *hal*

double mutant cells, the relative contributions of Hal4 and Hal5 to these phenotypes

have not been addressed. I hypothesized that Hal4 and Hal5 have redundant (or

partially-redundant) functions with respect to regulation of endocytosis. Alternatively, the

broad trafficking phenotypes observed might result from the sum of distinct cargo

specificities. To distinguish between these possibilities, I characterized endocytic

trafficking in *Δhal4* and *Δhal5* cells to determine if single mutants exhibited phenotypic

differences compared to *hal* double mutant cells. Importantly, I found that *Δhal4* and

Δhal5 single mutant cells both exhibited increased vacuolar localization of Mup1-GFP

relative to wildtype cells (**Figure 4.10A-B**). However, unlike *hal* double mutant cells

(**Figure 4.1A-B**), *Δhal4* and *Δhal5* single mutant cells both exhibited significant Mup1

PM localization (**Figure 4.10A-B**), suggesting partially redundant functions with respect

to Mup1 trafficking.

To more specifically characterize Mup1 signal at the PM, I measured fluorescence of

Mup1 tagged with pHluorin, a pH-sensitive GFP variant that quenches upon

encountering acidic intracellular compartments (Prosser *et al.*, 2010). Strikingly, I found

that *hal* double mutant cells exhibited no Mup1-pHluorin signal at steady state (**Figure**

4.10C), consistent with fluorescence microscopy analysis that revealed complete

vacuolar localization of Mup1 in these cells (**Figure 4.1A-B**). In contrast, *Δhal4* and

Δhal5 single mutant cells exhibited significant Mup1-pHluorin signal intensity at steady
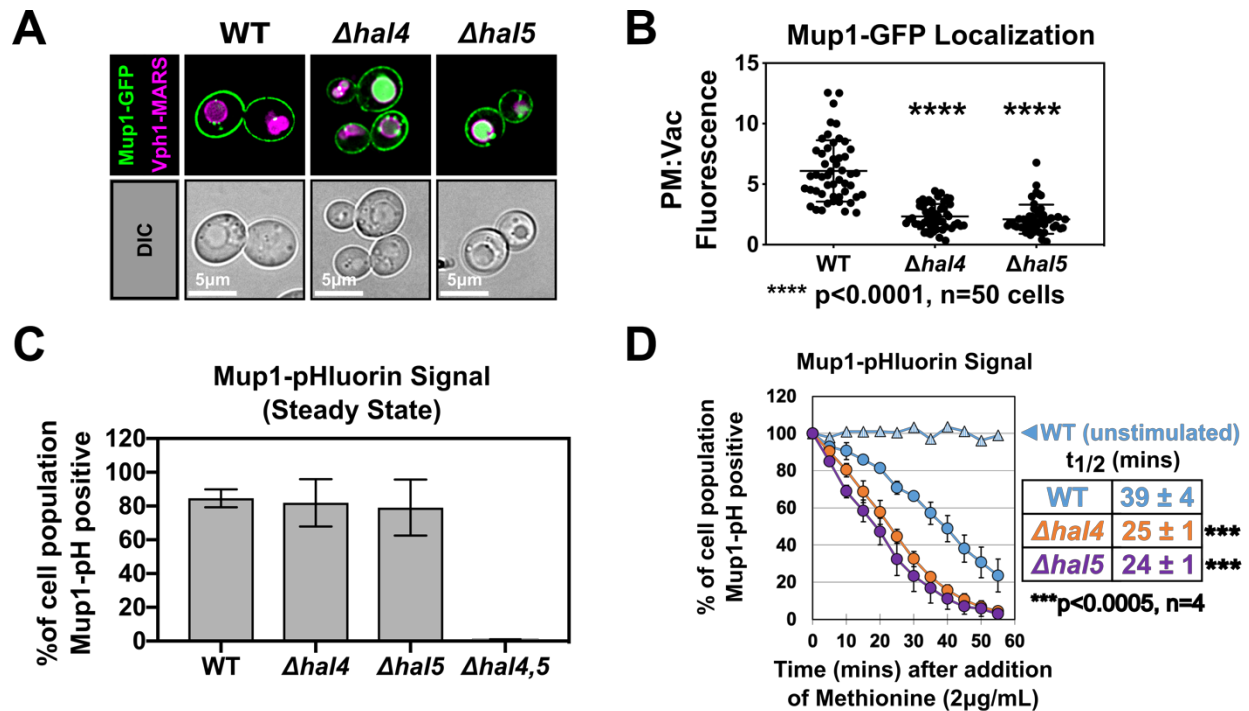
FIGURE 4.10 Hal4 and Hal5 are partially redundant with respect to Mup1 (A) Representative images of Mup1-GFP expressed from a centromeric plasmid under native promoter control in the presence of endogenously MARS tagged Vph1, a marker for the limiting membrane of the vacuole. WT, *Δhal4,* or *Δhal5* cells were cultured to mid-log phase in selective media. **(B)** Quantification of Mup1-GFP localization in (A) performed by measuring the ratio of Mup1-GFP signal at the PM compared to the vacuole (PM:VAC). PM:VAC ratio graphed as an average of 50 cells $\pm$ standard deviation. **(C)** Percentage of cell population expressing endogenously tagged Mup1-pHluorin as measured by cells that fall within a defined FITC gate by flow cytometry at steady state (10,000 cells counted per condition, n=4 biological replicates graphed as an average $\pm$ standard deviation). **(D)** Percentage of cell population expressing endogenously tagged Mup1-pHluorin as measured by cells that fall within a defined FITC gate by flow cytometry (10,000 cells counted per condition, n=4 biological replicates graphed as an average $\pm$ standard deviation) over time in the presence of excess methionine, an endocytic stimulant. Mup1-pH PM half-time ($t_{1/2}$) was estimated based on initial and final time points and elapsed time.

state (**Figure 4.10C**), consistent with fluorescence microscopy analysis revealing PM

localization of Mup1-GFP in these cells (**Figure 4.10A-B**). I speculated that *Δhal4* and

Δhal5 single mutant cells may exhibit increased endocytic trafficking of Mup1. To test

this, I measured the rate of internalization of Mup1-pHluorin from the plasma membrane

in response to methionine (Prosser *et al.*, 2016) and found that Mup1 internalizes faster

in *Δhal4* and *Δhal5* single mutant cells compared to wildtype cells (**Figure 4.10D**).

Taken together, these results indicate that both Hal4 and Hal5 contribute to the

regulation of Mup1 endocytic trafficking, and loss of either kinase results in increased

rate of Mup1 delivery to the vacuole.

To further explore the endocytic trafficking phenotypes of *Δhal4* and *Δhal5* single

mutant cells, I next examined localization of the arginine transporter Can1-GFP, which

localizes primarily to the PM in wildtype cells and exclusively to the vacuole in *hal*

double mutant cells (**Figure 4.2A-B**). Interestingly, Can1-GFP in *Δhal4* single mutant

cells exhibited an intermediate phenotype with a significant increase in vacuolar

localization, while distribution of Can1-GFP in *Δhal5* single mutant cells and wildtype

cells was not significantly different (**Figure 4.11A-B**). This data indicates that Hal4

contributes to the stabilization of Can1 at the plasma membrane, and Hal5 kinase

activity partially stabilizes Can1 at the PM in the absence of Hal4. In contrast to Can1-

GFP and Mup1-GFP, Fur4-GFP subcellular localization in *Δhal4* and *Δhal5* single

mutant cells was indistinguishable from wildtype cells (**Figure 4.12A-B**). Taken

together, these data suggest that Hal4 and Hal5 negatively regulate endocytic trafficking

64
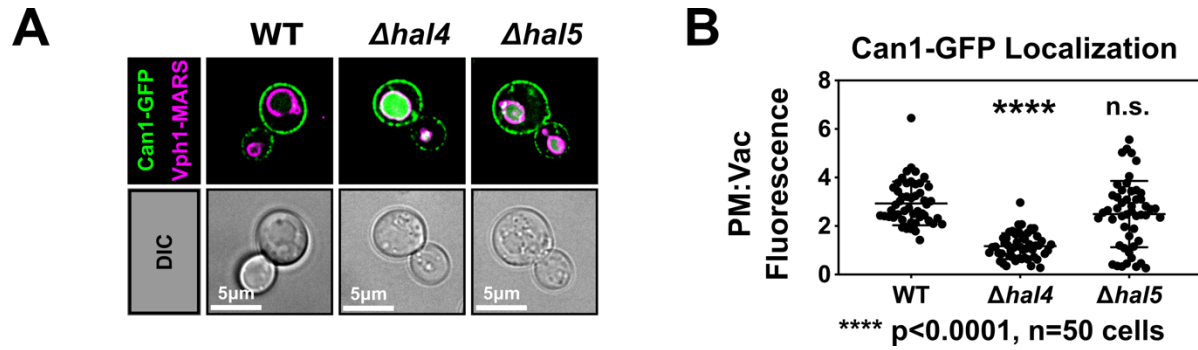
FIGURE 4.11 Hal4 and Hal5 are partially redundant with respect to Can1 (A) Representative images of Can1-GFP expressed from a centromeric plasmid under native promoter control in the presence of endogenously MARS tagged Vph1, a marker for the limiting membrane of the vacuole. WT, *Δhal4,* or *Δhal5* cells were cultured to mid-log phase in selective media. **(B)** Quantification of Can1-GFP localization in (A) performed by measuring the ratio of Can1-GFP signal at the PM compared to the vacuole (PM:VAC). PM:VAC ratio graphed as an average of 50 cells $\pm$ standard deviation.
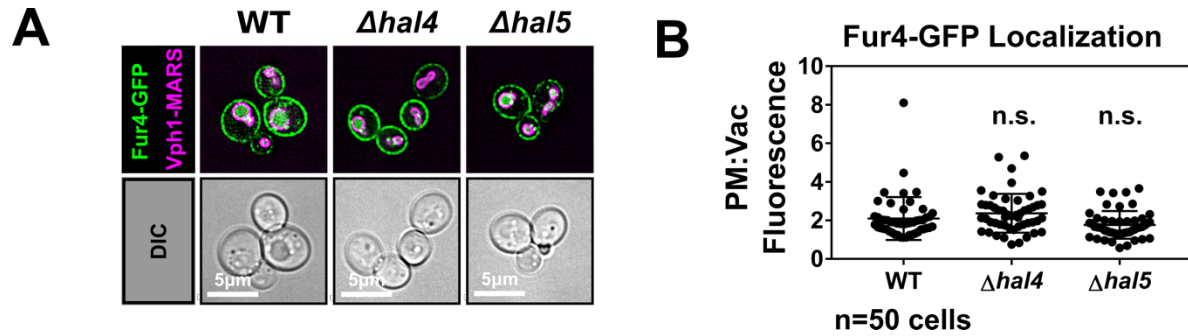
FIGURE 4.12 Hal4 and Hal5 exhibit fully redundant roles with respect to Fur4(A)
Representative images of Fur4-GFP expressed from a centromeric plasmid under
native promoter control in the presence of endogenously MARS tagged Vph1, a marker
for the limiting membrane of the vacuole. WT, *Δhal4,* or *Δhal5* cells were cultured to
mid-log phase in selective media. **(B)** Quantification of Fur4-GFP localization in (A)
performed by measuring the ratio of Fur4-GFP signal at the PM compared to the
vacuole (PM:VAC). PM:VAC ratio graphed as an average of 50 cells $\pm$ standard
deviation.
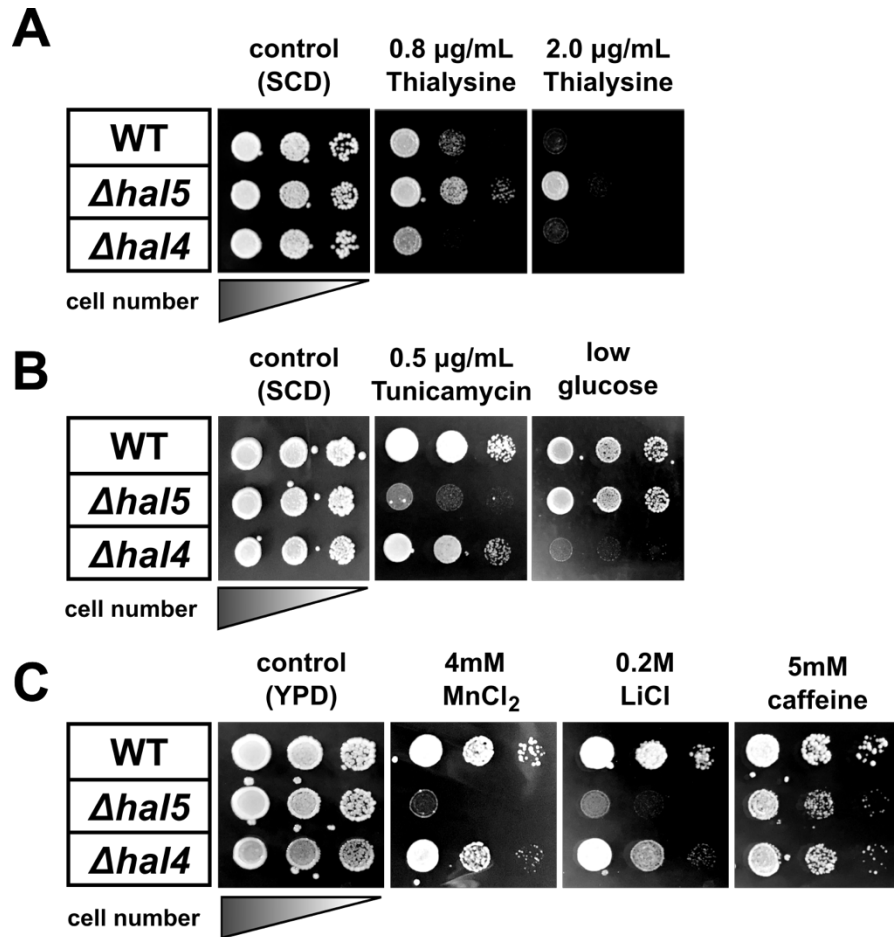
FIGURE 4.13 Hal4 and Hal5 exhibit distinct roles in some cellular contexts
Representative image of cells serially diluted onto indicated media and grown for 3
(YPD) or 5 (SCD) days to assess growth of Δ*hal4* and Δ*hal5* single mutants under **(A)**
thialysine stress, a toxic analog to lysine and indicator of trafficking fitness or **(B)**
Tunicamycin, an ER protein folding stress, or low glucose (0.2% glucose compared to
2% in control) and **(C)** manganese, lithium, or caffeine stresses.

and can function in a manner that is fully redundant (as for Fur4) or partially redundant (as for Mup1 and Can1).

Additionally, I found that *Δhal4* and *Δhal5* single mutant cells exhibited different sensitivities when exposed to a variety of stress conditions (**Figure 4.13A-C**). For example, *Δhal5* single mutant cells were resistant to thialysine (a toxic analog to lysine (Lin *et al.*, 2008)) while *Δhal4* single mutant cells were thialysine-sensitive (**Figure 4.13A**), which is indicative of a cargo-specific function with respect to lysine transport. Strikingly, *Δhal5* single mutant cells were sensitive to ER stress (tunicamycin), while *Δhal4* single mutant cells were sensitive to low glucose conditions (**Figure 4.13B**), suggesting distinct roles for Hal4 and Hal5 in different environmental conditions. Furthermore, *Δhal5* single mutant cells, but not *Δhal4* cells, exhibited sensitivity to metal ion ($MnCl_2$) and salt (LiCl) stresses (**Figure 4.13C**). Importantly, both *Δhal4* and *Δhal5* single mutant cells exhibited growth comparable to WT cells in the presence of caffeine or sodium dodecyl sulfate **(Figure 4.13C** and data not shown, Nathaniel Hepowit, PhD)**,** or DNA replication stress (methyl methanesulfonate) (data not shown, Nathaniel Hepowit, PhD). Overall, my data suggest that Hal4 and Hal5 exhibit partial or full redundancy with respect to endocytic trafficking phenotypes observed, arguing against a cargo-specific role in the regulation of endocytosis, although broader phenotypic characterization indicates that Hal4 and Hal5 may also have distinct functions in the cell.

4.2.3 Hal-mediated regulation of endocytosis requires both Art1-dependent and Art1-independent endocytosis

My results indicate that Hal kinases do not regulate endosome-to-PM recycling (**Figure 4.7** and **4.8**) and may instead function at the level of endocytic internalization from the PM (**Figure 4.10D**). To better define the precise trafficking step regulated by Hal kinases, I tested if endocytosis is required for aberrant accumulation of nutrient transporters in the vacuole. Methionine-induced endocytic downregulation of Mup1 requires Art1, an adaptor protein for the Rsp5 E3 ubiquitin ligase (Lin *et al.*, 2008). Importantly, I found that loss of Art1 stabilized Mup1 at the PM in the absence of Hal kinases (**Figure 4.14A-B**), indicating that Art1-mediated endocytosis is required for vacuolar trafficking in *hal* mutant cells. However, I also found that deletion of *ART1* did not restore the growth defect observed in *hal* mutant cells (**Figure 4.15**), suggesting that Art1-independent mechanisms of internalization may contribute to transporter instability.

Based on these results, I hypothesized that Art1-mediated internalization only accounts for aberrant vacuolar trafficking of a subset of Hal-regulated cargo. To test this, I analyzed trafficking of Fur4, an endocytic cargo known to be Art1-independent (Nikko and Pelham, 2009). I found that loss of Art1 does not restore Fur4-GFP to the PM (**Figure 4.16A-B**). In contrast, treatment with Latrunculin A (LatA), an actin polymerization inhibitor known to block endocytosis (Coué *et al.*, 1987; Kübler and Riezman, 1993; Engqvist-Goldstein and Drubin, 2003)), restored PM stability of both Fur4-GFP and Mup1-GFP in *hal* mutant cells (**Figure 4.15A-B** and **4.16A-B**). I extended my analysis to Pma1-GFP, a cargo not known to be subject to endocytic
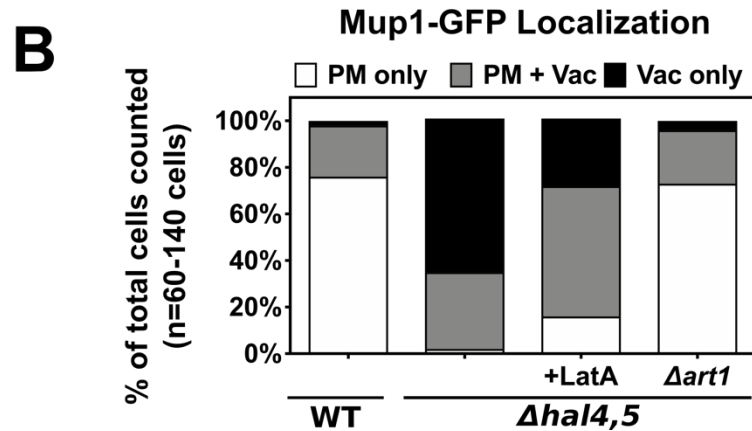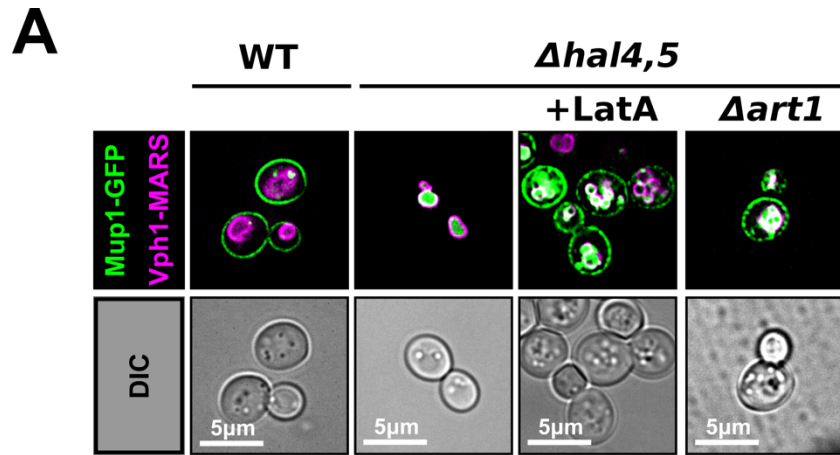
FIGURE 4.14 Hal4 and Hal5 regulate Art1-dependent endocytosis of Mup1 (A) Representative images of Mup1-GFP expressed from a centromeric plasmid under native promoter control in the presence of endogenously MARS tagged Vph1, a marker for the limiting membrane of the vacuole. WT *Δhal4Δhal5* cells, or *Δhal4Δhal5Δart1* cells were cultured to mid-log phase in selective media and treated with LatA for 1 hour were indicated. **(B)** Quantification of Mup1-GFP localization in (A) performed by binning cells into localization categories as indicated.
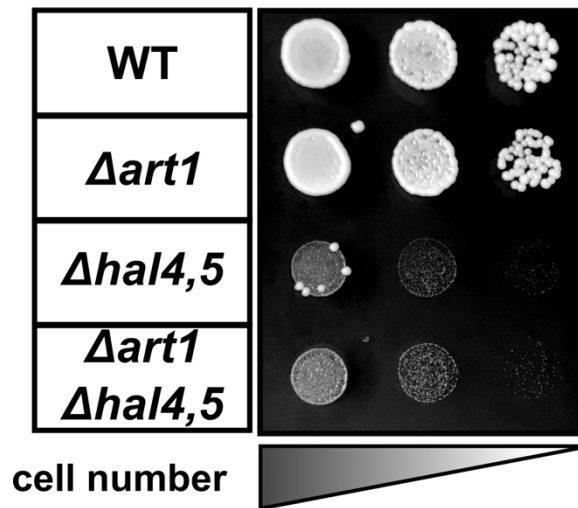
FIGURE 4.15 Deletion of *art1* does not restore growth in *hal* mutants
Representative image of cells serially diluted on synthetic complete media and grown for 3 days.
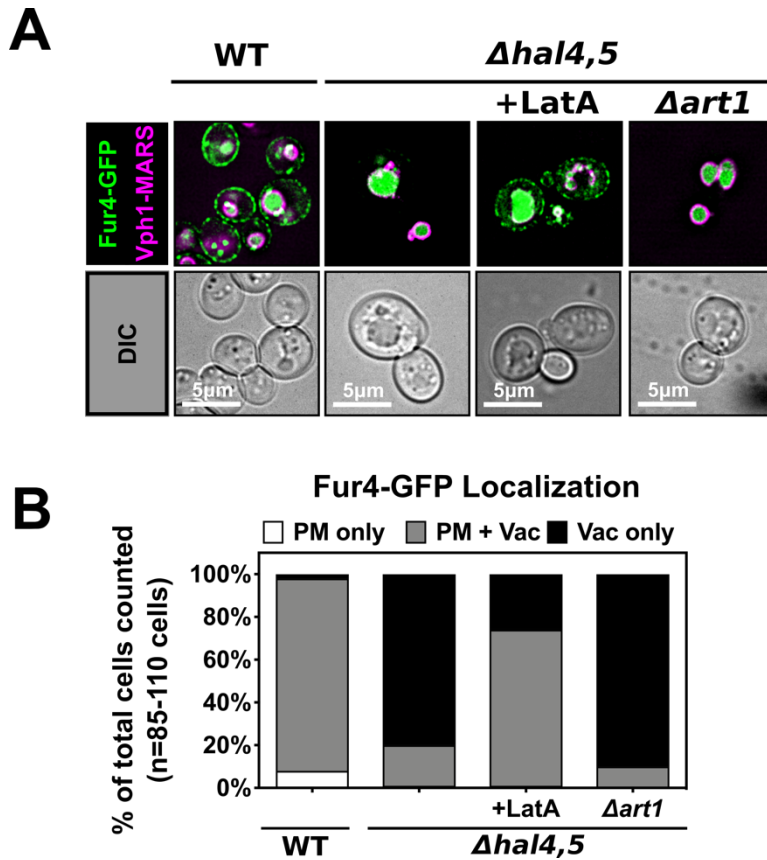
FIGURE 4.16 Hal4 and Hal5 regulate Art1-independent endocytosis of Fur4 (A)
Representative images of Fur1-GFP expressed from a centromeric plasmid under
native promoter control in the presence of endogenously MARS tagged Vph1, a marker
for the limiting membrane of the vacuole. WT *Δhal4Δhal5* cells, or *Δhal4Δhal5Δart1* cells
were cultured to mid-log phase in selective media and treated with LatA for 1 hour were
indicated. **(B)** Quantification of Fur4-GFP localization in (A) performed by binning cells
into localization categories as indicated.
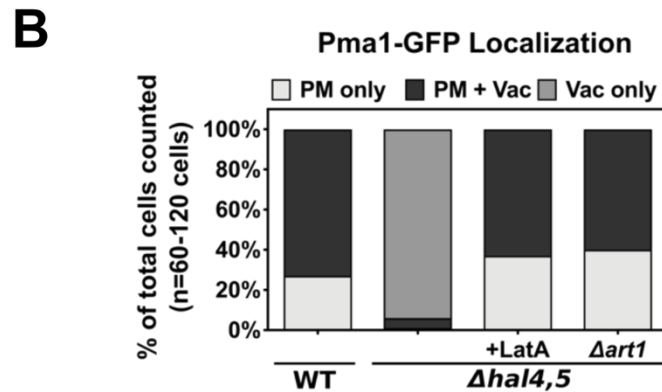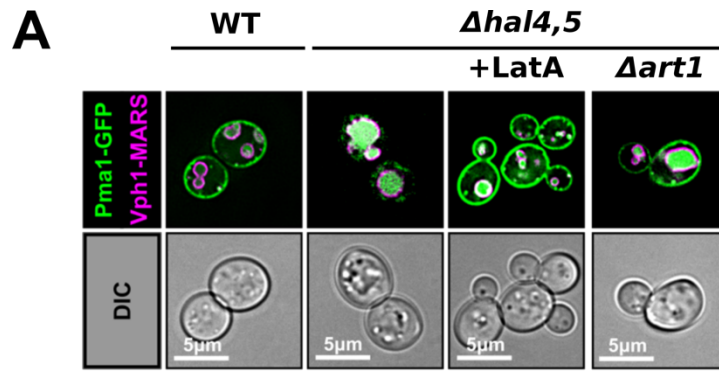
FIGURE 4.17 Hal4 and Hal5 regulate Art1-dependent endocytosis of Pma1 (A) Representative images of Fur1-GFP expressed from a centromeric plasmid under native promoter control in the presence of endogenously MARS tagged Vph1, a marker for the limiting membrane of the vacuole. WT *Δhal4Δhal5* cells, or *Δhal4Δhal5Δart1* cells were cultured to mid-log phase in selective media and treated with LatA for 1 hour were indicated. **(B)** Quantification of Fur4-GFP localization in (A) performed by binning cells into localization categories as indicated.

downregulation, and found that like Mup1-GFP, both loss of Art1 and treatment with LatA restored Pma1 signal to the PM (**Figure 4.17A-B**). These results indicate that Pma1 is subject to Art1-dependent internalization in the absence of Hal kinases.

4.3 Discussion

Combined with previous reports, these findings indicate that (i) loss of Hal4 and Hal5 kinases broadly affects the stability of integral PM transporters, extending beyond the APC-type superfamily to include the essential proton pump Pma1, (ii) Hal4 and Hal5 regulation of transporter stability is partially-redundant, and (iii) Hal kinases achieve this regulation by inhibiting endocytosis, reminiscent of related kinases Snf1 and Npr1. These findings are important because they contribute to the understanding of Hal kinase function with respect to maintenance of cellular homeostasis.

4.3.1 Hal4 and Hal5 are novel regulators of endocytosis

Hal-mediated regulation of endocytosis appears limited to integral membrane proteins that act as nutrient transporters (including carbon, ion, and nitrogen transport), since loss of Hal4 and Hal5 does not appear to affect the stability of peripheral membrane proteins, like structural components of eisosomes. One possibility is that Hal5 regulates endocytic downregulation through inhibition of Art1, perhaps by a mechanism similar to that reported for Npr1 (MacGurn *et al.*, 2011). In contrast to Npr1, which appears to promote endocytosis of some nutrient transporters, such as the tryptophan transporter Tat2 (Schmidt *et al.*, 1998), but inhibit endocytosis of other transporters such as Can1 (MacGurn *et al.*, 2011) and Gap1(Merhi and André, 2012), Hal kinases appear to exert

negative regulatory control over every nutrient transporter examined to-date, spanning

multiple nutrient classes and utilizing a variety of ART adaptor molecules. Consistent

with these findings, *art1* is clearly epistatic to *npr1* in the context of membrane trafficking

(MacGurn *et al.*, 2011), indicating that most *npr1* phenotypes can be attributed to Art1.

Although some *hal* mutant phenotypes can be attributed to Art1, as is the case for Mup1

and Pma1 instability, Art1 activity does not account for the growth defects observed in

Hal5. Thus, while many of the phenotypes associated with loss of Npr1 are attributable

to Art1 hyper-activation, this does not appear to be the case in the absence of Hal

kinases.

The role Hal kinases play in regulating the endocytosis of a diverse cargo could suggest

that they operate on an endocytic bypass mechanism that promotes endocytosis

independent of the normal regulatory control by the Art-Rsp5 network. An example of

such a mechanism involves the COS proteins, which were recently described to

promote endocytic downregulation of many nutrient transporters in stationary phase

(MacDonald *et al.*, 2015). However, one important feature of COS-mediated

endocytosis is that it occurs independently of the ARTs (MacDonald *et al.*, 2015). Thus,

since Hal-mediated endocytosis can be Art1-dependent, it is unlikely that Hal-mediated

endocytosis proceeds through induction of the COS pathway. Instead, the observation

that induced trafficking of some proteins, like Mup1 and Pma1, are Art1-dependent

suggests that loss of Hal kinases mimics changes in nutrient availability that typically

induce Art1-mediated endocytosis. Although the data presented here do not exclude the

possibility that Hal kinases regulate the function of Art1 and other ART adaptors, the

aberrant vacuolar trafficking of multiple transporters observed upon loss of Hal4 and

Hal5 requires both Art1-dependent and Art1-independent mechanisms, suggesting that

Hal regulation likely occurs upstream of the Art-RSP5 adaptor network, rather than via a

bypass mechanism.

4.3.2 Hal4 and Hal5 exhibit redundant and partially redundant functions

Although many previous studies reported phenotypes of *hal* double mutants,

phenotypes for *hal4* and *hal5* single mutants have not been previously reported. Here, I

present evidence that Hal4 and Hal5 kinases are not fully redundant, as previously

reported (Pérez-Valle *et al.*, 2007). While Hal kinases are fully redundant in the context

of growth, they are partially redundant in the regulation of nutrient transporters such as

Mup1 and Can1, which may indicate that Hal kinases operate in concert on different

pathways or distinct substrates, to regulate nutrient transporter stability. One possibility

is that Hal kinases operate together to form a kind of logic gate, whereby each kinase

operates independently and signals in a manner that is sufficient to maintain normal

growth and nutrient transporters at the cell surface. Consistent with the idea that Hal

kinases may not perform exactly the same cellular functions, *hal4* and *hal5* single

mutants appear to have distinct phenotypes, which suggests they may have separate

functions (**Figure 4.13A-C**).

4.3.3 A novel mechanism for regulation of Pma1 endocytic trafficking

Pma1, a P-type ATP-ase that pumps protons out of the cell and is essential for viability,

generates an electrochemical gradient that maintains cellular pH homeostasis and

drives nutrient transport across the PM. Most *pma1* trafficking mutants described in the literature either fail to export from the ER, and are degraded via the ERAD (ER-associated degradation) quality control pathway (Harris *et al.*, 1994; DeWitt *et al.*, 1998; Wang and Chang, 1999), or they export from the ER but fail to arrive at the PM and instead are trafficked to the vacuole (Chang and Fink, 1995; Luo and Chang, 2000). Once at the PM, Pma1 is thought to be tightly regulated and resistant to endocytosis due to its remarkable stability, with a half-life of approximately 11 hours (Benito *et al.*, 1991). The observed instability of Pma1 in *hal* mutant cells, though surprising, is consistent with the dysregulation of cytosolic pH and nutrient transport reported in previous studies (Pérez-Valle *et al.*, 2010).

At least one mutant *pma1* allele, called *pma1-10*, effectively targets to the PM but is hypo-phosphorylated and unstable (Gong and Chang, 2001), suggesting that phosphorylation stabilizes Pma1 at the cell surface. Interestingly, Ptk2, a ySnf1-RK related to Hal4 and Hal5, is observed to regulate Pma1 activity through direct phosphorylation in response to glucose (Eraso *et al.*, 2006), although it is not clear whether this regulates catalytic efficiency, trafficking, stability, or some combination. Consistent with these findings, Pma1 was recently observed to undergo endocytic downregulation, and replacement with Pma2, in response to heat stress (Zhao *et al.*, 2013). Additionally, loss of vacuolar proton pump activity in *vma* mutants results in aberrant endocytic trafficking of Pma1 (Velivela and Kane, 2018), suggesting that pH stress also triggers endocytic downregulation of Pma1. These findings suggest that, despite the fact that Pma1 is essential and stable at the cell surface, the cell has

mechanisms for downregulating Pma1 in response to environmental stresses. Art1 was observed to be dispensable for the endocytic downregulation of Pma1 in *vma* mutants, which was mediated exclusively by Art9 (Velivela and Kane, 2018). In contrast, instability of Pma1 in *hal* mutants can be attributed exclusively to Art1. Thus, it appears yeast cells have evolved multiple mechanisms for targeting the endocytic downregulation of Pma1, which is perhaps not surprising given that its abundance at the PM has been observed to be tightly regulated independently of transcription (Eraso *et al.*, 1987; Na *et al.*, 1995).

Deletion of *pma1* in yeast is inviable, thus one prediction is that *hal* mutants grow slowly due to the aberrant and accelerated endocytic downregulation of Pma1. If this were true, I expected restoration of Pma1 to the PM, as I see with the deletion of *art1* or treatment with LatA, to restore growth in *hal* mutant cells. However, *art1* fails to restore growth upon loss of both Hal kinases despite stabilizing Pma1 at the cell surface. Therefore, I think it is likely that the broad loss of nutrient transporters, rather than the specific loss of Pma1, contributes to the constitutively-starved state and slow growth phenotypes observed for *hal* mutant cells in previous studies (Mulet *et al.*, 1999; Pérez-Valle *et al.*, 2010).

The evidence presented in this chapter improves our understanding of Hal kinases and their individual contributions to the regulation of nutrient transporter endocytosis. Additionally, it places Hal kinases in a specific membrane trafficking pathway for the first time. Although the instability of nutrient transporters in *hal* mutants has been

appreciated for decades, it remains unknown if kinase activity contributes to this regulatory function, and Hal substrates remain to be identified. In Chapter 5, I explore the role of Hal5 catalytic activity in regulation of endocytosis and a candidate substrate, Art1.

CHAPTER 5

Hal5 Catalytic Activity is Critical for Regulation of Endocytosis

5.1 Introduction

Conventionally, protein kinases function enzymatically to phosphorylate protein targets and coordinate diverse biological outcomes. However, a growing body of evidence indicates that the functions of many active protein kinases extend beyond simply phosphorylation to include non-catalytic roles, such as allosteric regulation and scaffolding (Kung and Jura, 2016). For example, in response to intracellular ATP depletion, AMPK activates PPARα-dependent transcription to ultimately increase cellular ATP yields independently of its kinase activity through allosteric activation of PPARα (Bronner *et al.*, 2004). As presented in Chapter 4, *hal* mutants grow very slowly and exhibit aberrant accumulation of nutrient transporters in the vacuole. While the literature attributes these phenotypes to the absence of Hal kinase activity, an important limitation of all previous studies regarding Hal kinases is that the mutant phenotypes have never been complemented. Therefore, phenotypes may be caused indirectly, either by off-target effects of disrupting endogenous HAL genes, by compensation which is often observed for slow-growing mutants, or Hals may regulate nutrient transporter abundance independently of kinase activity. Some targets of Hal kinases have been hypothesized, such as the potassium transporters Trk1 and Trk2 (Casado *et al.*, 2010), and the transcription factor Gln3 (Hirasaki *et al.*, 2011), however; no substrates have been confirmed for either Hal4 or Hal5 kinase.

In Chapter 4, I determined that Hal kinases control nutrient transporter abundance at the cell surface through negative regulation of endocytosis. In this chapter, I present evidence that Hal5 catalytic activity is required for Hal-mediated regulation of endocytosis. Importantly, I find that endocytic downregulation of nutrient transporters is an acute effect of loss of Hal5 catalytic activity, rather than a chronic effect. I examine the possibility that Hal5 inhibits endocytosis by phosphorylating the Rsp5 adaptor protein Art1, as is the case for related kinase Npr1, but find no evidence to support this conclusion. Thus, despite the phenotypic similarities of Npr1 and Hal mutants, my studies indicate distinct mechanisms of action with respect to regulation of endocytosis. The evidence presented suggests that Hal5 undergoes auto-phosphorylation, the first evidence ever presented for a Hal substrate, but the physiological significance of these phosphorylation events remains unknown.

5.2 Results

5.2.1 Catalytic features of Hal5 are conserved with Snf1

To pinpoint catalytic and gatekeeper resides of Hal5, and gain other insights into possible structural features of the Hal5 kinase catalytic domain, I began by performing a pairwise alignment of Snf1 and Hal5, and then modeling Hal5 catalytic domain sequence onto a determined Snf1 X-Ray crystal structure (PDB 2FH9) (Nayak *et al.*, 2006) (**Figure 5.1A-B**). I found a conserved ATP-coordinating lysine reside at amino acid 546 (K546), a conserved bulky, hydrophobic amino acid within the ATP-binding pocket, called the gatekeeper residue, at amino acid 620 (M620), and a conserved

A

HAL5/503-855	**503** GKSIGVVGAGAYGVVKICARCKTAKDVLPYSTYSNGKKLFFAVKEL	**548**
SNF1/55-305	**55** YQIVKTLGEGSFGKVK----------LAYHT-TTGQKV--ALKII	**86**

HAL5/503-855	**549** KPKPGDQIDKFCTRLTSEFIIGHSLSHPHFEANAMIAGNVSRTTPP	**594**
SNF1/55-305	**87** NKK------------------------VLAKSDMQGRIEREISY	**106**

HAL5/503-855	**595** KHVFNAPNILKILDLMEYSNSFVEVMEFCASGDLYSLLTRNNISNE	**640**
SNF1/55-305	**107** LRLLRHPHIIKLYDVIKSKDEIIMVIEY-AGNELFDYIVQRDKMSE	**151**

HAL5/503-855	**641** SNNGSSRLIQTVKEGSGSPLHPLEADCFMKQLLNGVQYMHDHGIAH	**686**
SNF1/55-305	**152** Q---------------------EARRFFQQIISAVEYCHRHKIVH	**175**

HAL5/503-855	**687** CDLKPENILFQPNGLLKICDFGTSSVFQTAWEKHVHFQSGAMGSEP	**732**
SNF1/55-305	**176** RDLKPENLLLDEHLNVKIADFGLSNIMTDG----NFLKTSCGSPN	**216**

HAL5/503-855	**733** YVAPEEFIRDAEYDPRLVDCWSCGIVYCTMVMGQYLWKIAIPEKDS	**778**
SNF1/55-305	**217** YAAP-EVISGKLYAGPEVDVWSCGVILYVMLCRR-----LPFDDE	**255**

HAL5/503-855	**779** ----LFKSFLSEIKDDGQFYLFEELRHVSSELNRLRKIALYRTFQV	**820**
SNF1/55-305	**256** SIPVLFKNI-----SNGVYTLPKFLSPGAAGL-------IKRMLIV	**289**

HAL5/503-855	**821** DPTKRITIEQLLQSSWMRKTKCCVVYRHLHTKVSK*	**855**
SNF1/55-305	**290** NPLNRISIHEIMQDDW*------------------	**305**

B

FIGURE 5.1 Pairwise alignment of Hal5 and Snf1 (A) A pairwise sequence alignment, performed using EMBOSS (EMBL-EBI) and visualized using JalView, of the Hal5 and Snf1 catalytic domains to identify important conserved residues at Hal5 K546, M620, and D688 as well as lack of a conserved threonine in the activation loop at Snf1 T210. **(B)** The pairwise alignment of Snf1 and Hal5 catalytic domains was then used to model Hal5 (pink) onto Snf1(cyan) structure using MODELLER through the Chimera interface. In the panel at the top-right is a zoomed-in view of the conserved catalytic aspartate residues in the active sites. In the panel at the bottom-right is a zoomed-in view of the conserved ATP-coordinating lysine residues (in red) and the gatekeeper residues (in light blue) in the ATP-binding pockets.

catalytic aspartate at residue 688 (D688) (**Figure 5.1A**). Overall, the predicted Hal5

catalytic domain fold overlays with Snf1, with a few regions (some corresponding to

insertions) modeling as loops (**Figure 5.1B**). One loop appears to be conserved with the

Snf1 activation loop, but lacks a conserved threonine residue (**Figure 5.1A**).

5.2.2 Chronic loss of Hal5 catalytic activity destabilizes Hal5

To determine if Hal5 kinase activity is required to negatively regulate endocytosis, I

generated and characterized a variant of Hal5 mutated for a conserved aspartic acid

residue critical for the catalytic mechanism (*hal5-D688A*) (**Figure 5.1A**). While wildtype

Hal5 (untagged and containing a C-terminal 6XHis-Tev-3XFLAG tag) complemented the

aberrant trafficking of Mup1-GFP to the vacuole as well as increased rate of

endocytosis observed for Mup1-pHluorin, catalytic dead Hal5 failed to complement

these phenotypes (**Figures 5.2A-C** and **5.3A-B**). However, immunoblot analysis

revealed that the Hal5-D688A catalytic dead variant was not stably expressed (**Figure

5.3C**), suggesting that kinase activity may be required for Hal5 stability. To explore this

further, I analyzed a variant of Hal5 mutated at a conserved lysine in the ATP binding

pocket of the kinase domain (*hal5-K546R*) (**Figure 5.1A**) and found that this variant also

exhibited loss of protein stability (**Figure 5.3C**). These findings indicate that Hal5

catalytic dead mutants are unstable, limiting our ability to draw conclusions about Hal5

mechanism of action using catalytic dead variants.
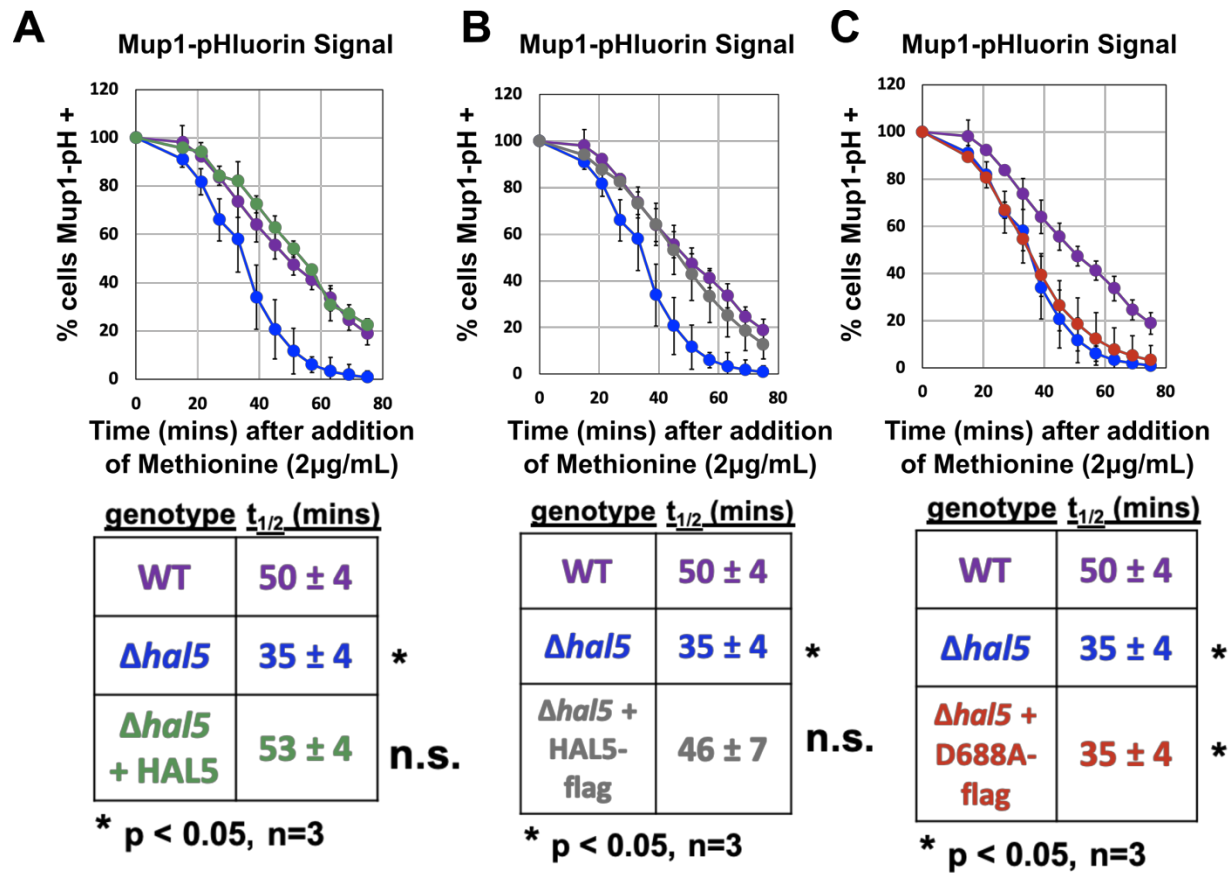
FIGURE 5.2 Hal5 catalytic activity is required for complementation $\Delta hal5$ mutant cells expressing endogenously-tagged Mup1-pHluorin and exogenously expressed **(A)** native Hal5 (HAL5), **(B)** C-terminally-tagged Hal5 (HAL5-HTF) or **(C)** C-terminally-tagged catalytic dead Hal5 (*hal5D688A-HTF*). Percentage of cell population expressing endogenously tagged Mup1-pHluorin as measured by cells that fall within a defined FITC gate by flow cytometry (10,000 cells counted per condition, n=3 biological replicates) over time in response to Methionine, an endocytic stimulant. Mup1-pH PM half-time ($t_{1/2}$) estimated based on initial and final time points and elapsed time**.**
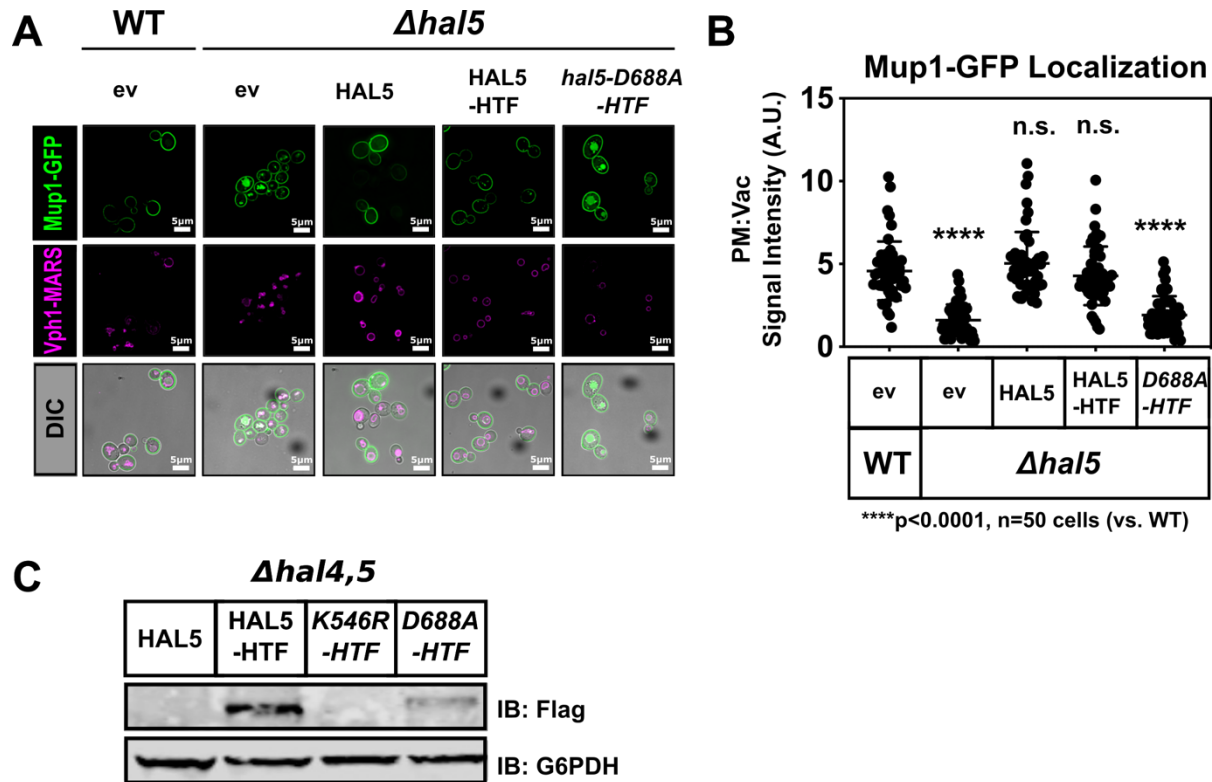
FIGURE 5.3 Hal5 catalytic point mutants are destabilized (A) Representative images of Mup1-GFP expressed from a centromeric plasmid in the presence of endogenously MARS tagged Vph1, a marker for the limiting membrane of the vacuole. HAL5 is exogenously expressed in the absence of endogenous Hal5 from a centromeric plasmid under native promoter control with either no tag (HAL5), a C-terminal 6xHIS-TEV-3xFLAG tag (HAL5-HTF), or a C-terminally-tagged catalytic dead variant (*hal5-D688A-HTF*). **(B)** Quantification of (A) by measuring the ratio of Mup1-GFP signal at the PM compared to the vacuole (PM:VAC). **(C)** Immunoblot analysis of C-terminally-tagged Hal5 variants described in (A) as well as an additional C-terminally-tagged catalytic dead variant (*hal5-K546R-HTF*).

5.2.3 Acute inhibition of Hal5 activity triggers rapid endocytic clearance of multiple cargo

To better understand the role of Hal5 catalytic activity in regulation of endocytic trafficking, I adapted a chemical-genetic strategy (Knight and Shokat, 2007) by developing an analog-sensitive allele of Hal5 (M620G, called *hal5AS*) through mutation of the conserved gatekeeper residue (M620) in the ATP binding pocket (based on the corresponding position of the kinase Snf1 (Shirra *et al.*, 2008)) (**Figure 5.1A**). Importantly, the *hal5AS* allele was functional and complemented the growth defect in *hal* mutant cells (**Figure 5.4A**) while addition of a PP1 analog (1-NA-PP1) induced a growth defect (**Figure 5.4B**). Thus, the *hal5AS* variant exhibits functional kinase activity that can be inhibited with 1-NA-PP1 and inhibition of Hal5 catalytic activity inhibits cell growth (in the absence of Hal4 kinase).

Using the *hal5AS* allele, I analyzed endocytic trafficking following acute inhibition of Hal5 kinase activity. Importantly, addition of 1-NA-PP1 induced Mup1-GFP trafficking to the vacuole in cells expressing *hal5AS* but not wildtype Hal5 (**Figure 5.5A**). Importantly, acute inhibition of Hal5AS by 1-NA-PP1 did not induce protein instability (following a 60-minute treatment) as observed with catalytic dead variants of Hal5 (**Figure 5.5B**), demonstrating that induction of vacuolar trafficking is not due to loss of Hal5 protein. To better characterize the kinetics of induced endocytosis following acute inhibition of Hal5 (in a *Δhal4* background), I analyzed Mup1-pHluorin trafficking and found that 1-NA-PP1 triggered loss of Mup1-pHluorin signal with a half-time of ~28 minutes (**Figure 5.5C**), which is faster than methionine-induced endocytosis measured in wildtype cells (**Figure 4.10D**). As expected, Art1 was required for endocytosis of fluorescently labeled Mup1
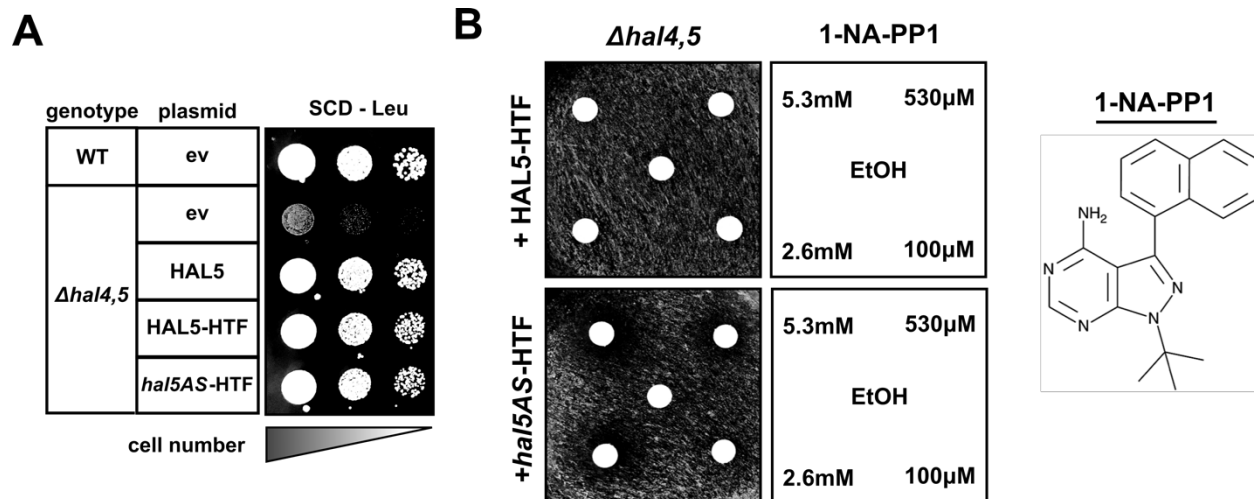
FIGURE 5.4 Hal5AS is functional and inhibited by 1-NA-PP1 (A) Cells were serially diluted onto synthetic selective media and grown for 3 days to assay functionality of *hal5AS* by growth. **(B)** Representative image of *Δhal4,5* mutant cells expressing either WT (HAL5-HTF) or analog-sensitive (*hal5AS-HTF*) Hal5 spread onto synthetic selective media as a lawn and treated with Whatman paper disks soaked in a solution of 1-NA-PP1 dissolved in vehicle (EtOH) at the indicated concentrations (grown for 3 days) to assess inhibition of *hal5AS* by 1-NA-PP1 (structure shown in right of panel).
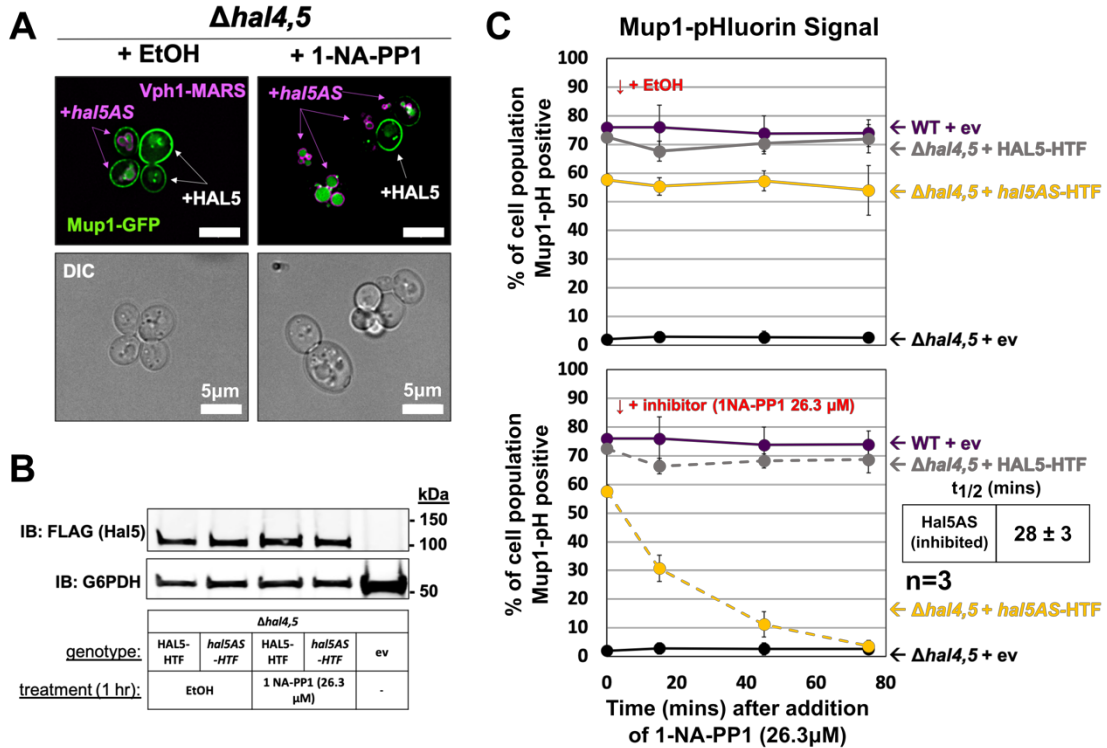
FIGURE 5.5 Hal5 catalytic activity is required for aberrant endocytic trafficking of Mup1 (A) Representative images of Mup1-GFP expressed from a centromeric plasmid in the presence of endogenously MARS tagged Vph1, a marker for the limiting membrane of the vacuole. HAL5 is exogenously expressed in the absence of endogenous Hal5 from a centromeric plasmid under native promoter control with either no tag (HAL5), a C-terminal 6xHIS-TEV-3xFLAG tag (HAL5-HTF), or a C-terminally-tagged catalytic dead variant (*hal5-D688A-HTF*). **(B)** Quantification of (A) by measuring the ratio of Mup1-GFP signal at the PM compared to the vacuole (PM:VAC). **(C)** Immunoblot analysis of C-terminally-tagged Hal5 variants described in (A) as well as an additional C-terminally-tagged catalytic dead variant (*hal5-K546R-HTF*).

variants (GFP and pHluorin) following acute inhibition of Hal5 (**Figure 5.6A-C**).

Importantly, acute inhibition of Hal5 triggered rapid endocytosis and vacuolar trafficking

of Fur4-GFP, a response which was inhibited by addition of LatA, but occurred

independently of Art1 (**Figure 5.7A-B**). Rapid sorting of cargo to the vacuole upon

inhibition of Hal kinase activity suggests that phosphatases antagonizing

phosphorylation on Hal-targets are acting very quickly in mutant cells. Previous studies

have shown that *ppz* phosphatase mutants exhibit endocytic trafficking defects (Lee *et*

al., 2019), leading me to hypothesize that Hal kinase activity is antagonized by Ppz

phosphatase activity. To test this hypothesis, I examined the genetic relationship of

PPZ1, PPZ2, and HAL5. I found that *hal5* is epistatic to *ppz1,2* (**Figure 5.8**)*,* suggesting

that Hal5 and Ppz phosphatases affect the same regulatory pathway. These results are

consistent with some overlap in Hal and Ppz targets in the cell.

5.2.4 Loss of Hal5 kinase activity produces no observable effect on Art1

My genetic evidence indicates that Hal kinases regulate both Art1-dependent and Art1-

independent endocytic events (**Figures 5.6A-C** and **5.7A-B**), suggesting that Hal

kinases operate upstream of the ART-Rsp5 network. However, given previous reports

that Art1 is tightly regulated by Npr1 (MacGurn *et al.*, 2011) - a kinase closely related to

Hal4 and Hal5 - I wanted to test the hypothesis that Hal kinases antagonize endocytosis

by inhibiting Art1 in a manner similar to Npr1. Unexpectedly, *hal* double mutant cells

(but not *Δhal4* or *Δhal5* single mutant cells) exhibited a slight but significant decrease in

Art1 abundance (**Figure 5.9**). To test if Hal kinases regulate Art1 phosphorylation, I
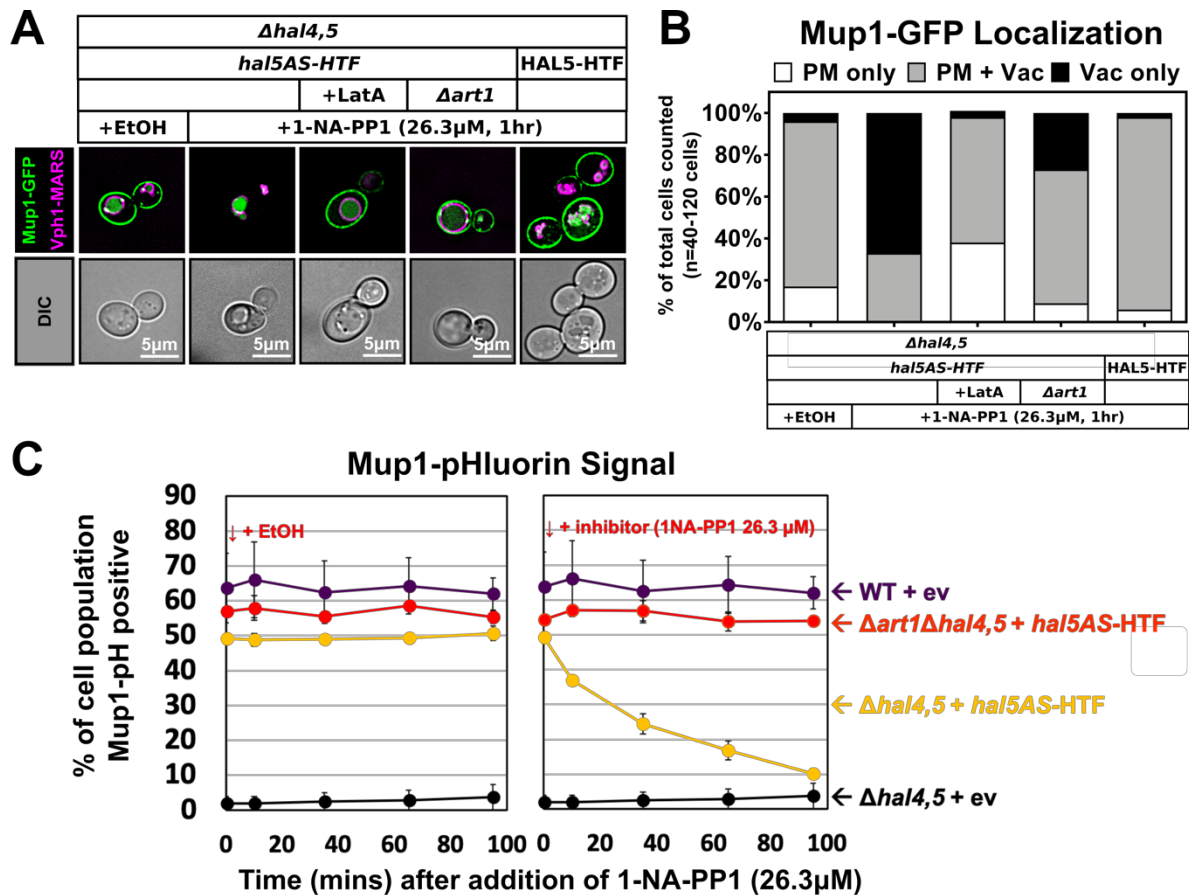
FIGURE 5.6 Acute inhibition of Hal5 activity triggers rapid endocytic clearance of Mup1 (A) Representative images of Mup1-GFP expressed from a centromeric plasmid in the presence of endogenously-tagged Vph1-MARS, a marker for the limiting membrane of the vacuole. WT or analog-sensitive HAL5 (HAL5-HTF or *hal5AS*-HTF) is exogenously expressed in *Δhal4,5* mutant cells from a centromeric plasmid under native promoter control. Cells were grown to mid-log phase in selective media and imaged after inhibitor treatment (1-NA-PP1) for 1 hour or further treated with LatA for 1 hour where indicated **(B)** Quantification of Mup1-GFP localization in (A) performed by binning cells into localization categories as indicated. **(C)** Percentage of cell population expressing endogenously tagged Mup1-pHlourin as measured by cells that fall within a defined FITC gate by flow cytometry at steady state (10,000 cells counted per condition, n=3 biological replicates) over time in the presence of *hal5AS* inhibitor 1-NA-PP1. WT or analog-sensitive HAL5 (HAL5-HTF or *hal5AS*-HTF) is exogenously expressed in *Δart1Δhal4,5* mutant cells from a centromeric plasmid under native promoter control. EV indicates empty vector.
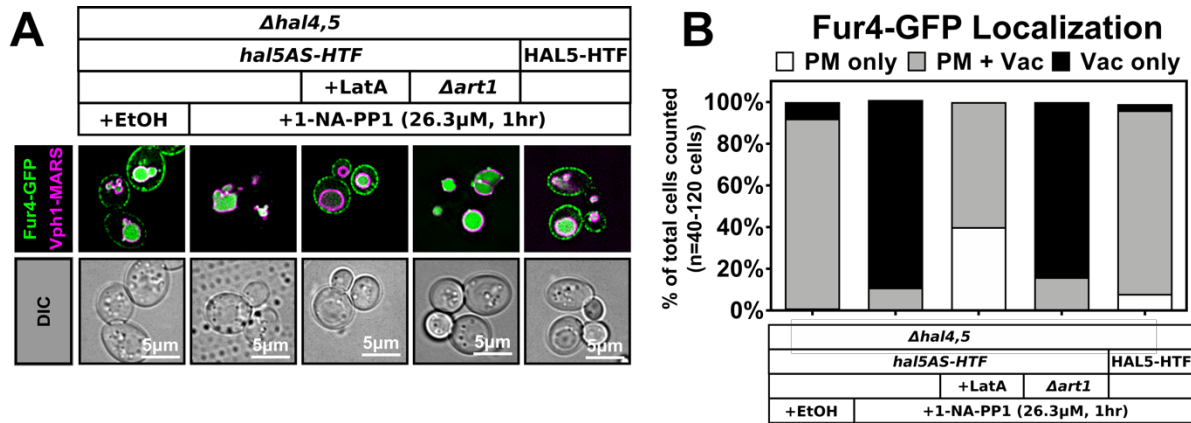
FIGURE 5.7 Acute inhibition of Hal5 activity triggers vacuolar localization of Fur4
(A) Representative images of Fur4-GFP expressed from a centromeric plasmid in the presence of endogenously-tagged Vph1-MARS, a marker for the limiting membrane of the vacuole. WT or analog-sensitive HAL5 (HAL5-HTF or *hal5AS*-HTF) is exogenously expressed in *Δhal4,5* mutant cells from a centromeric plasmid under native promoter control. Cells were grown to mid-log phase in selective media and imaged after inhibitor treatment (1-NA-PP1) for 1 hour or further treated with LatA for 1 hour where indicated **(B)** Quantification of Fur4-GFP localization in (A) performed by binning cells into localization categories as indicated.

	YPD:	control	5 mM Caffeine	4 mM MnCl$_2$	200 mM LiCl
WT					
Δppz1,2					
Δhal5					
Δhal5Δppz1					
Δhal5Δppz2					
Δhal5Δppz1,2					
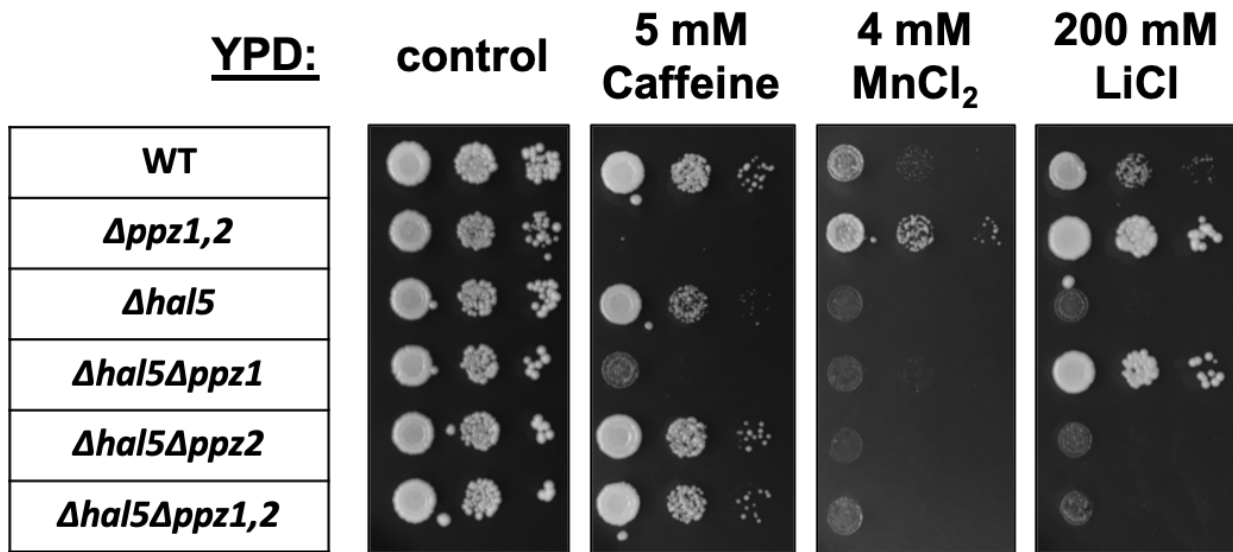
FIGURE 5.8 Hal5 and Ppz phosphatases genetically interact Representative images of cells serially diluted onto indicated media and grown for 3 days to assess growth of mutant combinations under caffeine stress as well as manganese and lithium ion stressors to assess growth.
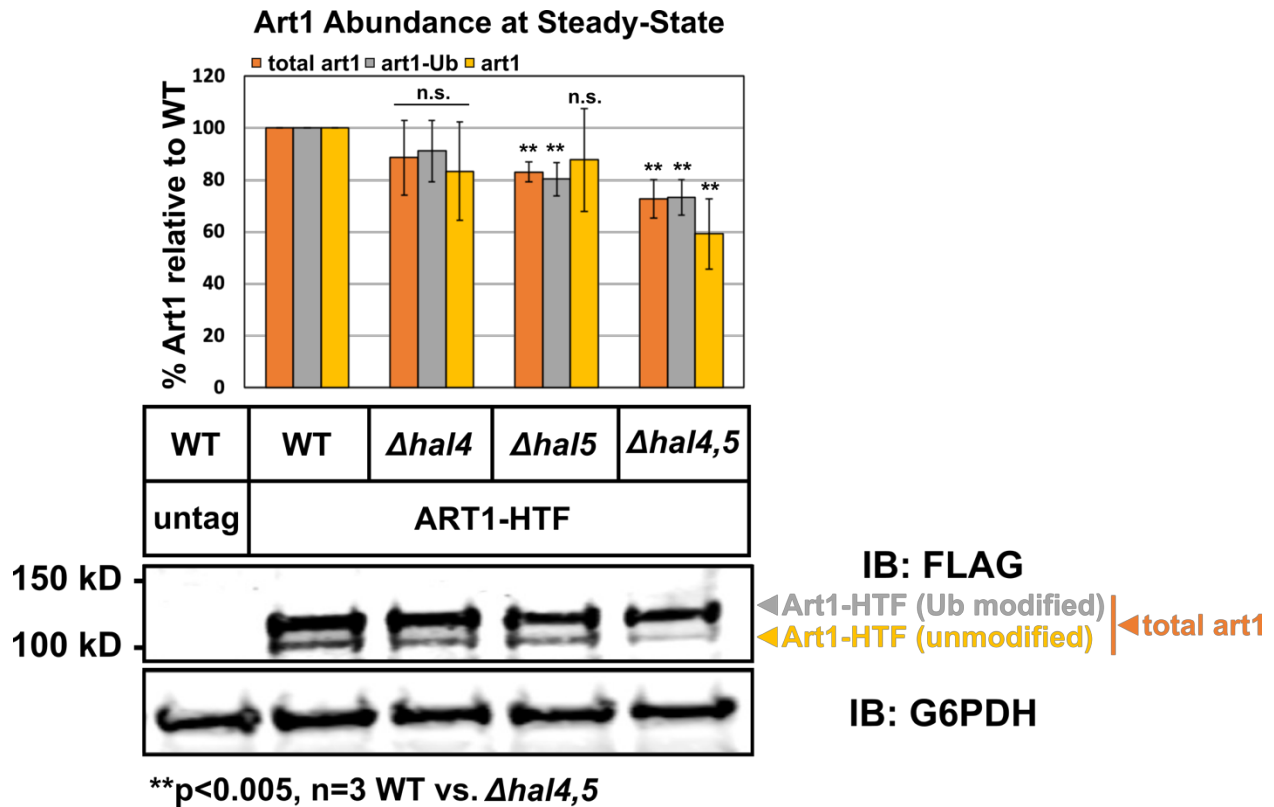
FIGURE 5.9 Art1 abundance is decreased in *hal* mutants Quantitative immunoblot analysis, with a representative immunoblot, of WT, *Δhal4*, *Δhal5*, or *Δhal4,5* cells expressing Art1 endogenously tagged with 6X-HIS-TEV-3XFLAG at the c-terminus (ART1-HTF). Total Art1 (orange bars) was quantified by measuring signal of both bands corresponding to Art1, and normalizing to G6PDH levels. Unmodified Art1 (yellow bars) was quantified by measuring signal of the bottom band, and normalizing to G6PDH levels. Ubiquitin-modified (Ub modified) Art1 (gray bars) was quantified by measuring signal of the top band, and normalizing to G6PDH levels. N=3

93

performed SILAC-MS quantitative phosphoprofiling analysis of Art1 (**Figure 5.10A-B**

and **5.11**). First, I compared Art1 phosphorylation in wildtype cells to *hal* double mutant

cells and detected only minor changes corresponding to slightly elevated

phosphorylation at some N-terminal sites in the absence of Hal kinases (**Figures 5.12**

and **5.13**). Additionally, I compared Art1 phosphorylation in the context of acute Hal5AS

inhibition and similarly detected only minor changes corresponding to slightly elevated

phosphorylation at some sites in the absences of Hal kinases (**Figure 5.14** and **5.15**).

Indeed, two regulatory modifications recently reported to inhibit Art1 activity –

phosphorylation of Thr93 and Thr795 (Lee *et al.*, 2019) – were either unaffected or

slightly elevated in the absence of Hal kinase activity (**Figures 5.12, 5.13,** and **5.14**).

Importantly, these experiments also reveal that loss of Hal kinase activity does not

impact the interaction between Art1 and Rsp5 (**Figures 5.12, 5.13,** and **5.14**).

Since Art1 activation is known to involve its translocation to the plasma membrane

(MacGurn *et al.*, 2011), I considered the possibility that Hal kinases might regulate Art1

localization. To test this, I analyzed Art1 subcellular localization and found that, in

contrast to *Δnpr1* mutant cells (MacGurn *et al.*, 2011), *hal* mutant cells exhibited no

observable increase in Art1 localization to the plasma membrane (**Figure 5.16**). Thus,

although I cannot exclude the possibility that Hal kinases antagonize endocytosis by

inhibiting Art1 function, the experiments shown here provide no evidence that Hal

kinases regulate phosphorylation or localization of Art1.
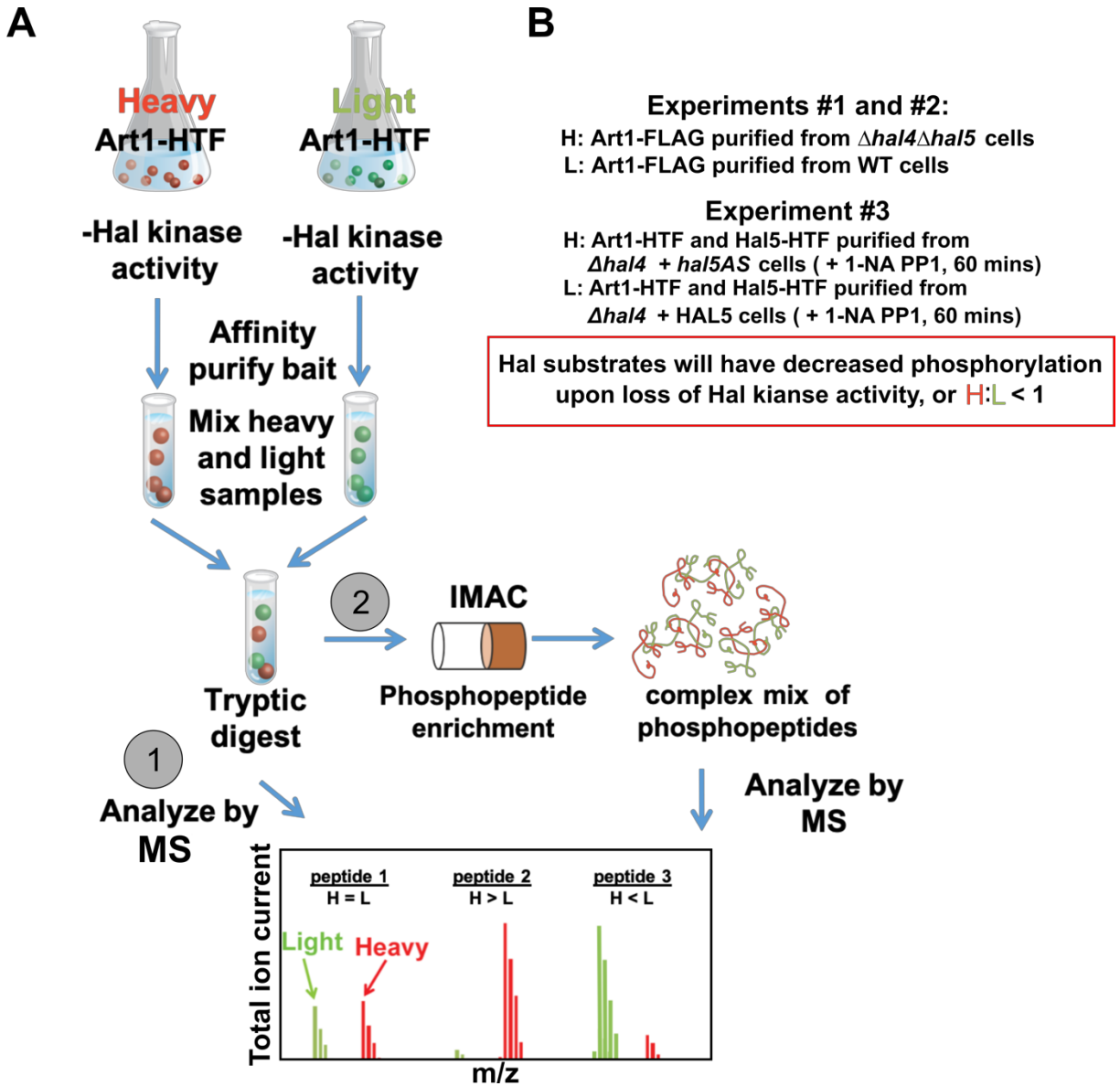
FIGURE 5.10 SILAC-MS experimental workflow (A) Schematic depicting the experimental workflow using SILAC coupled with immunoprecipitation, tryptic digest, and quantitative mass spectrometry analysis (1). To analyze phosphorylation, peptides are subjected to phosphopeptide enrichment prior to quantitative mass spectrometry analysis (2). **(B)** Description of how three different SILAC-MS experiments were performed to profile Art1 (Art1 and Hal5 in the case of Experiment #3) phosphorylation with and without Hal4 and Hal5 kinase activity.
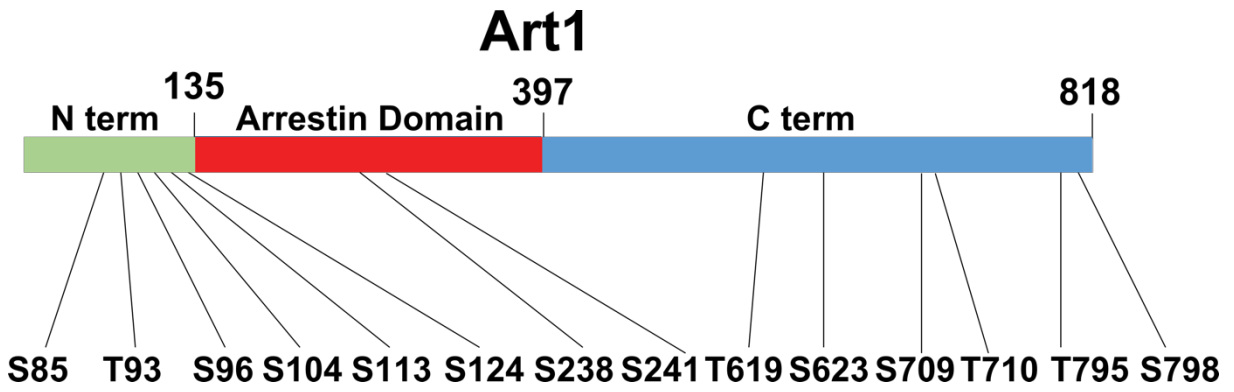
Figure 5.11 Art1 domain architecture and phosphosites Schematic of the domain architecture of the Art1 protein, with known phosphorylation sites indicated.
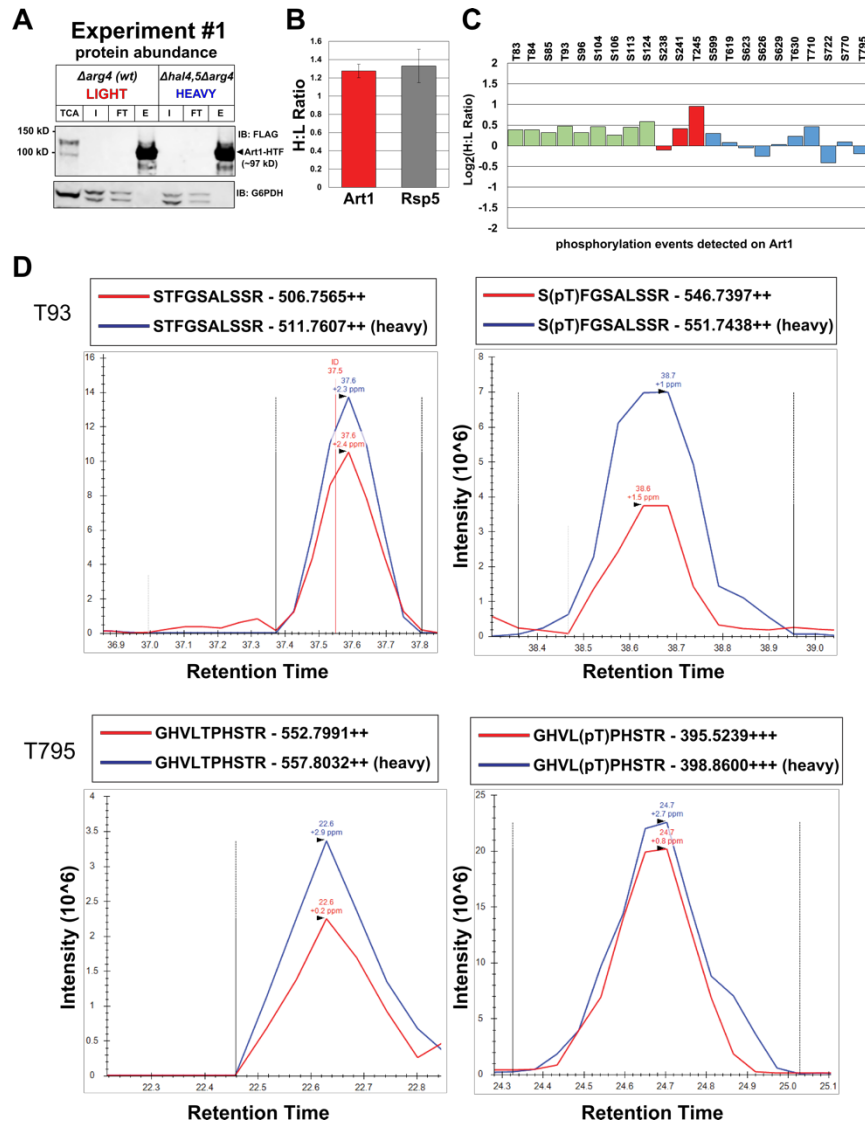
FIGURE 5.12 Art1 phosphorylation is unchanged (SILAC-MS experiment #1)
Analysis of experiment #1 described in Figure 5.10B. **(A)** 2% of prepared samples were analyzed by immunoblot to confirm Art1-HTF bait purification. Samples were subsequently submitted for mass spectrometry analysis. **(B)** The H:L ratio for all peptides of the indicated proteins were averaged to compute a measurement of the H:L ratio for the protein in the indicated experiment. Additional cell material was collected from *hal* mutant cells was to compensate for the observed loss in Art1 abundance (Figure 5.9) (i.e 1L of 0.5 OD WT cells vs 0.75 OD *hal* cells). **(C)** The LOG$_2$(H:L ratio) (normalized to total Art1) for each phosphorylation event detected is plotted and color-coded to correspond to the region of the Art1 protein as indicated in Figure 5.11. **(D)** Filtered chromatography data is shown for the indicated peptides (light peptide in red and heavy peptide in blue). Phosphopeptides identifying phosphorylation at Thr93 (top right) and Thr795 (bottom right) and the corresponding unmodified peptides (top left and bottom left, respectively) are depicted.

FIGURE 5.13 Art1 phosphorylation is unchanged (SILAC-MS Experiment #2)
Analysis of experiment #2 described in Figure 5.10B. **(A)** 2% of prepared samples were analyzed by immunoblot to confirm Art1-HTF bait purification. Samples were subsequently submitted for mass spectrometry analysis. **(B)** The H:L ratio for all peptides of the indicated proteins were averaged to compute a measurement of the H:L ratio for the protein in the indicated experiment. Additional cell material was collected from *hal* mutant cells was to compensate for the observed loss in Art1 abundance (Figure 5.9) (i.e 1L of 0.5 OD WT cells vs 0.75 OD *hal* cells). **(C)** The LOG_2(H:L ratio) (normalized to total Art1) for each phosphorylation event detected is plotted and color-coded to correspond to the region of the Art1 protein as indicated in Figure 5.11. **(D)** Filtered chromatography data is shown for the indicated peptides (light peptide in red and heavy peptide in blue). Phosphopeptides identifying phosphorylation at Thr93 (top right) and Thr795 (bottom right) and the corresponding unmodified peptides (top left and bottom left, respectively) are depicted.

98

FIGURE 5.14 Art1 phosphorylation is unchanged (SILAC-MS Experiment #3)
Analysis of experiment #3 described in Figure 5.10B. **(A)** 2% of prepared samples were analyzed by immunoblot to confirm Art1-HTF bait purification. Samples were subsequently submitted for mass spectrometry analysis. **(B)** The H:L ratio for all peptides of the indicated proteins were averaged to compute a measurement of the H:L ratio for the protein in the indicated experiment. Additional cell material was collected from *hal* mutant cells was to compensate for the observed loss in Art1 abundance (Figure 5.9) (i.e 1L of 0.5 OD WT cells vs 0.75 OD *hal* cells). **(C)** The LOG_2(H:L ratio) (normalized to total Art1) for each phosphorylation event detected is plotted and color-coded to correspond to the region of the Art1 protein as indicated in Figure 5.11. **(D)** Filtered chromatography data is shown for the indicated peptides (light peptide in red and heavy peptide in blue). Phosphopeptides identifying phosphorylation at Thr93 (top right) and Thr795 (bottom right) and the corresponding unmodified peptides (top left and bottom left, respectively) are depicted.

FIGURE 5.15 Growth of cells after acute inhibition of Hal5 kinase activity (A) For experiment #3 described in Figure 5.10B, following treatment of cultures with 1-NA-PP1 (and just prior to sample collection) 10mL of each culture was removed from the sample and cultured for an additional 24 hours in order to confirm inhibition by the compound. **(B)** Data in A plotted to better visualize time points from t=0 through t=12.
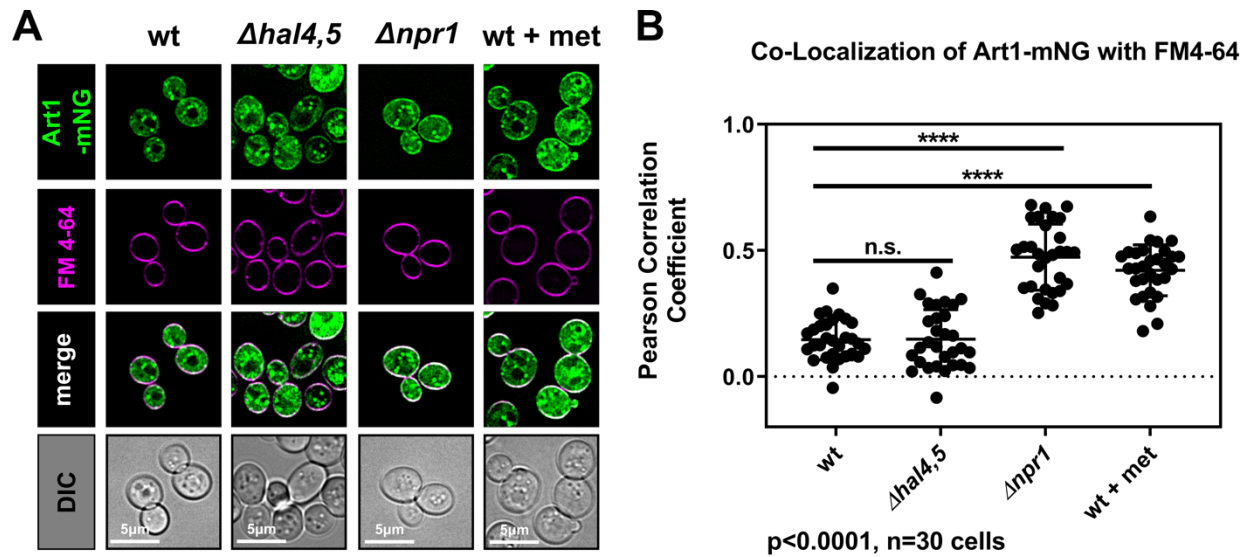
FIGURE 5.16 Art1 localization is unchanged in *hal* mutants Representative images of WT, *Δhal4,5*, *Δnpr1,* cells expressing Art1-mNG from a plasmid were grown to mid-log phase in selective media and imaged after a brief FM 4-64 pulse to label PM immediately prior to imaging. In the far right column of the panel, WT cells were treated with methionine (2μg/mL) for 10 minutes prior to FM 4-64 pulse. **(B)** Art1 localization to the PM in (A) was quantified by measuring Pearson's correlation coefficient of Hal5-mNG signal with FM 4-64 signal.

5.2.5 Quantitative phosphoprofiling of Hal5 indicates N-terminal phosphorylation

In the course of phosphoprofiling Art1 following acute inhibition of Hal5AS, I was also able to perform a similar phosphoprofiling analysis for Hal5 (since Hal5 was FLAG-tagged in these experiments and thus was captured as a bait). Interestingly, this analysis revealed two phosphorylation events proximal to the kinase domain at Ser358 and Ser395 that were dramatically reduced following acute inhibition of Hal5 kinase activity (**Figure 5.17**), suggesting that these modifications may occur by autophosphorylation. This is the first evidence of a substrate for Hal5, but the physiological significance of these phosphorylation events remains unclear.

5.3 Discussion

Taken together, these data indicate that (i) Hal5 kinase activity is required for its role in the regulation of endocytic trafficking, (ii) Hal5 kinase activity stabilizes PM proteins and inhibition of Hal5 kinase activity (in the absence of Hal4) triggers rapid endocytosis and vacuolar trafficking, and (iii) induction of endocytosis and vacuolar trafficking is an acute and rapid response to loss of Hal kinase activity, rather than a chronic adaptive condition in hal double mutant cells. The work presented in this chapter includes the first complementation analysis for Hal5, the first demonstration that kinase activity is required for function, and the first evidence of a substrate (itself).

5.3.1 Hal5 regulation of transcription may result from loss of nutrient transporters

Using an analog-sensitive allele of *hal5* has allowed me to interrogate acute consequences of inhibiting Hal5 catalytic activity in the cell. This approach was used to
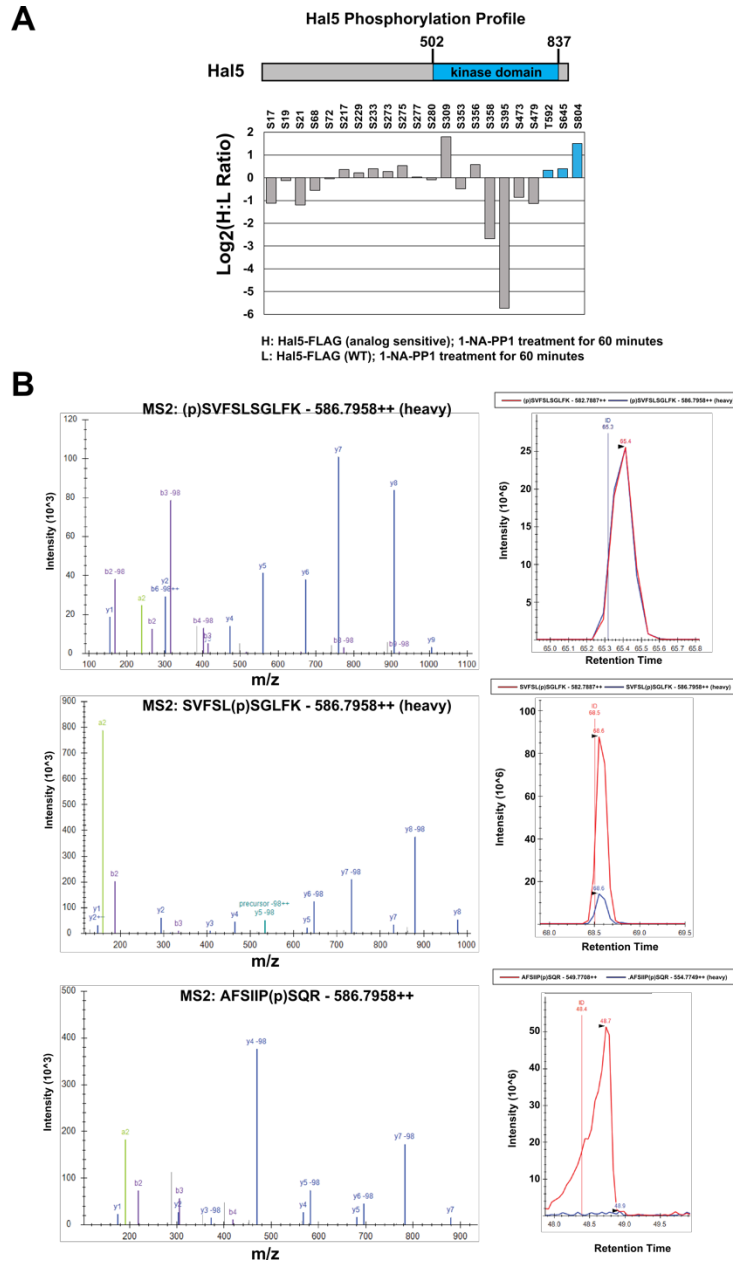
FIGURE 5.17 Acute inhibition of Hal5AS results in decreased phosphorylation of the non-catalytic region Analysis of Hal5 phosphorylation from data collected in Experiment #3 from Supplemental Figure 6. **(A)** Quantitative phosphoprofiling analysis Hal5 based on SILAC-MS data. Schematic of the domain architecture of Hal5 is shown at the top. **(B)** Fingerprinting and quantification of individual phosphorylation events resolved for Hal5. MS2 spectra for individual phosphopeptides (left panels) and filtered chromatograms for quantification of light (red) and heavy (blue) peptides (right panels) are shown for Ser353 (top), Ser358 (middle) and Ser395 (bottom).

characterize the role of Snf1 in glucose-responsive transcriptional regulation, but not

transporter abundance, and has not been used in the characterization of Npr1-mediated

regulation of transporter abundance. Thus, a question of whether these changes to

endocytic trafficking were acute or chronic, not only in Hal mutants but in other mutants

with similar phenotypes, remain. Upon acute inhibition of *hal5-AS*, in the absence of

Hal4, rapid internalization of nutrient transporters occurs within minutes (**Figure 5.6C**),

while growth of cells does not slow for at least 90 minutes after inhibition (**Figure

5.15B**). This result suggests that loss of nutrient transporters occurs first, and that slow-

growth in *hal* mutant cells occurs subsequent to broad loss of nutrient transporters.

Many transcriptional changes have been documented in *hal* mutant cells (Pérez-Valle *et

al.*, 2010), suggesting that Hal kinases maintain cellular homeostasis in part through

regulation of transcription. However, many of these transcriptional changes are

regulatory pathways turned on in response to starvation, a condition that may be

provoked by the chronic and broad loss of nutrient transporters from the cell surface in

hal mutant cells. Thus, it is possible that the transcriptional changes observed in *hal*

mutant cells are due to compensation in *hal* mutant cells, rather than due to the direct

loss of Hal kinases. Further studies comparing the kinetics of induced endocytosis and

transcriptional effects associated with loss of Hal function will be required to determine

which effects are primary and which are secondary.

5.3.2 The mechanism of Hal5 endocytic regulation appears distinct from Npr1 and Snf1
Npr1 phosphorylates Art1 in the N-terminal region to release Art1 from the PM, and

inactivate it (MacGurn *et al.*, 2011), thereby promoting stability of the Can1 at the cell

surface. Ppz phosphatases dephosphorylate Art1 at T93 and T795, promoting PM-localization of Art1 and physical interaction with cargo such as Mup1 (Lee *et al.*, 2019). Considering the observed similarities between *npr1* and *hal* mutant phenotypes, and the genetic interaction of *hal* mutants with *ppz* mutants (**Figure 5.8**), one model for Hal-mediated inhibition of endocytosis is through hyper-activation of Art1. This model predicts increased PM-localization of Art1, increased Art1 abundance at steady-state, or decreased phosphorylation on Art1 at sites known to be inhibitory in the absence of Hal kinases. However, phosphorylation sites on Art1 thought to be inhibitory were either slightly elevated or unchanged in *hal* mutant backgrounds (**Figures 5.12, 5.13 and 5.14**), PM-localization of Art1 was unchanged, and Art1 protein abundance decreases slightly at steady-state. Taken together, these data do not support a model whereby loss of Hal kinases triggers hyper-activation of Art1. is inconsistent with a hyper-activation model of Art1 upon loss of Hal kinases, which distinguishes Hal-mediated regulation of endocytosis from Npr1. Additional experimental analysis of Art4 upon loss of Hal5 will be required to determine whether Hal-mediated regulation of endocytosis is distinct from Snf1. This may be difficult, as considerably less is known about the activation of Art4 compared to Art1.

5.3.3 The non-catalytic region of Hal5 is subject to auto-regulation

To my knowledge, data presented in this chapter provides the first evidence of a substrate for Hal5 kinase activity (itself), and suggests that Hal5 may regulate the function of an uncharacterized feature upstream of the kinase domain. One way in which Hal5 autophosphorylation may regulate its function is through regulation of its

stability. Consistent with this hypothesis, chronic catalytic-dead point mutants of Hal5 (D688A and K546R) are not expressed. Other ways in which Hal5 autophosphorylation may regulate its function include regulation of protein-interaction partners, substrate selection, or subcellular localization. In Chapter 6 of this thesis, I test the function of the non-catalytic region of Hal5 and present evidence that there are features within this region important for both Hal5 function and localization.

In this chapter, I presented evidence that Hal-kinase activity is critical for regulation of endocytosis, and that the mechanism of regulation appears to be distinct from related kinases that have been previously characterized. In Chapter 6, I extend my characterization of Hal5 kinase beyond its catalytic role in negative regulation of endocytosis to investigate the uncharacterized non-catalytic region.

CHAPTER 6

Kinase-proximal Domains of Hal5 are Critical for Localization to the PM and Endocytic Function

6.1 Introduction

As I demonstrated in Chapter 3, my phylogenetic analysis of full amino acid sequences for the 130 protein kinases in yeast resulted in 6 distinct clades which do not perfectly align with the previously established classical kinase groupings. One possible explanation is that this analysis used full amino acid sequences, encompassing both catalytic domains and non-catalytic regions of protein kinases, while early analyses compare exclusively sequences corresponding to catalytic domains. This is consistent with a 2010 phylogenetic analysis of kinases across evolution, where more than 60% of kinases from nearly 500 distinct genomes spanning all domains of life were found to contain at least one non-kinase accessory domain (Martin *et al.*, 2010), implying that non-catalytic domains within protein kinases are a globally important facet of kinase function. Accessory domains may augment protein kinase catalytic activity by conferring substrate specificity, determining intracellular localization, performing scaffolding functions, or auto-regulatory functions (Sali and Blundell, 1993). One hallmark of the yeast AMPK/Snf1-related kinases is the presence of large regions of non-catalytic sequence. For example, Snf1 contains an auto-inhibitory ubiquitin-associated (UBA) domain proximal to the kinase domain, and an adenylate sensing domain at the C-terminus that appears to bind ADP molecules (Mayer *et al.*, 2011). Additionally, Gin4 and Kcc4 contain kinase-associated (KA1) domains that directly bind anionic

phospholipids at the plasma membrane to confer plasma-membrane localization (Chi *et al.*, 2012). For most of the yeast AMPK/Snf1-related kinases, the non-catalytic regions of protein sequence remain uncharacterized.

In Chapter 5, I determined that catalytic activity of the yeast AMPK/Snf1-related kinase Hal5 is required for Hal-mediated inhibition of nutrient transporter endocytosis. In this chapter, I investigate the function of the non-catalytic region of Hal5 and find that elements proximal to the kinase domain in the N-terminal region are critical for Hal5 function in endocytosis, Hal5 localization to the PM, and Hal5 response to nutrient availability.

6.2 Results

6.2.1 *N-terminal elements of Hal5 are required for its function*

Hal5 consists of a C-terminal kinase domain (amino acids 502-837) with a large N-terminal region (amino acids 1-501) that has not been characterized. To test for features at the N-terminus of Hal5 that are important for function, I first used JPred (Drozdetskiy *et al.*, 2015) to predict secondary structure in the N-terminal region (**Figure 6.1A**). Based on the predicted secondary structure, I designed a truncation series deleting elements up to the beginning of the kinase domain (**Figure 6.1B**). Using this truncation series, I determined that *hal5Δ1-493* and *hal5Δ1-339* truncations failed to complement the growth defect in *hal* double mutant cells (**Figure 6.1C**) despite high levels of protein

A
Secondary Structure Prediction of Hal5 AA 1-493 (N-terminal Region)
H=helix E=Sheet

```
AA   1 MGDEKLSRHTSLKRARSLSESIKGLFKPSGISGSNNAAAPSSRPGQDQAHSHQTARIITSNVSSPSISPVHSPVLQA 77
         -------------HHHHHHHHH------------------------------------------------------
      78 APKHHKLGVPNIAKLSLSPSREPSLNSENEMFSQESFISEKDEDEANLLEREDLQNKKEEKARAKHVRSKEAYVPHH 154
         ---------------------------------------------------------------------------
     155 RYTVGSDEVERQPRERLKNFPQNAGSSNPANSNANHVLDQENNFSIDAMLDYDEESKLRRRNSLGVRNHSNRTRSRK 231
         ---------------------------------------------------------------------------
     232 NSLSTPRSPPMKNGNGGMNSNATNNVGNGTGNRIYMRGRNHSDSISASSLPKFQEIECKCILDLGHFKVFENGYHEH 308
         ---------------------------------------------------------EEEEE--EEEE----EEE
     309 SLRVLPIITNNKNVDSGDEKDADASVNSGDDGDNDSEANMHKQKSVFSLSGLFKSHKDGNQQQQQQQQQQEENGEQIN 385
         --EEEEEEE------------------------------------------HHHHHH----------HHH--------
     386 LEKAFSIIPSQRFIKSQTLKKSRTSNLKNGNNDELMKNDGKNIPQIVNPNAAVGVEELKLINALSEKIRKGLKSENT 462
         ---HHHH---------------------------------------------HHHHHHHHHHHHHHHHHHHHHH---
     463 KGNNGEGRSNSNKQEDSDDTEGKAGTTNDDT 493
         --------------------------HHH
```

B

HAL5 (AA 1-855) — kinase domain 502-837

hal5Δ1-493 (AA 494-855) — 502-837

hal5Δ1-339 (AA 340-855) — 502-837

hal5Δ1-248 (AA 249-855) — 502-837

hal5Δ1-99 (AA 100-855) — 502-837

C

Δhal4,5   SCD -Leu

+ HAL5
+ hal5Δ1-493
+ hal5Δ1-339
+ hal5Δ1-248
+ hal5Δ1-99

cell number

D

HAL5	-	+	+	+	+
HTF tag	-	-	+	+	+
hal5Δ1-493	-	-	-	+	-
hal5Δ1-339	-	-	-	-	+

IB: Flag
◀HAL5-HTF
◀hal5Δ1-339-HTF
◀hal5Δ1-493-HTF

IB: G6PDH
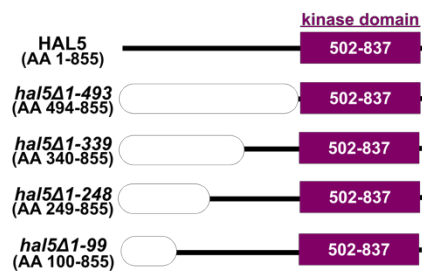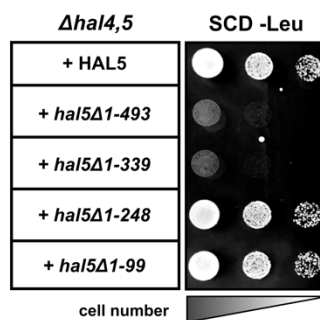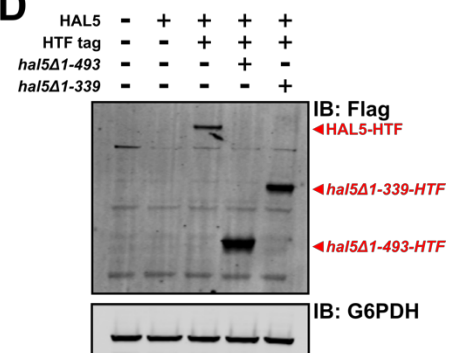
FIGURE 6.1 N-terminal elements proximal to the kinase domain are important for Hal5 function in growth **(A)** Secondary structure prediction performed in JPred for the N-terminal region of Hal5 **(B)** Schematic representation of Hal5 truncation variants compared to WT Hal5. **(C)** Representative image of cells serially diluted on synthetic selective media and grown for 3 days. Cells exogenously expressing either empty vector (EV) or a variant of Hal5 as indicated **(D)** Immunoblot analysis to examine expression of Hal5 variants that fail to complement growth in *hal* mutant cells

expression (**Figure 6.1D**). Furthermore, these truncations failed to complement aberrant Mup1 trafficking to the vacuole observed in *hal* double mutant cells (**Figure 6.2A-C**). In contrast, *hal5Δ1-248* and *hal5Δ1-99* truncation variants fully complemented growth and trafficking phenotypes observed in *hal* double mutant cells (**Figure 6.1C-D** and **6.2A-C**). Together, these data indicate that the kinase domain of Hal5 is not sufficient for regulation of endocytosis and suggest that features of Hal5 proximal to the kinase domain are critical for its function in the regulation of endocytic trafficking.

6.2.2 Hal5 localizes to the plasma membrane

Based on the functional data provided in my truncation analysis (**Figures 6.1C-D** and **6.2A-C**), I hypothesized that features proximal to the kinase domain might be important for Hal5 subcellular localization. Since Hal5 localization in cells has not been reported, I analyzed the subcellular localization of Hal5 tagged at the C-terminus with mNeonGreen (mNG, (Shaner *et al.*, 2013)) (both endogenous and exogenous expression) and observed cytosolic and peripheral localization (**Figure 6.3A-B**). Importantly, C-terminal tagging of Hal5 with mNG did not result in loss of function as assayed by growth complementation (**Figure 6.3C**). To test if peripheral Hal5 localized to the plasma membrane (PM), I imaged Hal5-mNG in cells pulse-labelled with FM4-64 (a lipophilic tracer dye that incorporates into the bilayer of the PM (Vida and Emr, 1995)) and detected significant colocalization, indicating that the peripheral pool of Hal5 indeed localizes to the PM (**Figure 6.4A-C**). Although this indicates Hal5 localizes to the PM, it does not address if Hal5 binds directly to lipids in the plasma membrane. To further
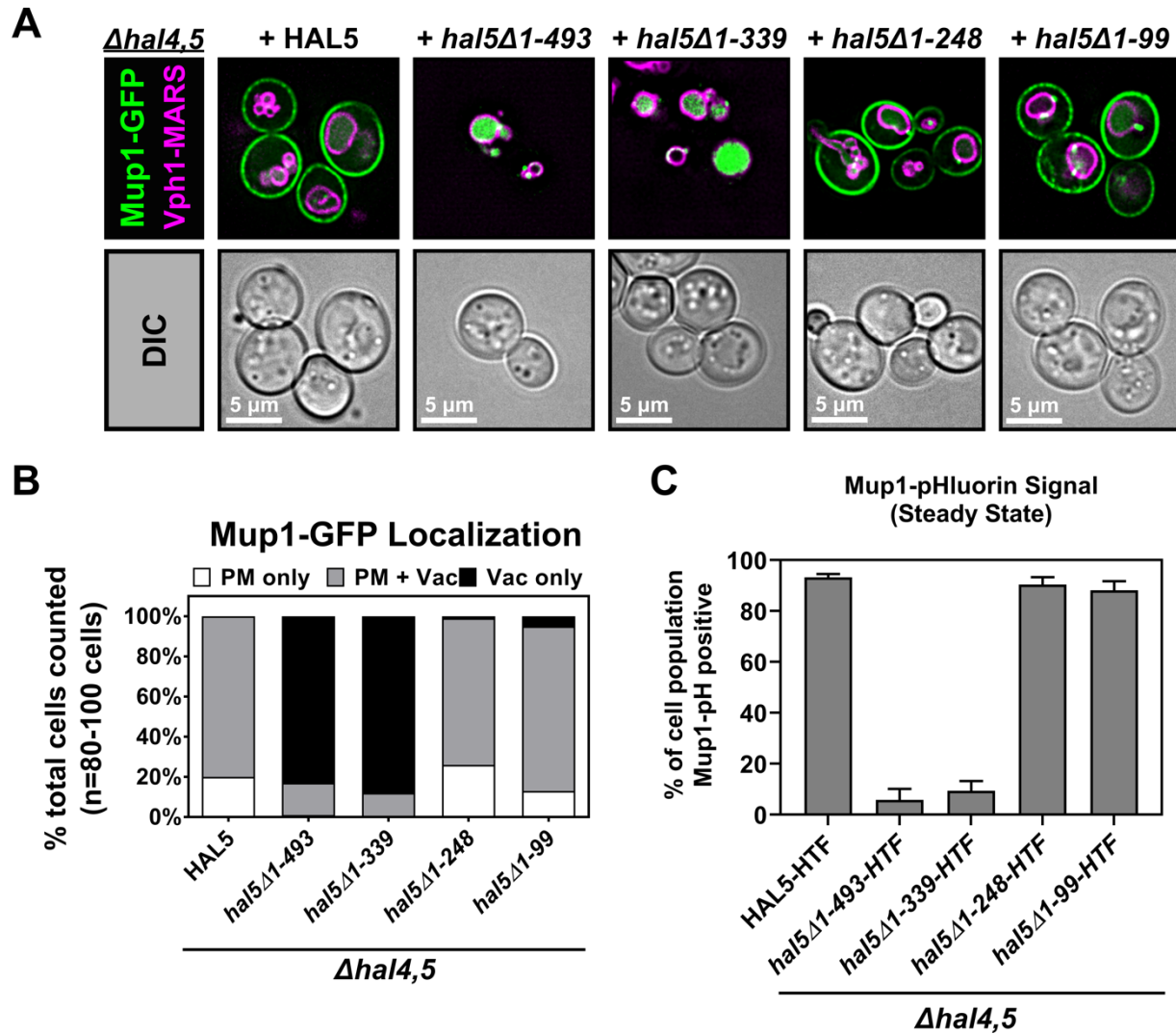
FIGURE 6.2 N-terminal elements proximal to the kinase domain are important for Hal5 function in endocytic trafficking (A) Representative images of Mup1-GFP expressed from a centromeric plasmid in the presence of endogenously-tagged Vph1-MARS, a marker for the limiting membrane of the vacuole. Empty vector (EV) or Hal5 variants are exogenously expressed in *Δhal4,5* mutant cells from a centromeric plasmid under native promoter control. **(B)** Quantification of Mup1-localization in (D) performed by binning cells into localization categories as indicated. **(C)** Percentage of cell population expressing endogenously tagged Mup1-pHluorin as measured by cells that fall within a defined FITC gate by flow cytometry at steady state (10,000 cells counted per condition, n=3 biological replicates).

A

Hal5-mNG | zoom | DIC

5 µm

B

endogenous

cell middle | cell surface

Hal5-mNG | DIC | Hal5-mNG | DIC

5 µm | 5 µm

zoom | zoom

C

SCD -LEU media

WT	ev	
Δhal4,5	ev	
	Hal5-mNG	

cell number
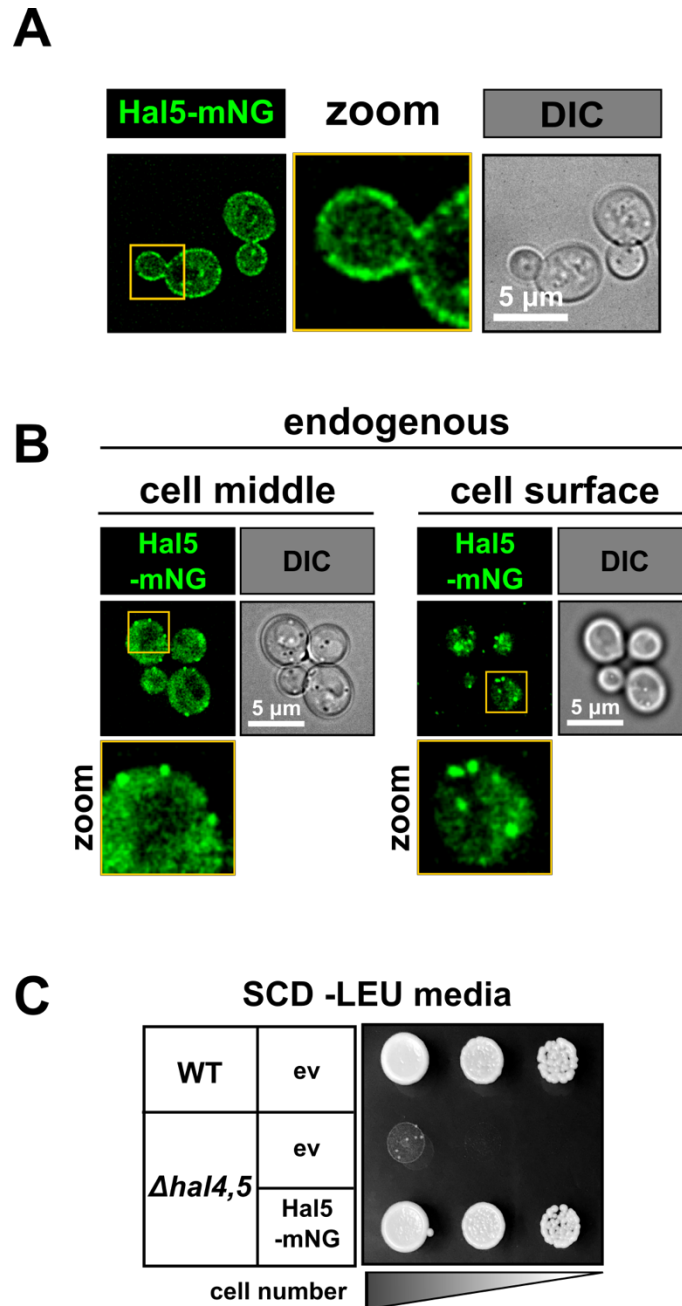
Figure 6.3 Hal5 localizes to the cell periphery (A) Representative image of WT cells grown to mid-log phase in selective media expressing Hal5 C-terminally-tagged with mNeonGreen (Hal5-mNG) from a centromeric plasmid under native promoter control. **(B)** Representative images of cells expressing endogenously-tagged Hal5-mNG grown to mid-log phase in rich media imaged near the cell middle (left) or cell surface (right) to asses Hal5 localization. **(C)** Cells expressing either empty vector (ev) or Hal5-mNG serially diluted onto synthetic selective media and grown for 5 days to assess functionality of C-terminally-tagged Hal5-mNG.
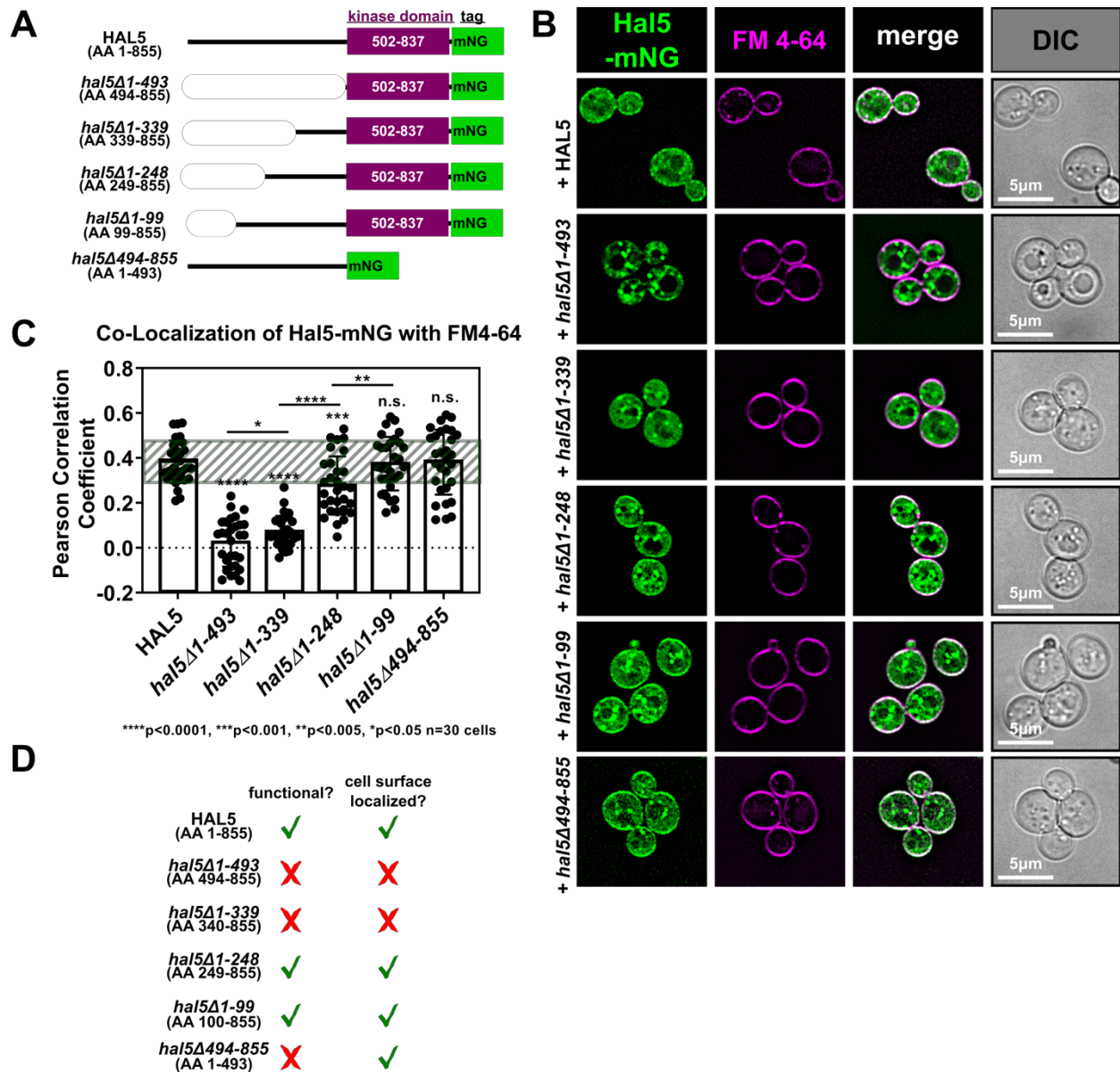
Figure 6.4 N-terminal elements proximal to the kinase domain are critical for Hal5 localization to the PM (A) Schematic representation of c-terminally mNeonGreen-tagged Hal5 variants compare to WT Hal5. **(B)** Representative images of WT cells grown to mid-log phase in selective media expressing Hal5-mNG after brief FM 4-64 pulse to label PM immediately prior to imaging **(C)** Hal5 localization to the PM was quantified in (B) by measuring Pearson correlation coefficient of Hal5-mNG signal with FM 4-64 signal. Standard deviation of cells expressing full-length Hal5-mNG is denoted by the green box. **(D)** Table summarizing each Hal5 variant tested, its functionality, and its localization.

characterize the PM-localized pool of Hal5, I imaged cells expressing Hal5-mNG along with mCherry-tagged endocytic site components including Ede1, Sla2, Ent1, and Abp1 (Weinberg and Drubin, 2012) and found that Hal5 only coincidentally co-localized with these structures (**Figure 6.5A**). Thus, Hal5 does not appear to associate with endocytic sites. Despite some co-localization of Hal5-mNG with Mup1-mCherry (a methionine transporter that localizes generally to the PM), I did not detect significant co-localization of Hal5-mNG with mCherry-tagged variants of the Rsp5 adaptor Art1 or the eisosome component Pil1 (**Figure 6.5B**). Interestingly, treatment of cells with LatA increased the extent of Hal5 localization to the PM (**Figure 6.6A-B**), indicating that inhibition of endocytosis and/or actin dynamics stabilizes Hal5 at the PM.

6.2.3 Hal5 N-terminal region is critical for PM localization

To determine whether the N-terminal region of Hal5 contains features critical for PM localization, I analyzed the subcellular location of an N-terminal truncation series of Hal5 (**Figure 6.4A**) and found that deletion of amino acids 1-493 and 1-339 resulted in loss of detection at the PM, while truncations deleted for amino acids 1-248 and 1-99 were retained at the PM (**Figure 6.4B-C**). Importantly, I also observed that deletion of the kinase domain did not alter PM localization – indicating that PM localization is determined by elements proximal to the kinase domain. As with full-length Hal5, treatment of cells with LatA increased the PM localization of the Hal5 N-terminal domain but had no effect on the localization of the kinase domain (**Figure 6.6C-D**). Thus, my data reveals a correlation between Hal5 function and localization of the kinase domain

114
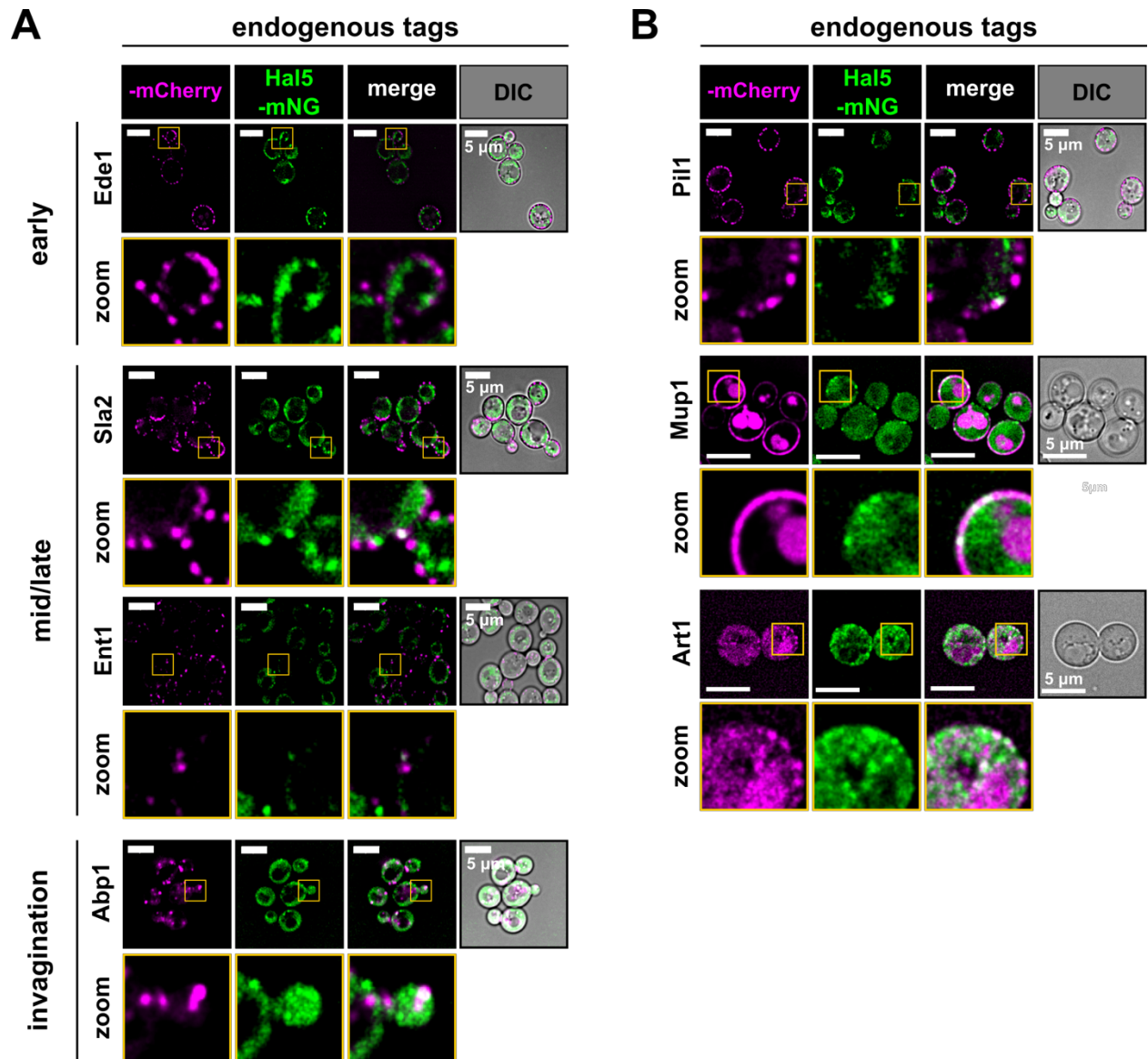
Figure 6.5 Hal5 does not colocalize with endocytic sites (A) Cells co-expressing endogenous Hal5-mNG and mCherry-tagged components of endocytic site machinery corresponding to either early (top), mid/late (middle), or invagination (bottom) events. **(B)** Cells co-expressing endogenous Hal5-mNG and mCherry-tagged Pil1 (eisosomes), Mup1 (nutrient transporter, broad PM marker), or Art1 (Rsp5 adaptor).
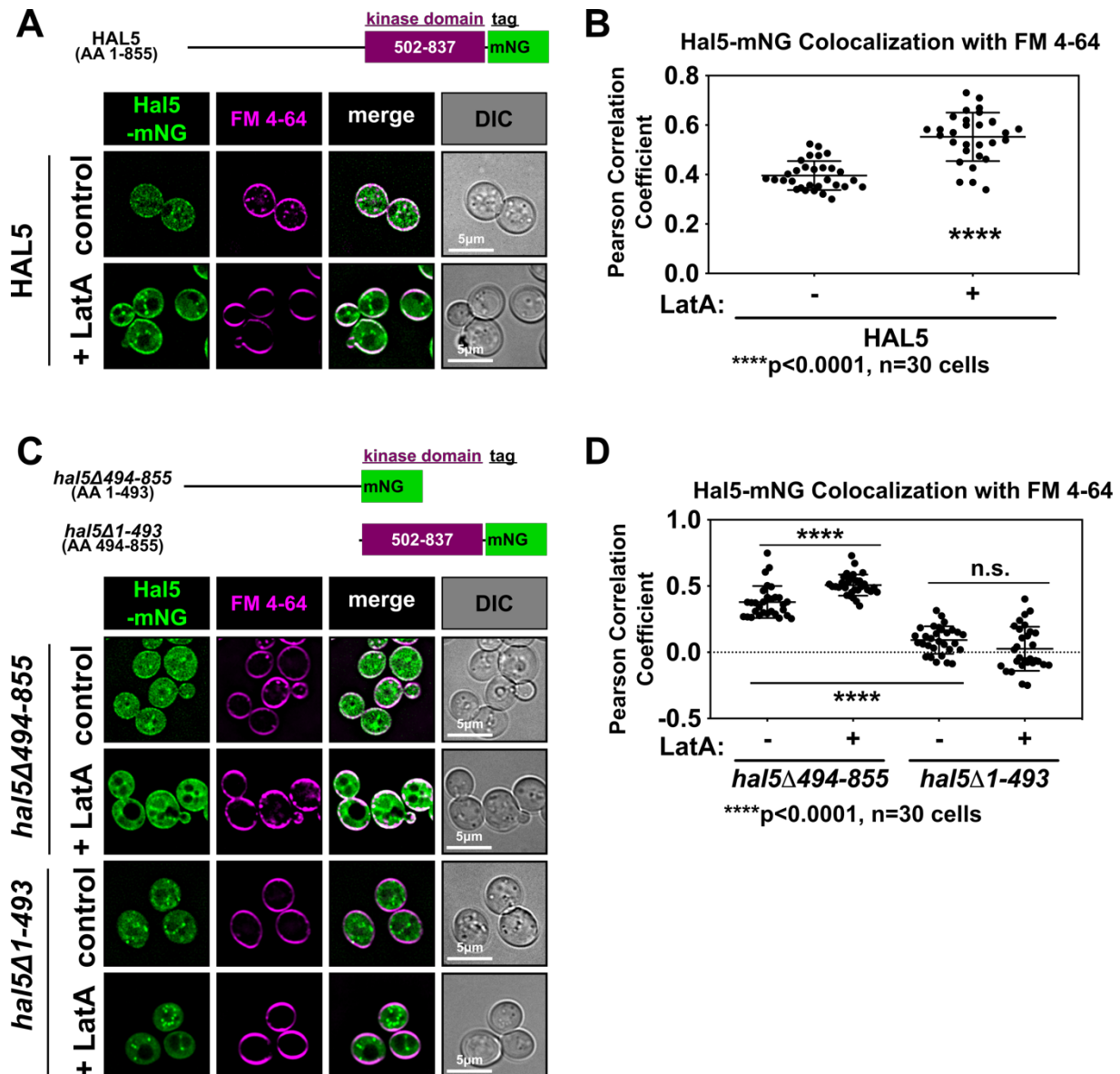
Figure 6.6 Acute inhibition of endocytosis increases Hal5 localization to the PM
(A) Representative images of WT cells grown to mid-log phase in selective media expressing Hal5-mNG (with or without 1 hour LatA treatment) after brief FM 4-64 pulse to label PM immediately prior to imaging **(B)** Localization of Hal5 to the PM was quantified in (A) by measuring Pearson correlation coefficient of Hal5-mNG signal with FM 4-64 signal. **(C)** Representative images using conditions described in (A) for WT cells expressing either a Hal5 variant deleted for the N-terminal region (*hal5Δ1-493-mNG*) or a Hal5 variant deleted for the kinase domain (*hal5Δ494-855-mNG*). **(D)** Quantification of Hal5 localization to the PM in (C) performed as described in (B).

to the PM (**Figure 6.4D**), suggesting that recruitment of Hal5 kinase activity to the plasma membrane is critical for its regulation of endocytic trafficking. One way in which Hal5 may localize to the PM is through interaction with a PM-bound or anchored protein. To test this hypothesis, I performed quantitative SILAC-MS interactome analysis of Hal5 (**Figure 6.7A-C**). In this analysis, Hal5 was significantly enriched from both crude (S5, to include membrane fractions) and cleared (S13, to exclude membrane fractions) yeast lysates, indicating successful SILAC labeling and immunoprecipitation. In both experiments, a few other proteins were enriched slightly above background, including Slx5, a subunit of the Sumo-targeted Ubiquitin Ligase complex. High background in the S5 SILAC-MS experiment, and low peptide abundance for putative interacting partners in both the S5 and S13 SILAC-MS experiments, limits my ability to make conclusions about the interactions of Hal5 with other proteins in the cell.

Another way in which Hal5 may localize to the PM is by binding directly to lipids through an uncharacterized lipid-binding domain. AMPK/Snf1-related kinases Gin4 and Kcc4 have been shown to localize to the PM through binding of anionic phospholipids by critical lysine residues in KA1 (kinase-associate 1) domains (Chi *et al.*, 2012). To test whether Hal5 may harbor an uncharacterized KA1 domain within its N-terminal region, I first performed a multiple sequence alignment of Hal5 (amino acids 1-493) with the KA1 domains of Gin4 (amino acids 1007-1142) and Kcc4 (amino acids 901-1037). Importantly, I found that the KA1 domains of Gin4 and Kcc4 aligned with elements of the Hal5 N-terminal region proximal to the kinase domain that are important for both function and localization of Hal5 (**Figure 6.8**). To further explore the possibility that Hal5

A

S5 (crude, soluble + membrane)
Hal5 interactome: Hal5 (L) vs. Hal5-HTF (H)

B

S13 (cleared, soluble only)
Hal5 interactome: Hal5 (L) vs. Hal5-HTF (H)

change in abundance
red indicates H:L ≥2
and at least 3 peptides detected
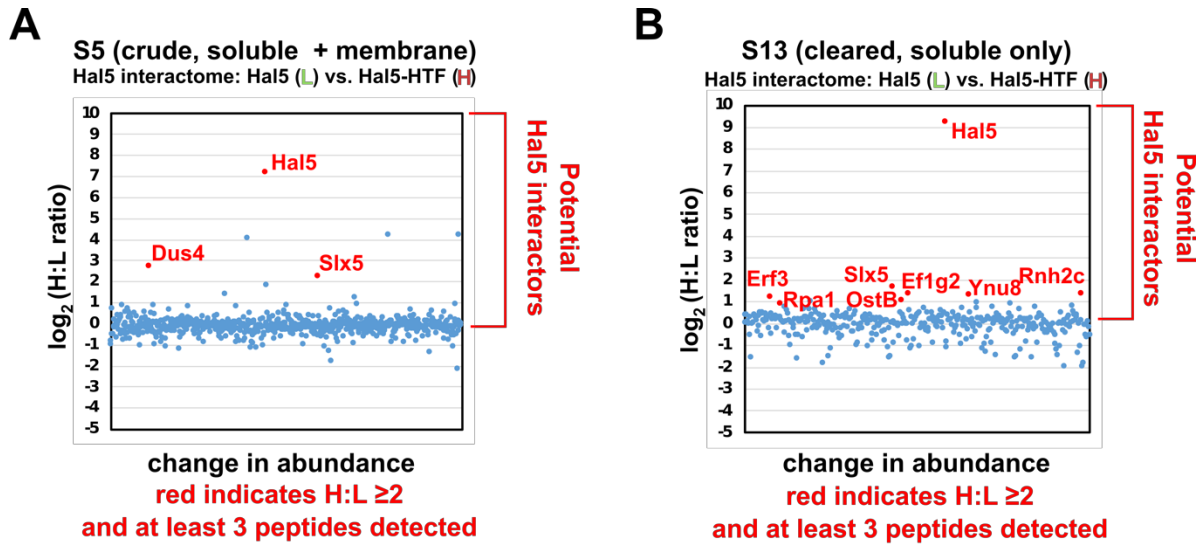
C

S5 (crude, soluble + membrane)

H:L	peptides	sequence coverage	protein	description (SGD)
142.79	55	61%	Hal5	putative protein kinase involved in regulation of potassium transporters
6.1563	6	26%	Dus4	dihydrouridine synthase
4.6995	3	7%	Slx5	Subunit of the Slx5-Slx8 SUMO-targeted Ub ligase (STUbL) complex

S13 (cleared, soluble only)

H:L	peptides	sequence coverage	protein	description (SGD)
599.51	52	68%	Hal5	putative protein kinase involved in regulation of potassium transproters
3.2446	3	7%	Slx5	Subunit of the Slx5-Slx8 SUMO-targeted Ub ligase (STUbL) complex
2.5798	3	27%	Rnh2c	ribonuclease H2 subunit involved in ribonucleotide excision repair
2.5489	4	12%	Ef1g2	alias: Tef4; elongation factor 1-gamma 2
2.4713	3	31%	Ynu8	uncharacterized protein YNL208W, may interact with ribosomes
2.3125	6	12%	Erf3	translation termination factor
2.0596	3	8%	OstB	alias: Wbp1; Beta subunit of the oligosaccharyl transferase glycoprotein complex; required for N-linked glycosylation of proteins in the endoplasmic reticulum
2.0075	3	3%	Rpa1	highly conserved single-stranded DNA binding protein involved in DNA replication, repair, and recombination

Figure 6.7 Quantitative SILAC-MS interactome analysis of Hal5 (A-B) The LOG$_2$(H:L ratio) for each protein group was graphed and color-coded based on the criteria indicated. Following the workflow described in Figure 5.10A, Untagged (L) or c-terminally flag-tagged Hal5 (6X-HIS-TEV-3XFLAG, Hal5-HTF) (H) was expressed from a centromeric plasmid and immunoprecipitated from **(A)** a crude yeast lysate, called S5, comprised of both soluble and membrane fractions, or **(B)** a cleared yeast lysate, called S13, comprised of only the soluble fraction. **(C)** Tables summarizing data meeting the criteria indicated in red.

118

```
HAL5/1-493        1 MGDEKLSRHTSLKRARSLSESIKGLFKPSGISGSNNAAAPSSRPGQ 46
KCC4/901-1037       ----------------------------------------------
GIN4/1007-1142      ----------------------------------------------

HAL5/1-493       47 DQAHSHQTARIITSNVSSPSISPVHSPVLQAAPKHHKLGVPNIAKL 92
KCC4/901-1037       ----------------------------------------------
GIN4/1007-1142      ----------------------------------------------

HAL5/1-493       93 SLSPSREPSLNSENEMFSQESFISEKDEDEANLLEREDLQNKKEEK 138
KCC4/901-1037       ----------------------------------------------
GIN4/1007-1142      ----------------------------------------------

HAL5/1-493      139 ARAKHVRSKEAYVPHHRYTVGSDEVERQPRERLKNFPQNAGSSNPA 184
KCC4/901-1037       ----------------------------------------------
GIN4/1007-1142      ----------------------------------------------

HAL5/1-493      185 NSNANHVLDQENNFSIDAMLDYDEESKLRRRNSLGVRNHSNRTRSR 230
KCC4/901-1037   901 ----------------------------------DNDKK----- 905
GIN4/1007-1142 1007 ----------------------------------KDHSK----- 1011

HAL5/1-493      231 KNSLSTPRSPPMKNGNGGMNSNATNNVGNGTGNRIYMRGRNHSDSI 276
KCC4/901-1037   906 -DNDTV-----------NAPTTVKKPPNSVLLKKFSKGKILELE- 937
GIN4/1007-1142 1012 -DHLKE-----------HKQDKNTAIGNGSFFRKFSKSSDKTME- 1043

HAL5/1-493      277 SASSLPKFQEIECKCILDLGHFKVFENGYHEHSLRVLPIITNNKNV 322
KCC4/901-1037   938 ------IHAKIPEKRLYE--GLHKLLEGWKQYGLKNLVFNITNMII 975
GIN4/1007-1142 1044 ------LYAKISAKQLFN--GLEKLLRGWTQYGLKNIKSHPNNLTL 1081

HAL5/1-493      323 DSGDEKDADASVNSGDDGDNDSEANMHKQKSVFSLSGLFKSHKDGN 368
KCC4/901-1037   976 TGKLVND--------------------SILFLRSTLFEIM--- 995
GIN4/1007-1142 1082 TGKLSSD--------------------NIFSLRSTLFEVN--- 1101

HAL5/1-493      369 QQQQQQQQQEENGEQINLEKAFSIIPSQRFIKSQTLKKSRTSNLKN 414
KCC4/901-1037   996 ----------------------------------------VLPN 999
GIN4/1007-1142 1102 ----------------------------------------IYPR 1105

HAL5/1-493      415 GNNDELMKNDGKNIPQIVNPNAAVGVEELKLINALSEKIRKGLKSE 460
KCC4/901-1037  1000 GD--------GRSLIKFNK---KTG--STKTLTKLATEIQIILQKE 1032
GIN4/1007-1142 1106 GK--------MSVVQFKK---VSG--SFKAVKKLVNEVENVLNKE 1137

HAL5/1-493      461 NTKGNNGEGRSNSNKQEDSDDTEGKAGTTNDDT 493
KCC4/901-1037  1033 --------GVLDK----------------- 1037
GIN4/1007-1142 1138 --------GVLQK----------------- 1142
```

Figure 6.8 MSA of Hal5 N-terminal region with known KA1 domains A multiple sequence alignment, performed using Clustal Omega (EMBL-EBI) and visualized in JalView, of the N-terminal region of Hal5 (amino acids 1-493) with the KA1 domains of Kcc4 (amino acids 901-1037) and Gin4 (amino acids 1007-1142). Positions corresponding to residues critical for Kcc4 PM localization and lipid binding (Moravcevic *et al.*, 2010) are denoted by black indicators.

localizes to the PM through a lipid binding domain, I analyzed the localization of Hal5-

mNG in temperature- sensitive PI-kinase mutants (Mayinger, 2012). Shifting both *pik1-*

ts and *vps34-ts* mutants (defective for PI(4) and PI(3) kinase activity, respectively

(Auger *et al.*, 1989; Garcia-Bustos *et al.*, 1994)) from permissive temperature (26°C) to

restrictive temperature (37°C) resulted in decreased PM localization of Hal5. One

limitation of this experiment is that *vps34-ts* mutants appear to exhibit defects in Hal5-

mNG localization at permissive temperature (26°C), which may indicate that *vps34-ts*

has loss of function at permissive temperature, impairing my ability to interpret a shift in

Hal5-mNG localization. Importantly, shifting *sec1-ts* mutants to restrictive temperature

(37°C) did not impact Hal5-mNG localization to the PM (**Figure 6.9A-B**), suggesting that

the secretory pathway is not required for Hal5-mNG localization (Carr *et al.*, 1999; Scott

et al., 2004). Additionally, Hal5-mNG localization to the PM was not disrupted in Δ*cho1*

mutants (**Figure 6.9C-D**), suggesting that phosphatidylserine is not important for Hal5-

mNG localization to the PM (Atkinson *et al.*, 1980). Taken together, these data suggest

that PI(P) lipids may be important for Hal5 localization to the PM, but does not indicate

whether Hal5-mNG localization to the PM is direct or indirect.

6.2.4 Nutrient availability regulates Hal5 localization

Based on previous studies reporting that the Npr1 kinase localizes to the plasma

membrane in response to changes in TORC1 signaling (MacGurn *et al.*, 2011), I

hypothesized that localization of Hal5 to the PM might be important for its regulation of

endocytosis. I observed no effect of acute inhibition on the PM localization of Hal5AS

(**Figure 6.10A-B**), indicating that Hal5 kinase activity, and N-terminal phosphorylation
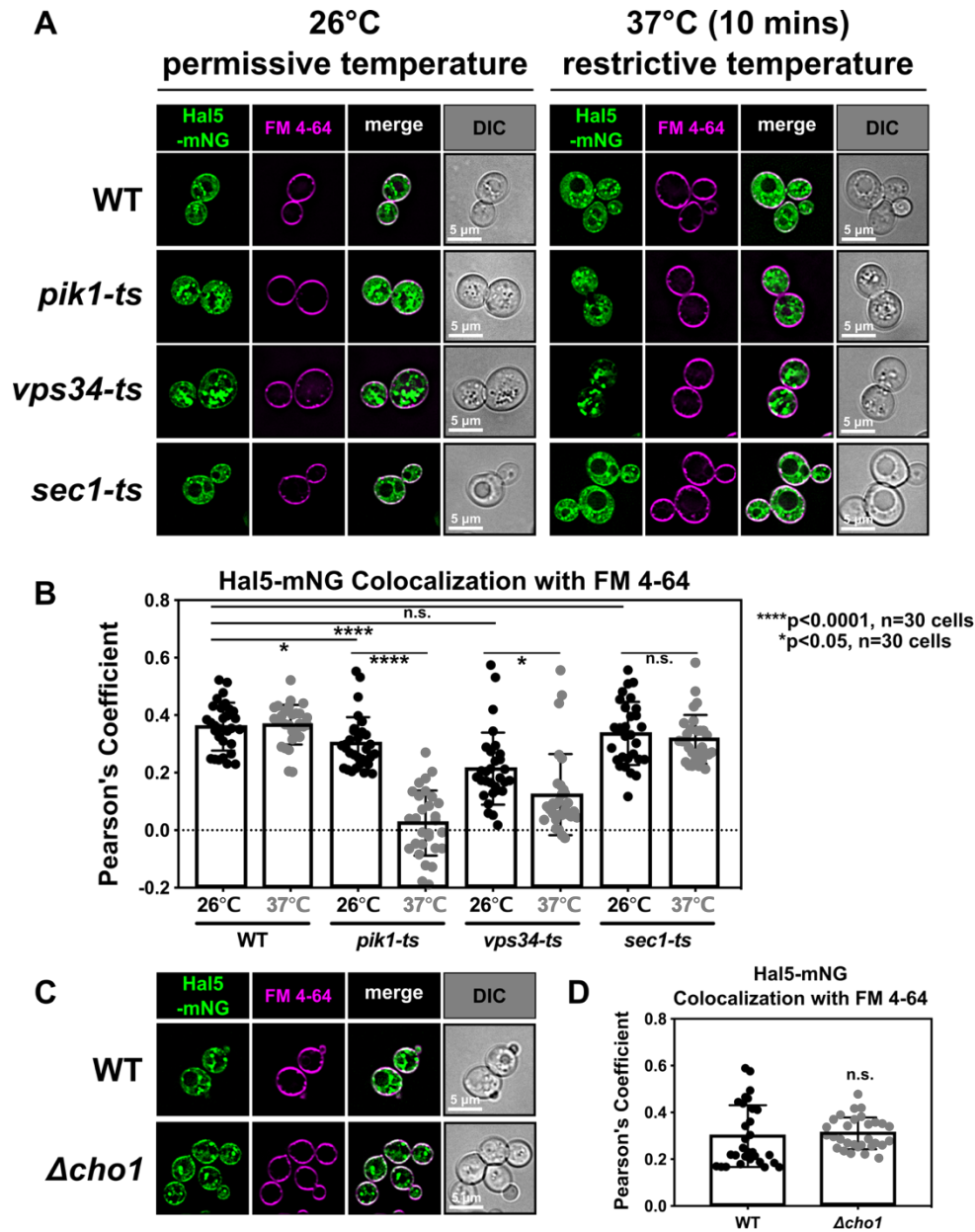
Figure 6.9 PI(P) lipids are important for Hal5 localization to the PM (A)
Representative images of WT cells expressing Hal5-mNG from a centromeric plasmid under native promoter control. Cells were grown to mid-log phase in selective media at permissive temperature then shifted to the restrictive temperature for 10 minutes, then briefly pulsed with FM 4-64 to label PM immediately prior to imaging. **(B)** Hal5 localization to the PM was quantified in (A) by measuring Pearson correlation coefficient of Hal5-mNG signal with FM 4-64 signal. **(C)** Representative images of *cho1* mutant cells expressing Hal5-mNG from a centromeric plasmid under native promoter control. Cells were grown to mid-log phase in selective media, then briefly pulsed with FM 4-64 to label PM immediately prior to imaging. **(D)** Hal5 localization was quantified in (C) as described in (B).
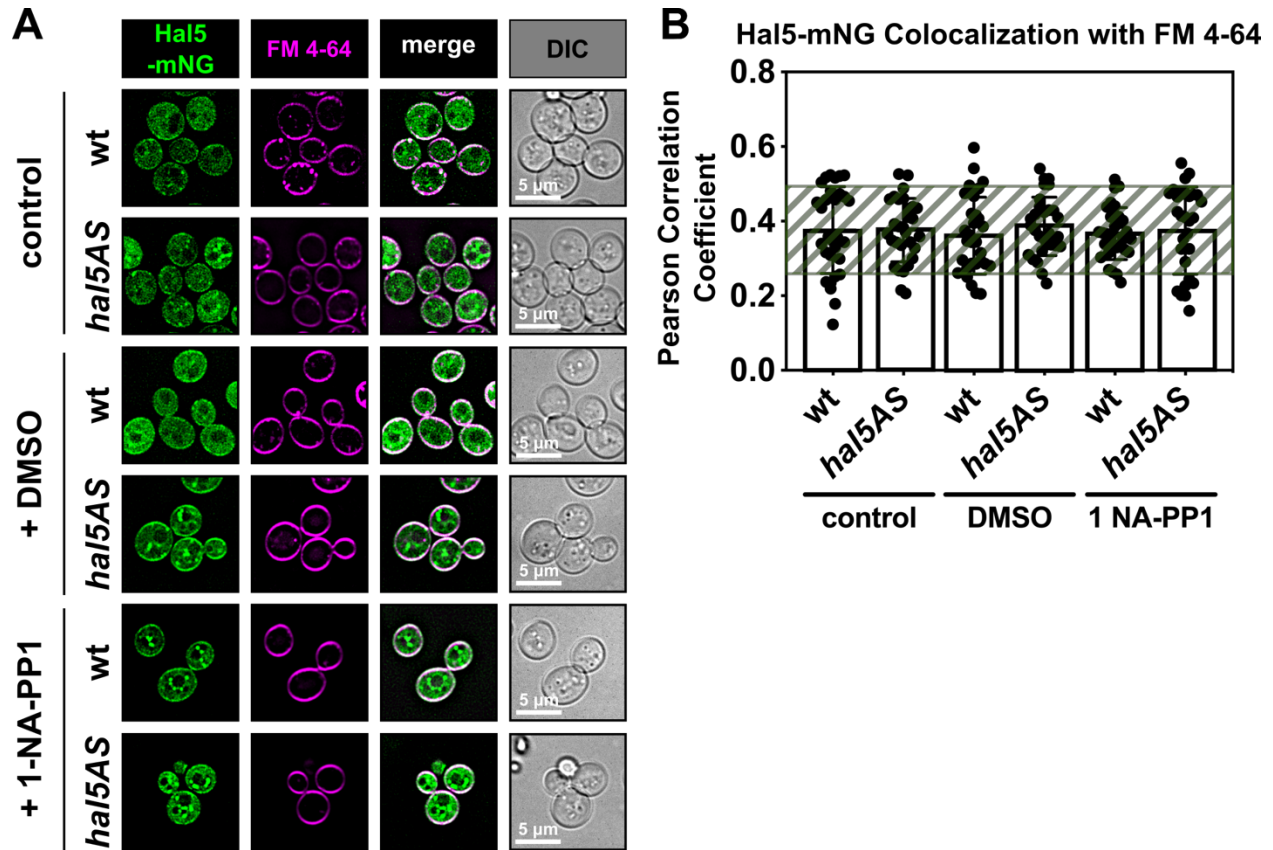
Figure 6.10 Hal5 catalytic activity does not regulate its localization to the PM (A) Representative images of WT cells expressing WT or analog-sensitive variants of Hal5-mNG (wt or *hal5AS*) from a centromeric plasmid under native promoter control. Cells were grown to mid-log phase in selective media. Cells were untreated (control), treated with vehicle (DMSO), or inhibitor (1-NA-PP1 26.3μM) for 10 minutes, then briefly pulsed with FM 4-64 to label PM immediately prior to imaging. **(B)** Hal5 localization to the PM was quantified in (A) by measuring Pearson correlation coefficient of Hal5-mNG signal with FM 4-64 signal. Standard deviation of control WT cells denoted by green box.

events dependent on Hal5 kinase activity (**Figure 5.17**), do not regulate its PM

association. I next hypothesized that Hal5 might respond to environmental changes that

trigger endocytic regulation. To test this, I analyzed the subcellular localization of Hal5

(both full-length Hal5 (**Figure 6.11A-B**) and the N-terminal domain (**Figure 6.12A-B**))

following a variety of different environmental stimuli. I found that conditions of high salt

(addition of excess sodium or potassium to the media) triggered a slight increase in the

PM localization of Hal5 (both the N-terminus and full-length Hal5), while switching to a

nutrient-starved media did not impact Hal5 PM association (**Figure 6.11A-B** and **Figure

6.12A-B**). In contrast, I detected a significant loss of Hal5 PM localization following

stimulation with uracil and methionine (**Figure 6.11A-B** and **Figure 6.12A-B**) – stimuli

that trigger the endocytosis of Fur4 and Mup1, respectively. Additionally, stimulation

with tryptophan, leucine, or rich media resulted in loss of Hal5 PM localization, while

stimulation with histidine did not (**Figure 6.11A-B**). In contrast to Npr1, which is

responsive to TORC1 signaling output (MacGurn *et al.*, 2011), inhibiting TORC1 by

treatment with rapamycin or activating TORC1 by treatment with cycloheximide did not

result in any detectable changes in Hal5 localization (**Figure 6.13A-B**) or SDS-PAGE

mobility (**Figure 6.13C**). Taken together, these data indicate that Hal5 responds to

changes in nutrient availability, with excess nutrients like uracil and methionine

triggering a decrease in Hal5 PM association.

6.3 Discussion

Taken together, these data indicate that (i) N-terminal elements proximal to the kinase

domain are important for both PM localization and endocytic regulation, (ii) localization

Figure 6.11 Nutrient availability regulates Hal5 localization (A) Representative images of WT cells expressing full-length c-terminally tagged Hal5-mNG from a centromeric plasmid under native promoter control. Cells were grown to mid-log phase in selective media then switched to media with the indicated nutrient conditions (10 μg/mL methionine (met), uracil (ura), leucine (leu), tryptophan (trp), histidine (his), 500mM NaCl, or 300 mM KCl) for 10 minutes, then briefly pulsed with FM 4-64 to label PM immediately prior to imaging. **(B)** Hal5 localiza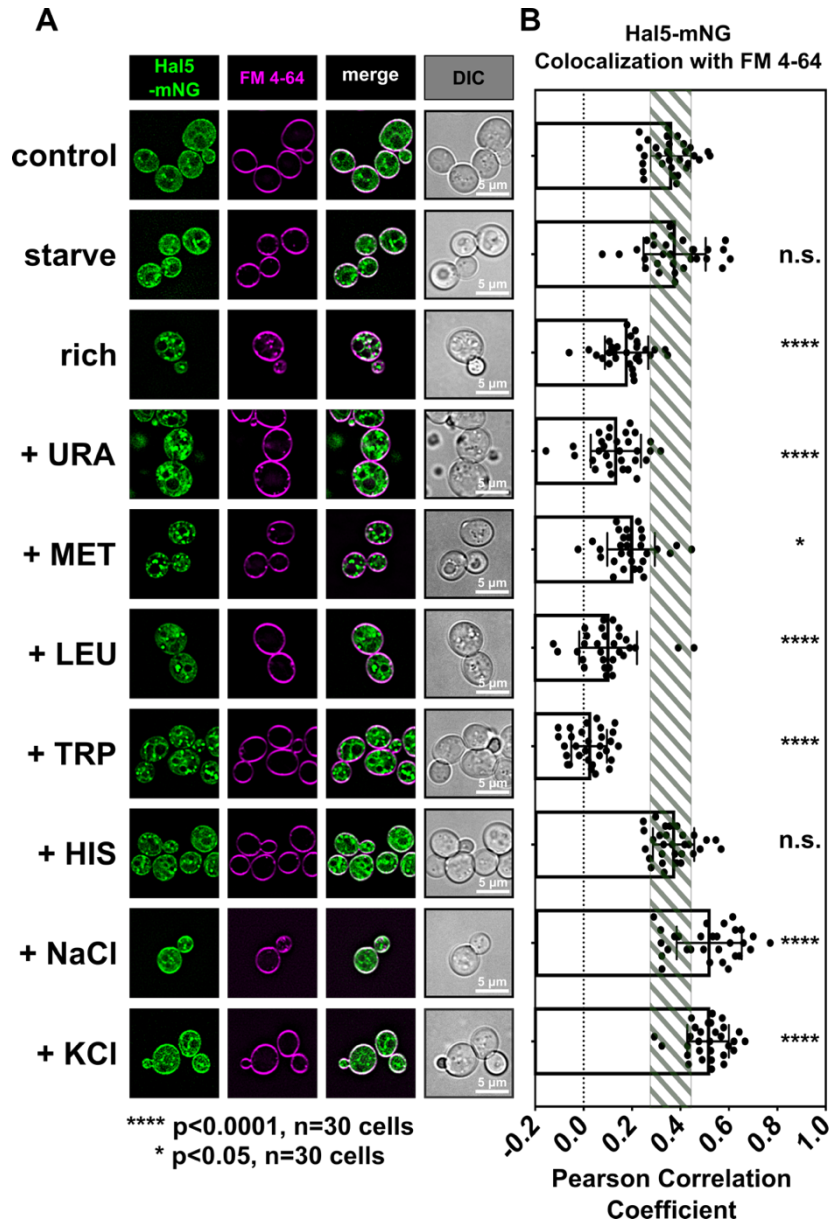tion to the PM was quantified in (A) by measuring Pearson correlation coefficient of Hal5-mNG signal with FM 4-64 signal. Standard deviation of WT cells is denoted by the green box
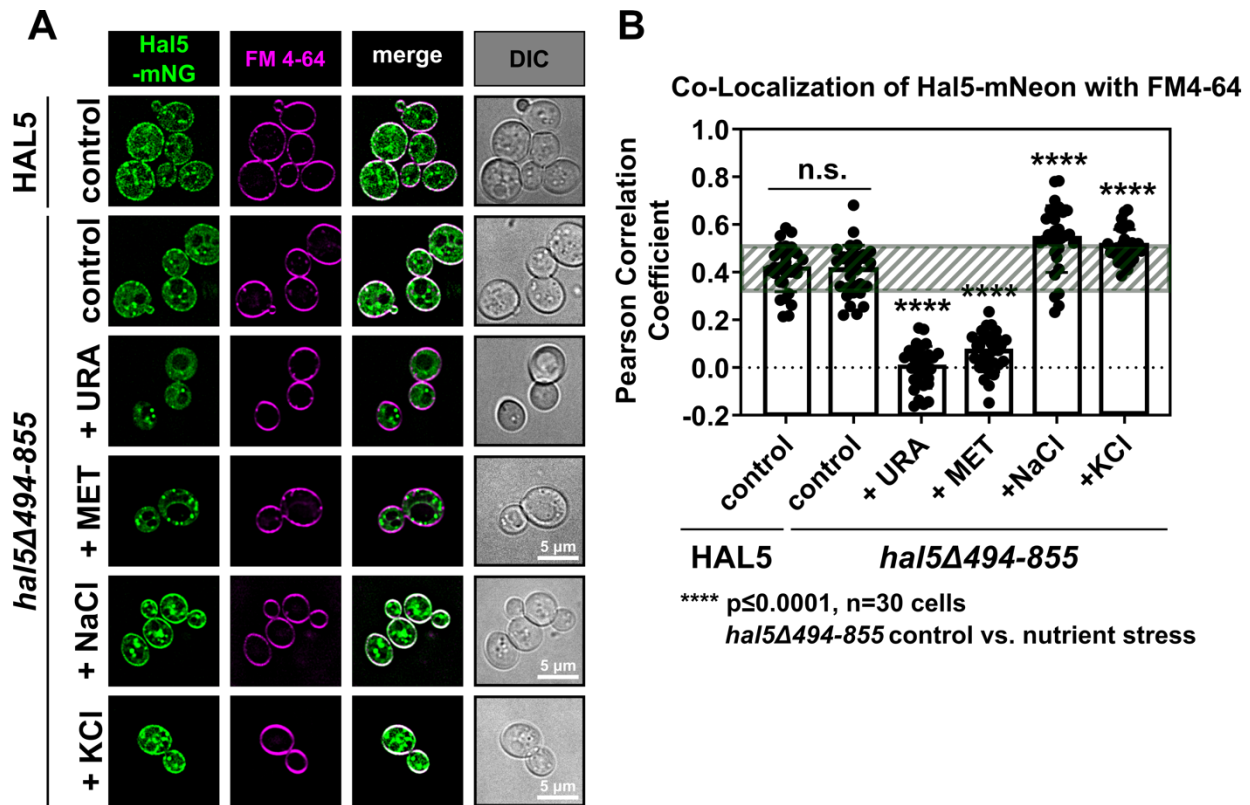
124

Figure 6.12 The N-terminal region of Hal5 is sufficient to mediate localization change in response to nutrients (A) Representative images of WT cells expressing a variant of Hal5-mNG deleted for the kinase domain from a centromeric plasmid under native promoter control. Cells were grown to mid-log phase in selective media then switched to media with the indicated nutrient conditions (10 μg/mL methionine (met), 10 μg/mL uracil (ura), 500mM NaCl, or 300 mM KCl) for 10 minutes, then briefly pulsed with FM 4-64 to label PM immediately prior to imaging. **(B)** Hal5 localization to the PM was quantified in (A) by measuring Pearson correlation coefficient of Hal5-mNG signal with FM 4-64 signal. Standard deviation untreated cells expressing full-length Hal5-mNG is denoted by the green box.
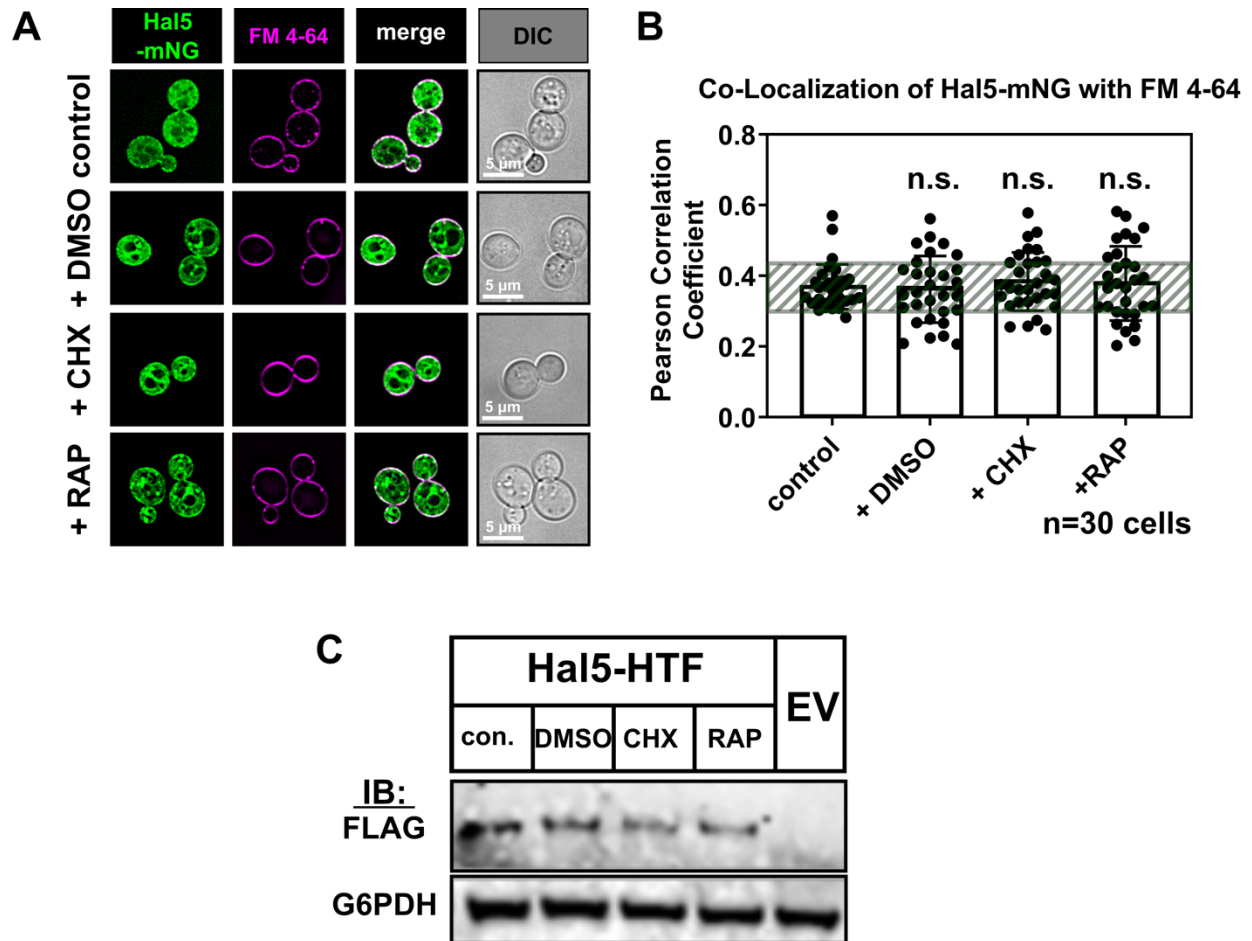
FIGURE 6.13 TORC1 activity does not regulate Hal5 localization to the PM (A) Representative images of WT cells expressing full-length Hal5-mNG as described in (A). Prior to pulsing with FM 4-64 to label the PM, cells were treated with either DMSO (mock), Cycloheximide (50 μg/mL) or Rapamycin (200 ng/mL) for 15 minutes. **(B)** Quantification of (C) as described in (B). **(C)** Immunoblot analysis of whole cell lysates collected from WT cells expressing full-length c-terminally tagged Hal5-HTF, treated with either DMSO (mock), Cycloheximide (50 μg/mL), or Rapamycin (200 ng/mL) for 15 minutes. EV indicates empty vector.

of Hal5 to the PM correlates with its role as an endocytic antagonist, and (iii) Hal5 PM localization is sensitive to changes in nutrient availability, with repletion of specific nutrients triggering Hal5 ejection from the PM. The work presented in this chapter includes the first analysis of Hal5 subcellular localization, builds on my previous findings to implicate non-catalytic regions of Hal5 in the regulation of endocytosis, and positions Hal5 as a potential signal transducer in a nutrient-sensing relay.

6.3.1 Regulation of Hal5 subcellular localization is distinct from that of Npr1

Both Hal5 and Npr1 are PM-localized in some conditions, and appear to be subject to extensive phosphorylation within the N-terminal region. In the case of Npr1, much of this phosphorylation appears to be TORC1-sensitive (MacGurn *et al.*, 2011). Inhibition of TORC1 using rapamycin results in decreased phosphorylation of Npr1, which correlates with increased PM-localization of Npr1 (MacGurn *et al.*, 2011). In contrast, PM-localization of Hal5 does not appear to be modulated by rapamycin or cycloheximide treatment (TORC1 inhibiting and activating, respectively), and is instead modulated by the availability of amino acids, nucleosides, and ions in the media (**Figures 6.11A-B** and **6.12A-B**). Upstream kinases mediating phosphorylation on Hal5 remain unidentified, although phosphorylation at serine residues 358 and 395 can be attributed to auto-regulation (**Figure 5.17A-B**), either directly through auto-phosphorylation or indirectly in some kind of feedback mechanism. Other Hal5 phosphorylation sites detected in quantitative SILAC-MS analysis were not sensitive to inhibition of Hal5AS (**Figure 5.17A-B**), suggesting trans-regulation by other kinases and phosphatases. For Hal5, it is clear that non-catalytic regions are important for function and PM-localization,

but the contribution of phosphorylation to this regulation remains unclear. Even though toggling TORC1 activity does not appear to impact Hal5 localization to the PM, it is possible that TORC1 mediates phosphorylation events on Hal5 to regulate some other facet of Hal5 function. As TORC1 ultimately functions in intracellular sensing of nitrogen availability, it is possible that, like Hal5, Npr1 localization to the PM may respond to changes in amino acid availability, although this has not been tested. For both Hal5 and Npr1, non-catalytic regions appear to be critical for PM-localization, but the mechanisms of regulation appear to be distinct. Further characterization of phosphorylation within the N-terminal region of Hal5 will be required to determine whether these events are critical for Hal5 function or localization, as has been established for the N-terminal phosphorylation of Npr1.

6.3.2 Localization determinants may be important functional features of the broader yeast AMPK/Snf1-related family

Several kinases in the yAMPK/Snf1-RK family have now been observed localizing to the PM. For example, Gin4, Kcc4, and Hsl1 exhibit strong localization to the PM, specifically at the bud-neck in dividing cells (Moravcevic *et al.*, 2010). Critical arginine and lysine residues within the KA1 domain of Kcc4 directly binds acidic phospholipids to mediate this localization, in conjunction with a septin-binding domain (Moravcevic *et al.*, 2010). In contrast to Hal5, phosphatidylserine appears to be critical for Kcc4 localization to the PM (Moravcevic *et al.*, 2010). Reminiscent to Kcc4 and KA1 domain containing kinases, a non-catalytic region of Hal5 appears to mediate PM-localization, though further characterization is necessary to determine whether this is mediated through lipid

binding. In contrast to non-catalytic regions of Hal5, it is not clear whether the KA1

domain in KCC4 is important for its function (Moravcevic *et al.*, 2010). However, the

KA1 domains of related kinases Gin4 and Hsl1 are essential for their functions

(Moravcevic *et al.*, 2010). The targeting of human AMPK-related Mark kinases to the

PM via lipid-binding determinants in KA1 domains suggests that regulation of catalytic

activity through targeted subcellular localization may be a conserved feature of the

broader AMPK/Snf1-related kinase family (Moravcevic *et al.*, 2010; Emptage *et al.*,

2017). Kin1 and Kin2 also have been identified as containing KA1 domains based on

sequence (Elbert *et al.*, 2005), but the localization of Kin1 and Kin2 remains

uncharacterized. In contrast to Hal5, deletion of these non-catalytic regions from Kin1

and Kin2 results in hyper-activation, indicating an auto-inhibitory role (Elbert *et al.*,

2005). Interestingly, the N-terminal region of Hal4, but not Hal5, is predicted to have a

mitochondrial membrane targeting sequence (Gey *et al.*, 2014). Consistent with this

prediction, previous studies have observed Hal4 fractionating with mitochondrial

membranes, and interacting with mitochondrial membrane proteins (Gey *et al.*, 2014),

although the subcellular localization of Hal4 has never been visualized. These studies

suggest that localization determinants may be an important feature of the large

uncharacterized non-catalytic regions of yeast AMPK/Snf1-related kinases.

6.3.3 Identification of Hal5 interaction partners may reveal functional insight

Hal5 has been reported to interact with many different proteins through a variety of high

and low-throughput protein-protein interaction studies (summarized in **Table 6.1**),

including proteins involved in metabolic processes such as the tryptophan biosynthesis

Interactor	Functional Description (BioGrid)	Role	Experimental Evidence Code	Dataset	Throughput
AIM3	Protein that inhibits barbed-end actin filament elongation; interacts with Rvs167p	HIT	**Biochemical Activity**	Ptacek J (2005)	High
ARC1	Protein that binds tRNA and methionyl- and glutamyl-tRNA synthetases; involved in tRNA delivery, stimulating catalysis, and ensuring localization	HIT	**Biochemical Activity**	Ptacek J (2005)	High
ATG31	Autophagy-specific protein required for autophagosome formation	HIT	**Biochemical Activity**	Ptacek J (2005)	High
BRE1	E3 ubiquitin ligase; forms heterodimer with Rad6p to monoubiquinate histone H2B-K123	HIT	**Biochemical Activity**	Ptacek J (2005)	High
CCR4	Component of the CCR4-NOT transcriptional complex; CCR4-NOT is involved in regulation of gene expression	BAIT	**Affinity Capture-RNA**	Miller JE (2017)	High
CDC28	Cyclin-dependent kinase (CDK) catalytic subunit; master regulator of mitotic and meiotic cell cycles	BAIT	**Affinity Capture-MS**	Yahya G (2014)	High
CDC37	Essential Hsp90p co-chaperone	BAIT	**Two-hybrid**	Millson S (2014)	Low
CLB2	B-type cyclin involved in cell cycle progression	HIT	**Biochemical Activity**	Ptacek J (2005)	High
CMR3	Putative zinc finger protein	HIT	**Biochemical Activity**	Ptacek J (2005)	High
CRM1	Major karyopherin; involved in export of proteins, RNAs, and ribosomal subunits from the nucleus; exportin	BAIT	**Affinity Capture-MS**	Kirli K (2015)	High
DAS2	Putative protein of unknown function	HIT	**Biochemical Activity**	Ptacek J (2005)	High
DHH1	Cytoplasmic DExD/H-box helicase, stimulates mRNA decapping	BAIT	**Affinity Capture-RNA**	Jungfleisch J (2017) and Miller JE (2017)	High
DMA2	Ubiquitin-protein ligase (E3); controls septin dynamics and spindle position checkpoint (SPOC) with ligase Dma1p by regulating recruitment of Elm1p to bud neck	HIT	**Biochemical Activity**	Ptacek J (2005)	High
DSN1	Essential component of the MIND kinetochore complex; joins kinetochore subunits contacting DNA to those contacting microtubules	BAIT	**Affinity Capture-MS**	Akiyoshi B (2010)	High
GPH1	Glycogen phosphorylase required for the mobilization of glycogen	BAIT	**Affinity Capture-MS**	Akiyoshi B (2010)	High
ISW1	ATPase subunit of imitation-switch (ISWI) class chromatin remodelers	HIT	**Biochemical Activity**	Ptacek J (2005)	High
ITR2	Myo-inositol transporter; member of the sugar transporter superfamily	HIT	**Affinity Capture-MS**	Ho Y (2002)	High
MBP1	Transcription factor; involved in regulation of cell cycle progression from G1 to S phase	HIT	**Biochemical Activity**	Ptacek J (2005)	High
MMF1	Mitochondrial protein required for transamination of isoleucine	HIT	**Affinity Capture-MS**	Breitkreutz A (2010)	High
NAB2	Nuclear polyadenylated RNA-binding protein; required for nuclear mRNA export and poly(A) tail length control	BAIT	**Affinity Capture-RNA**	Batisse J (2009)	High
NUP53	FG-nucleoporin component of central core of nuclear pore complex (NPC)	HIT	**Biochemical Activity**	Lusk CP (2007)	Low
PAH1	Mg2+-dependent phosphatidate (PA) phosphatase; dephosphorylates PA to yield diacylglycerol	HIT	**Biochemical Activity**	Ptacek J (2005)	High

Table 6.1 Summary of previously identified Hal5 protein interactions from high and low-throughput protein interaction studies This table displays data that has been curated by BioGrid, and augmented with functional information available about each interactor from SGD.

Interactor	Functional Description (BioGrid)	Role	Experimental Evidence Code	Dataset	Throughput
PCL10	Pho85p cyclin; recruits, activates, and targets Pho85p cyclin-dependent protein kinase to its substrate	HIT	**Biochemical Activity**	Ptacek J (2005)	High
PDS5	Cohesion maintenance factor; involved in sister chromatid condensation and cohesion	BAIT	**Affinity Capture-MS**	Graumann J (2004)	High
PPX1	Exopolyphosphatase; hydrolyzes inorganic polyphosphate (poly P) into Pi residues; located in the cytosol, plasma membrane, and mitochondrial matrix	HIT	**Biochemical Activity**	Ptacek J (2005)	High
PRM7	Pheromone-regulated protein; predicted to have one transmembrane segment; promoter contains Gcn4p binding elements	HIT	**Biochemical Activity**	Ptacek J (2005)	Low
RFA1	Subunit of heterotrimeric Replication Protein A (RPA); RPA is a highly conserved single-stranded DNA binding protein involved in DNA replication, repair, and recombination	HIT	**Biochemical Activity**	Ptacek J (2005)	High
RGT1	Glucose-responsive transcription factor; regulates expression of several glucose transporter (HXT) genes in response to glucose	HIT	**Biochemical Activity**	Kim JH (2006)	Low
RBP10	RNA polymerase subunit ABC10-beta; common to RNA polymerases I, II, and III	HIT	**Biochemical Activity**	Ptacek J (2005)	High
RPN3	Essential non-ATPase regulatory subunit of the 26S proteasome lid; similar to the p58 subunit of the human 26S proteasome	BAIT	**Affinity Capture-MS**	Krogan NJ (2006)	High
RPN11	Metalloprotease subunit of 19S regulatory particle; part of 26S proteasome lid	BAIT	**Affinity Capture-MS**	Kaake RM (2010)	High
RSC30	Component of the RSC chromatin remodeling complex	HIT	**Biochemical Activity**	Ptacek J (2005)	High
RVB2	ATP-dependent DNA helicase	BAIT	**Affinity Capture-MS**	Lakshminarasimhan	High
SHR3	Endoplasmic reticulum packaging chaperone	HIT	**Biochemical Activity**	Ptacek J (2005)	High
SMF1	Divalent metal ion transporter	HIT	**Biochemical Activity**	Ptacek J (2005)	High
SSA1	ATPase involved in protein folding and NLS-directed nuclear transport	BAIT	**Affinity Capture-MS**	Truman AW (2015)	High
SSD1	Translational repressor with a role in polar growth and wall integrity	HIT	**Biochemical Activity**	Ptacek J (2005)	High
TRP1	Phosphoribosylanthranilate isomerase; tryptophan bisynthesis enzyme	HIT	**Biochemical Activity**	Ptacek J (2005)	High
VAM6	Subunit of the HOPS endocytic tethering complex	HIT	**Biochemical Activity**	Ptacek J (2005)	High
YCF1	Vacuolar glutathione S-conjugate transporter	BAIT	**Affinity Capture-MS**	Elbaz-Alon Y (2014)	High
YCR016W	putative protein of unknown function	HIT	**Reconstituted Complex**	Fasolo J (2011)	High
YCR099C	putative protein of unknown function	HIT	**Biochemical Activity**	Ptacek J (2005)	High
YGR130C	putative protein of unknown function	HIT	**Biochemical Activity**	Ptacek J (2005)	High
YMC1	Putative mitochondrial inner membrane transporter; proposed role in oleate metabolism and glutamate biosynthesis	HIT	**Biochemical Activity**	Ptacek J (2005)	High
YML037C	putative protein of unknown function	HIT	**Biochemical Activity**	Ptacek J (2005)	High
YOR29C	putative protein of unknown function	HIT	**Biochemical Activity**	Ptacek J (2005)	High

Table 6.1 continued

enzyme Trp1 and glycogen phosphorylase Gph1, ubiquitin-protein ligases such as

Dma2 and Bre1, proteasome components Rpn3 and Rpn11, nutrient transporters like

Itr2, Smf1, and Ycf1, a subunit of the HOPS endocytic tethering complex called Vam6,

and glucose-responsive transcription factor Rgt1. Though many of these reported

interactions are from high-throughput studies, and still require validation, they are

consistent with a role for Hal5 in the regulation of cellular homeostasis, including

transcriptional regulation and endocytosis. It is possible that particular cellular

conditions induce Hal5 to associate with interacting partners, and that quantitative

SILAC-MS interactome analysis may need to be optimized for cell conditions to detect

physiological interactions. For example, excess extracellular amino acids promote the

physical interaction of Yck1 and Yck2 with SPS sensor components at the cell surface

in a mechanism to control substrate selection for otherwise constitutively active kinases

(Ljungdahl, 2009). Similarly, Tor1 relocalizes from a cytoplasmic pool to a lysosomal

membrane pool in response to intracellular amino acids concentrations in mammalian

cells, which promotes Tor1 association with active TORC1 complex subunits (Lawrence

et al., 2018). Therefore, one possibility is that nutrient stresses, like the ones that alter

Hal5 subcellular localization (**Figures 6.11A-B** and **6.12A-B**), may improve resolution of

physiological Hal5 interacting partners. Ultimately, characterizing Hal5 protein

interactions will provide mechanistic insight into its regulation of endocytosis.

In this Chapter, I shifted my focus to the functional role of the previously

uncharacterized N-terminal region of Hal5 kinase. I present evidence that elements in

the N-terminal region proximal to the kinase domain are critical for regulation of

endocytosis, subcellular localization, and nutrient response. These findings provide

novel insight into the underlying mechanism of Hal5 function in regulation of nutrient

transporter endocytosis.

CHAPTER 7

Discussion

7.1 Summary of results

By investigating the role of Hal kinases in stabilization of nutrient transporters, I present evidence that Hal kinases contribute to cellular homeostasis by functioning to antagonize endocytosis and broadly stabilize nutrient transporters at the PM (**Figure 7.1**). Specifically, I report that *(i)* Hal inhibition of endocytosis likely occurs upstream of the ART-Rsp5 network, *(ii)* both the Hal5 kinase activity and elements in the uncharacterized N-terminal domain are critical for regulation of endocytosis, *(iii)* localization of Hal5 to the PM correlates with its role as an endocytic antagonist, and *(iv)* Hal5 PM localization is responsive to changes in nutrient availability, with repletion of specific nutrients triggering Hal5 ejection from the PM. Generally, my findings contribute to the broader understanding of how endocytosis and signaling events are coupled to nutrient sensing to coordinate complex physiological processes like the adaptive growth response.

7.2 Conclusions

7.2.1 Hal kinases as antagonists of nutrient transporter endocytosis

Although the protein networks and machinery involved in endocytosis have been well characterized, mechanisms that regulate endocytic site assembly and cargo selection
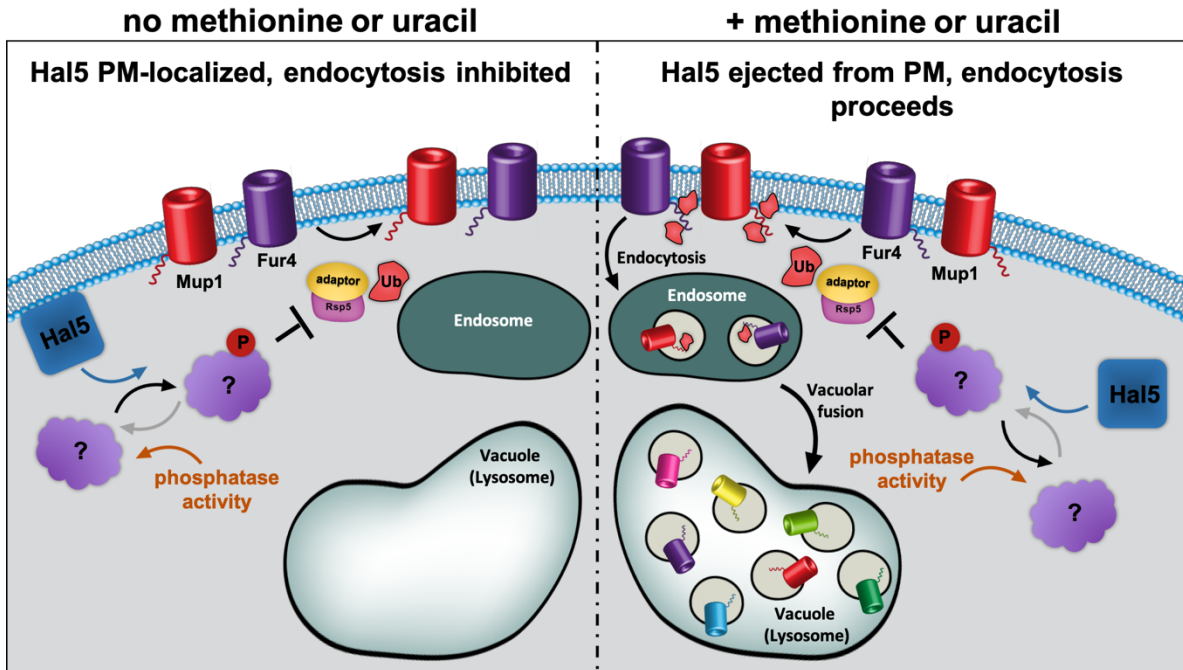
Figure 7.1 Model of Hal5 inhibition of nutrient transporter endocytosis Hal5 acts as an endocytic gatekeeper, localizing to the plasma-membrane to inhibit nutrient transporter endocytosis until the appropriate signal received. In conditions of excess nutrients, such as methionine or uracil, Hal5 is ejected from the plasma-membrane, allowing endocytosis of nutrient transporters to proceed.

remain poorly understood. Phospho-regulation is known to occur at different stages

along the endocytic trafficking route, and can involve regulation of cargo selection

(MacGurn *et al.*, 2011; Alvaro *et al.*, 2016; Lee *et al.*, 2019), endocytic site assembly

(Chi *et al.*, 2012; Peng *et al.*, 2015), multi-vesicular body (MVB) sorting (Morvan *et al.*,

2012), or recycling from endosomes (Lee *et al.*, 2017).

Npr1 and Snf1 represent well-characterized examples of phospho-regulation at the level

of cargo-selection. Snf1 phosphorylates arrestin-like adaptor protein Art4 to inhibit

endocytosis of glucose and lactate transporters (Coccetti *et al.*, 2018), while Npr1

phosphorylates arrestin-like adaptor proteins Art1, Bul1, and Bul2 to inhibit endocytosis

of arginine transporter Can1 the general amino acid permease Gap1 (Merhi and André,

2012). Similar to Npr1 and Snf1, Hal5 inhibits endocytosis of nutrient transporters,

although the list of transporters impacted by Hal kinases is more expansive than that

reported for Npr1 and Snf1, spanning multiple nutrient classes that are known to require

a wide variety of arrestin-related adaptor proteins. Thus, the negative regulatory control

that Hal kinases exert over endocytosis appears to be broader than Npr1 or Snf1. At

least two Art1 phosphorylation events, at Thr93 and Thr795, are important for endocytic

downregulation of Art1-dependent cargo (Lee *et al.*, 2019). However, phosphorylation at

these residues does not appear to be regulated by Hal5 kinases (**Figures 5.12D, 5.13D,**

and **5.14D**). Globally, phosphorylation of Art1 appears unchanged or slightly elevated in

hal mutants (**Figures 5.12C, 5.13C,** and **5.14C**), inconsistent with the possibility that

Hal5 inhibition of endocytosis occurs through phosphorylation of Art1, as is

demonstrated for Npr1. This may indicate that Hal5 regulates Art1 through an

uncharacterized mechanism, although this seems unlikely due to Hal-regulation of Art1-indepndent endocytosis of Fur4 (**Figures 4.16A-B** and **5.7A-B**). Instead, it seems more likely that Hal5 regulation of endocytosis could occur at the level of Rsp5, which interacts with all arrestin-related adaptor proteins, or even upstream of the ART-Rsp5 network.

A well-characterized example of regulation of endocytic assemblies in yeast involves the casein kinase Hrr25 (CKδ/ε in mammalian cells) which localizes to the PM in a discrete punctate pattern (Peng *et al.*, 2015). Hrr25 was found to localize to endocytic sites and arrives concurrently with the early endocytic site protein Ede1, which is itself a substrate for the Hrr25 kinase (Peng *et al.*, 2015). Thus, Hrr25 is an example of a kinase that generally regulates endocytosis by direct phosphorylation of endocytic site components. Like Hrr25, Hal5 also localizes to the PM in a punctate pattern, but in contrast to Hrr25 I find that Hal5 does not exhibit significant co-localization with known endocytic site components (**Figure 6.5A**). Although I cannot exclude the possibility that Hal5 may regulate the endocytic machinery, I believe my data suggests that Hal kinases operate upstream of endocytic site assembly, which is triggered by Rsp5/Art-mediated ubiquitylation.

One possible mechanism of action for Hal kinases could involve direct phosphorylation of a broad array of nutrient transporters at the PM. A demonstrated example of cargo phosphorylation is illustrated by regulation of the essential yeast plasma membrane proton pump, Pma1, by Ptk2 (Eraso *et al.*, 2006; Lecchi *et al.*, 2007; Mazón *et al.*,

2015). Ptk2, a ySnf1-RK related to Hal4 and Hal5, localizes to the PM and

phosphorylates Serine 899 within the C-terminal tail of Pma1 to activate it in response

to glucose stimulation (Eraso *et al.*, 2006). Due to demonstrated roles for the C-terminal

cytoplasmic tail of Pma1 in secretion to the PM, stability at the PM, as well as glucose-

activated enzymatic activity (Mason *et al.*, 2014), it is not clear whether this

phosphorylation event regulates enzymatic activity, protein abundance, or some

combination. My study, along with previous reports, suggests that regulation by Hal

kinases is quite broad and extends beyond APC superfamily transporters that move

amino acids and nucleosides into the cell to include glucose transporters as well as ion

transporters and the essential proton pump, Pma1 (Mulet *et al.*, 1999; Pérez-Valle *et al.*,

2007). Given the diverse portfolio of transporters subject to Hal kinase regulation, I think

a model involving direct phosphorylation of cargo by Hal kinases at the PM is unlikely.

Alternatively, Hal kinases may broadly inhibit nutrient transporter endocytosis by

regulation of plasma membrane organization. The eukaryotic plasma membrane is often

described as having a patchwork organization of many different microdomains, each

with a unique identity and distinct function marked by enrichment in particular proteins

and lipids (Grossmann *et al.*, 2007; Douglas and Konopka, 2014; Schuberth and

Wedlich-Söldner, 2015). For example, eisosomes are endocytosis-resistant

microdomains of the yeast PM that protect cargo from access by ubiquitylation

machinery (Grossmann *et al.*, 2008; Douglas *et al.*, 2011; Ziółkowska *et al.*, 2011;

Gournas *et al.*, 2018; Moharir *et al.*, 2018). Nutrient transporters Can1 and Fur4

organize into eisosome compartments in the absence of substrate (arginine and uracil,

respectively) while stimulation of cells with excess substrate triggers re-organization of

nutrient transporters away from eisosomal compartments (Gournas *et al.*, 2018; Moharir

et al., 2018). This movement may depend on conformational changes induced by

substrate binding, as mutations that prevent conformational changes during substrate

transport result in increased association with the eisosomal compartment (Gournas *et

al.*, 2018). Interestingly, structural components of the eisosome undergo extensive

phosphorylation, but the physiological significance of such phosphorylation events is not

currently understood (Douglas *et al.*, 2012; Douglas and Konopka, 2014; Roelants *et

al.*, 2017; Gournas *et al.*, 2018). Thus, it is possible that Hal kinases may antagonize

endocytosis by regulating the function of eisosomes at the PM. However, I did not

observe appreciable co-localization of Hal5 with eisosomes (**Figure 6.5B**) or disruption

of eisosome microdomains in *hal* mutant cells (**Figure 4.5**). Thus, more detailed

experimentation will be required to determine if Hal kinases regulate eisosome

composition or function.

7.2.2 Hal kinases are PM-localized nutrient-responsive trafficking regulators

My localization of Hal5 to the PM (**Figures 6.3A-B** and **6.4B-C**), and characterization of

its response to changing environmental conditions (**Figure 6.11A-B** and **6.12A-B**)

suggests that Hal5 kinase activity at the PM may be inhibited upon changes in the

availability of specific nutrients, like methionine and uracil. TORC1 (mTORC1) is a well-

characterized nutrient-sensing kinase that signals from the limiting membrane of the

vacuole to control catabolic and anabolic decisions (including protein synthesis or

autophagy) in response to availability of specific nutrients including nitrogen, glucose,

and lipids (Lawrence and Zoncu, 2019). Despite a significant cytosolic population of mTORC1, and a relatively small fraction of mTORC1 localized to lysosomal membranes, it is thought that most mTORC1 kinase activity occurs at the lysosomal/vacuolar membrane (Lawrence *et al.*, 2018). High cytoplasmic amino acid concentrations (mainly leucine, arginine, and glutamine) promote the ability of mTORC1 to localize to lysosomal/vacuolar membranes (Sancak *et al.*, 2008; Zoncu *et al.*, 2011; Jewell *et al.*, 2015). My data suggests that Hal5 may be regulated in a manner analogous to TORC1, since nutrient availability affects its ability to localize to the PM.

Despite the spatial restriction of active mTORC1 in mammalian cells (as well as yeast), TORC1 has recently been demonstrated to exert regulatory control over endocytosis in yeast. One way in which it does this is through negative regulation of Npr1 (an NPR1/HAL5 kinase related to Hal4 and Hal5) to regulate composition of the PM proteome, and therefore nutrient influx (Schmidt *et al.*, 1998; MacGurn *et al.*, 2011; Merhi *et al.*, 2011; Merhi and André, 2012). In contrast to my findings for Hal kinases, Npr1 is thought to antagonize endocytosis at the level of specific Rsp5 adaptor proteins, including Art1, Bul1, and Bul2, and therefore impact a more specific subset of endocytic cargo (MacGurn *et al.*, 2011; Merhi *et al.*, 2011; Merhi and André, 2012). Surprisingly, previous reports indicate that overexpression of Npr1 improves *hal* mutant growth defects through stabilization of nutrient transporters at the PM (Primo *et al.*, 2017), suggesting that Npr1 may compensate for some Hal functions. Furthermore, phosphoinhibition of Art1 is antagonized, at least in part, by Ppz phosphatases, although the mechanism is orthogonal to Npr1-mediated phospho-inhibition of Art1 (Lee

et al., 2019). Similar to Hal kinases, Ppz phosphatases are well-characterized for their

role in potassium and ion homeostasis (Posas *et al.*, 1993; Yenush *et al.*, 2002; Ruiz *et*

al., 2004). Given that both Hal kinases and Ppz phosphatases regulate potassium and

ion homeostasis, and the observed genetic interactions of *hal* and *ppz* mutants (**Figure**

5.8), I speculate that Ppz phosphatases may also antagonize Hal kinase activities that

regulate endocytosis of nutrient transporters.

7.2.3 Regulation of ySnf1-RKs by elements in the N-terminal domains

The ySnf1-RK family of kinases shares conservation restricted to the catalytic domains

(**Figure 3.4**). Outside of the catalytic domains, sequences are divergent. For example,

the N-terminal regions of Hal4 and Hal5 do not exhibit any considerable degree of

sequence conservation with each other or other family members, which have been

largely uncharacterized. Snf1 (AMPK in mammalian cells), one of the best characterized

nutrient-sensing kinase regulators of endocytic downregulation, exists as a catalytic

subunit (α) in a heterotrimeric complex that is autoinhibited, and that autoinhibition is

released as glucose is depleted (Coccetti *et al.*, 2018). Other members of this

heterotrimeric complex include Snf4, an invariant stimulatory subunit (γ), and a variable

(β) subunit which consists of either Sip1, Sip2, or Gal83 (Coccetti *et al.*, 2018). In Snf1

complexes, the β subunit confers specificity to activated Snf1 by targeting subcellular

localization and mediating substrate interactions (Schmidt and McCartney, 2000;

Vincent *et al.*, 2001). Interestingly, inactivate Snf1 in complex with any one of the three

β subunits localizes to the cytosol, while active Snf1 in complex with Sip1 re-localizes to

the vacuole and association with Gal83 re-localizes active Snf1 to the nucleus (Vincent

et al., 2001). Active Snf1 association with Sip2 remains localizes to the cytosol (Vincent

et al., 2001). Thus, the nutrient-sensing capabilities, subcellular localization, and

substrate interactions of Snf1 are governed by its association with different subunits *in-*

trans. My data suggests that nutrient-responsiveness and subcellular localization of

Hal5 are controlled by its N-terminal region *in-cis*. Alternatively, it is possible that Hal

kinases may interact with regulatory subunits that contribute to its regulation or

localization, although such interacting proteins are yet to be identified. In contrast to

Snf1, it is currently unknown if Hal kinases are capable of directly sensing nutrients or if

they indirectly respond to changes in nutrient availability, as has been established for

the Npr1 kinase.

Considering the divergence of N-terminal domains of ySnf1-RKs, I speculate that the N-

terminal regions confer substrate targeting and subcellular localization of these kinases,

similar to the accessory subunits of the heterotrimeric Snf1 complexes. Consistent with

this hypothesis, active Npr1 localizes to the PM, and inhibition of TORC1 signaling with

rapamycin treatment alters both Npr1 localization as well as phosphorylation events in

the N-terminal region (Bonenfant *et al*., 2003; Breitkreutz *et al.*, 2010; MacGurn *et al.*,

2011). In addition to those identified in this study, high-throughput proteomics studies

have identified multiple phosphorylation events on Hal5 that occur throughout the N-

terminal region (Chi *et al.*, 2007; Li *et al.*, 2007; Albuquerque *et al.*, 2008; Holt *et al.*,

2009), but the physiological significance of those events is not currently understood.

Thus, similar to Npr1, it is possible that Hal kinases are regulated by phosphorylation

events that occur within the N-terminal domain, and such phosphorylation may impact

the ability of Hal5 to localize to the PM. Although there are clear differences in Npr1 and

Hal5 function, in each case regulatory elements of otherwise divergent N-terminal

regions control subcellular localization, are nutrient-responsive, and are important for

function. Therefore, I propose that regulation ySnf1-RKs, like Npr1 and Hal5, may be

similar to regulation of Snf1, except that *cis*-acting elements in the N-terminal regions

may function in regulation of localization or substrate selection, analogous to the β

subunits of Snf1. Interestingly, Hal4 is predicted to have a mitochondrial targeting

sequence and has been found to sediment in mitochondrial subcellular fractions (Gey *et*

al., 2014). In contrast, Hal5 is not predicted to have a mitochondrial targeting sequence,

and I speculate that differential subcellular localization of Hal4 and Hal5 kinases is

critical for understanding how these activities are coordinated. Furthermore, differential

subcellular localization of Hal4 and Hal5 may explain why their functions appear to be

distinct in some cases (**Figure 5.8**).

7.3 Future directions

7.3.1 What is the catalytic mechanism of Hal5 inhibition of nutrient transporter

endocytosis?

My findings indicate that Hal5 maintains cellular homeostasis through negative

regulation of nutrient transporter endocytosis, that catalytic activity is required, and that

regulation is distinct from that observed for Npr1. Unlike Npr1, Hal5 substrates remain

to be identified. The *hal5AS* allele developed and characterized in my work can be used

in future studies to address this knowledge gap. For example, quantitative SILAC-MS

experiments may be used in an unbiased or candidate approach to identify

phosphorylation events that change during acute inhibition of Hal5AS. Some important

experiments include identification of the global Hal5 phosphoproteome, an examination

of Hal5 phosphorylation at the plasma-membrane, and investigation of Rsp5 and

nutrient transporters as candidate Hal5 substrates. Importantly, identifying Hal5

substrates will reveal a molecular mechanism for Hal5-mediated regulation of endocytic

trafficking, and will more broadly provide mechanistic insight into regulation of endocytic

trafficking by signaling networks.

Using quantitative SILAC-MS experiments, Hal5 itself has been identified as a putative

substrate during the course of my work. Even though this experiment was performed

under acute inhibition, which suggests direct auto-phosphorylation, indirect

phosphorylation by upstream kinases cannot be excluded. Furthermore, the

physiological significance of these phosphorylation events is unclear. *In vitro*

reconstitution of Hal5 activity would confirm Hal5 auto-phosphorylation, and phosphor-

resistant point mutations of Hal5, like Ser358Ala or Ser395Ala, can be used in

complementation assays developed during this study to interrogate the physiological

significance of these phosphorylation events. Due to the instability observed for catalytic

dead point mutants of Hal5 (**Figure 5.3C**), and the stabilization observed for N-terminal

truncations of Hal5 (**Figure 6.1D**), one prediction is that Hal5 auto-phosphorylation

regulates its stability. Parallel to these observations, acute inhibition of endocytosis with

LatA treatment results in stabilization of Hal5 at the PM (**Figure 6.6A-D**). Taken

together, these results suggest that the cell may regulate Hal5 activity in a feedback

mechanism that involves auto-regulation and endocytic trafficking. Ultimately, understanding auto-phosphorylation of Hal5 may contribute to our understanding of how the cell manages Hal5 activity, which is important for maintenance of cellular homeostasis and nutrient transporter stability at the cell surface.

7.3.2 How does Hal5 localize to the plasma-membrane?

My findings indicate that PM-localization of Hal5 correlates with its functional role in endocytic trafficking, and that non-catalytic regions of Hal5 are critical for this. Hal5 is not predicted to have any transmembrane spanning regions, and the secretory pathway is not required for Hal5 localization to the PM (**Figure 6.9A-B**), arguing against Hal5 integration into the PM. Furthermore, Hal5 localization to the PM is altered by nutrient availability (**Figures 6.11A-B** and **6.12A-B**). Thus, it seems likely that Hal5 localization to the PM is regulated, and that this likely regulates proximity of Hal5 to substrates important for its role in nutrient transporter endocytosis. However, it is not clear from my studies whether Hal5 is targeted to the PM through direct binding of lipids at the PM, indirect binding of peripheral membrane proteins, or some combination. A portion of the N-terminal region of Hal5 that is important for PM-localization and function appears to align with KA1 domains from other yAMPK/Snf-RKs (**Figure 6.8**), and PI(P) lipids appear to be important for Hal5 PM-localization (**Figure 6.9A-B**). Based on these results, one hypothesis is that Hal5 is capable of directly binding lipids at the PM. To test this hypothesis, purified recombinant Hal5, both full-length and the N-terminal region, can be used in lipid dot-blots and liposome binding assays to determine whether Hal5 is capable of binding lipids *in vitro* and to determine lipid composition preference.

Additionally, the quantitative SILAC-MS interactome analysis performed for Hal5 (**Figure 6.7A-C**) might be optimized to resolve relevant physiological interacting partners. For example, Hal5 PM-localization increases in response to salt treatment (**Figure 6.11A-B** and **6.12A-B**) or acute inhibition of endocytosis with LatA (**Figure 6.6A-D**). One prediction is that Hal5 interaction with peripherally bound proteins may increase under these conditions. Parallel to that, Hal5 PM-localization decreases in response to methionine and uracil treatment (**Figures 6.11A-B** and **6.12A-B**), suggesting that Hal5 interactions may shift to cytosolic under these conditions. Characterizing the nature of Hal5 PM association will reveal mechanistic insight underlying its regulation of endocytosis and its nutrient-responsiveness, and will inform our broader understanding of Snf/AMPK-RKs.

7.3.3 What is the contribution of Hal4 to regulation of nutrient transporter endocytosis?
Given the complexity of phenotypes associated with loss of both Hal4 and Hal5, I deliberately chose to focus on a single kinase (Hal5) over the course of my studies in an effort to better elucidate the mechanism by which these kinases regulate nutrient transporter stability. Thus, important questions regarding Hal4 have not yet been addressed. A similar characterization and analysis that I have performed for Hal5 should be applied to Hal4 to determine whether *hal4* phenotypes are due to off-target effects, whether Hal4 catalytic activity is required, and to investigate the function of the large uncharacterized N-terminal region of Hal4, including its subcellular localization and nutrient-responsiveness. Hal4, but not Hal5, is predicted to have a mitochondrial targeting sequence (Gey *et al.*, 2014), suggesting that, in contrast to Hal5, Hal4 may

localize to mitochondria. Consistent with this hypothesis, *hal4* single mutants, but not

hal5 single mutants, are defective for growth in glucose-scarce conditions (**Figure**

4.13B). This growth defect is suppressed by treatment with antimycin (data not shown,

Nathaniel Hepowit, PhD.), an inhibitor of cellular respiration, consistent with a role for

Hal4 at the mitochondria. One prediction is that, in addition to its role in nutrient

transporter homeostasis, Hal4 has a distinct role in signaling from the mitochondria to

control energy metabolism. Perhaps a more interesting hypothesis is that differential

subcellular localization of Hal4 and Hal5 allows the cell to maintain nutrient homeostasis

and nutrient transporter stability by coordinating signals about nutrient status across

different subcellular compartments. This idea is not unlike what is observed for

TORC1/Npr1-mediated regulation of nutrient transporter endocytosis, where TORC1

senses nutrient status at the limiting membrane of the vacuole to regulate endocytosis

of nutrient transporters through the activity of PM-localized Npr1. Ultimately,

characterizing the activity and subcellular localization of Hal4 will improve our

understanding of how Hal kinases maintain cellular homeostasis, and will help us to

understand how cells sense and respond to environmental cues.

References

Ahalawat, N., and Murarka, R.K. (2017). Molecular Mechanism of Nucleotide-Dependent Allosteric Regulation in AMP-Activated Protein Kinase. J Phys Chem B *121*, 2919-2930.

Albuquerque, C.P., Smolka, M.B., Payne, S.H., Bafna, V., Eng, J., and Zhou, H. (2008). A multidimensional chromatography technology for in-depth phosphoproteome analysis. Mol Cell Proteomics *7*, 1389-1396.

Alvaro, C.G., Aindow, A., and Thorner, J. (2016). Differential Phosphorylation Provides a Switch to Control How α-Arrestin Rod1 Down-regulates Mating Pheromone Response in Saccharomyces cerevisiae. Genetics *203*, 299-317.

Andréasson, C., Heessen, S., and Ljungdahl, P.O. (2006). Regulation of transcription factor latency by receptor-activated proteolysis. Genes Dev *20*, 1563-1568.

Ardito, F., Giuliani, M., Perrone, D., Troiano, G., and Lo Muzio, L. (2017). The crucial role of protein phosphorylation in cell signaling and its use as targeted therapy (Review). Int J Mol Med *40*, 271-280.

Atkinson, K.D., Jensen, B., Kolat, A.I., Storm, E.M., Henry, S.A., and Fogel, S. (1980). Yeast mutants auxotrophic for choline or ethanolamine. J Bacteriol *141*, 558-564.

Auger, K.R., Carpenter, C.L., Cantley, L.C., and Varticovski, L. (1989). Phosphatidylinositol 3-kinase and its novel product, phosphatidylinositol 3-phosphate, are present in Saccharomyces cerevisiae. J Biol Chem *264*, 20181-20184.

Azzam, Z.S., Kinaneh, S., Bahouth, F., Ismael-Badarneh, R., Khoury, E., and Abassi, Z. (2017). Involvement of Cytokines in the Pathogenesis of Salt and Water Imbalance in Congestive Heart Failure. Front Immunol *8*, 716.

Beck, T., and Hall, M.N. (1999). The TOR signalling pathway controls nuclear localization of nutrient-regulated transcription factors. Nature *402*, 689-692.

Becuwe, M., Vieira, N., Lara, D., Gomes-Rezende, J., Soares-Cunha, C., Casal, M., Haguenauer-Tsapis, R., Vincent, O., Paiva, S., and Léon, S. (2012). A molecular switch on an arrestin-like protein relays glucose signaling to transporter endocytosis. J Cell Biol *196*, 247-259.

Benito, B., Moreno, E., and Lagunas, R. (1991). Half-life of the plasma membrane ATPase and its activating system in resting yeast cells. Biochim Biophys Acta *1063*, 265-268.

Bertram, P.G., Choi, J.H., Carvalho, J., Ai, W., Zeng, C., Chan, T.F., and Zheng, X.F. (2000). Tripartite regulation of Gln3p by TOR, Ure2p, and phosphatases. J Biol Chem *275*, 35727-35733.

Blazek, A.D., Paleo, B.J., and Weisleder, N. (2015). Plasma Membrane Repair: A Central Process for Maintaining Cellular Homeostasis. Physiology (Bethesda) *30*, 438-448.

Bonenfant, D., Schmelzle, T., Jacinto, E., Crespo, J.L., Mini, T., Hall, M.N., and Jenoe, P. (2003). Quantitation of changes in protein phosphorylation: a simple method based on stable isotope labeling and mass spectrometry. Proc Natl Acad Sci U S A *100*, 880-885.

Breitkreutz, A., Choi, H., Sharom, J.R., Boucher, L., Neduva, V., Larsen, B., Lin, Z.Y., Breitkreutz, B.J., Stark, C., Liu, G., Ahn, J., Dewar-Darch, D., Reguly, T., Tang, X., Almeida, R., Qin, Z.S., Pawson, T., Gingras, A.C., Nesvizhskii, A.I., and Tyers, M. (2010). A global protein kinase and phosphatase interaction network in yeast. Science *328*, 1043-1046.

Bright, N.J., Thornton, C., and Carling, D. (2009). The regulation and function of mammalian AMPK-related kinases. Acta Physiol (Oxf) *196*, 15-26.

Bronner, M., Hertz, R., and Bar-Tana, J. (2004). Kinase-independent transcriptional co-activation of peroxisome proliferator-activated receptor alpha by AMP-activated protein kinase. Biochem J *384*, 295-305.

Carr, C.M., Grote, E., Munson, M., Hughson, F.M., and Novick, P.J. (1999). Sec1p binds to SNARE complexes and concentrates at sites of secretion. J Cell Biol *146*, 333-344.

Carroll, S.Y., Stimpson, H.E., Weinberg, J., Toret, C.P., Sun, Y., and Drubin, D.G. (2012). Analysis of yeast endocytic site formation and maturation through a regulatory transition point. Mol Biol Cell *23*, 657-668.

Casado, C., Yenush, L., Melero, C., Ruiz, M.e.C., Serrano, R., Pérez-Valle, J., Ariño, J., and Ramos, J. (2010). Regulation of Trk-dependent potassium transport by the calcineurin pathway involves the Hal5 kinase. FEBS Lett *584*, 2415-2420.

Chang, A., and Fink, G.R. (1995). Targeting of the yeast plasma membrane [H+]ATPase: a novel gene AST1 prevents mislocalization of mutant ATPase to the vacuole. J Cell Biol *128*, 39-49.

Chi, A., Huttenhower, C., Geer, L.Y., Coon, J.J., Syka, J.E., Bai, D.L., Shabanowitz, J., Burke, D.J., Troyanskaya, O.G., and Hunt, D.F. (2007). Analysis of phosphorylation sites on proteins from Saccharomyces cerevisiae by electron transfer dissociation (ETD) mass spectrometry. Proc Natl Acad Sci U S A *104*, 2193-2198.

Chi, R.J., Torres, O.T., Segarra, V.A., Lansley, T., Chang, J.S., Newpher, T.M., and Lemmon, S.K. (2012). Role of Scd5, a protein phosphatase-1 targeting protein, in phosphoregulation of Sla1 during endocytosis. J Cell Sci *125*, 4728-4739.

Coccetti, P., Nicastro, R., and Tripodi, F. (2018). Conventional and emerging roles of the energy sensor Snf1/AMPK in. Microb Cell *5*, 482-494.

Coué, M., Brenner, S.L., Spector, I., and Korn, E.D. (1987). Inhibition of actin polymerization by latrunculin A. FEBS Lett *213*, 316-318.

Cox, K.H., Kulkarni, A., Tate, J.J., and Cooper, T.G. (2004). Gln3 phosphorylation and intracellular localization in nutrient limitation and starvation differ from those generated by rapamycin inhibition of Tor1/2 in Saccharomyces cerevisiae. J Biol Chem *279*, 10270-10278.

DeWitt, N.D., dos Santos, C.F., Allen, K.E., and Slayman, C.W. (1998). Phosphorylation region of the yeast plasma-membrane H+-ATPase. Role in protein folding and biogenesis. J Biol Chem *273*, 21744-21751.

Douglas, L.M., and Konopka, J.B. (2014). Fungal membrane organization: the eisosome concept. Annu Rev Microbiol *68*, 377-393.

Douglas, L.M., Wang, H.X., Keppler-Ross, S., Dean, N., and Konopka, J.B. (2012). Sur7 promotes plasma membrane organization and is needed for resistance to stressful conditions and to the invasive growth and virulence of Candida albicans. MBio *3*.

Douglas, L.M., Wang, H.X., Li, L., and Konopka, J.B. (2011). Membrane Compartment Occupied by Can1 (MCC) and Eisosome Subdomains of the Fungal Plasma Membrane. Membranes (Basel) *1*, 394-411.

Drozdetskiy, A., Cole, C., Procter, J., and Barton, G.J. (2015). JPred4: a protein secondary structure prediction server. Nucleic Acids Res *43*, W389-394.

Elbert, M., Rossi, G., and Brennwald, P. (2005). The yeast par-1 homologs kin1 and kin2 show genetic and physical interactions with components of the exocytic machinery. Mol Biol Cell *16*, 532-549.

Emptage, R.P., Lemmon, M.A., and Ferguson, K.M. (2017). Molecular determinants of KA1 domain-mediated autoinhibition and phospholipid activation of MARK1 kinase. Biochem J *474*, 385-398.

Engqvist-Goldstein, A.E., and Drubin, D.G. (2003). Actin assembly and endocytosis: from yeast to mammals. Annu Rev Cell Dev Biol *19*, 287-332.

Eraso, P., Cid, A., and Serrano, R. (1987). Tight control of the amount of yeast plasma membrane ATPase during changes in growth conditions and gene dosage. FEBS Lett *224*, 193-197.

Eraso, P., Mazón, M.J., and Portillo, F. (2006). Yeast protein kinase Ptk2 localizes at the plasma membrane and phosphorylates in vitro the C-terminal peptide of the H+-ATPase. Biochim Biophys Acta *1758*, 164-170.

Forsberg, H., Gilstring, C.F., Zargari, A., Martínez, P., and Ljungdahl, P.O. (2001). The role of the yeast plasma membrane SPS nutrient sensor in the metabolic response to extracellular amino acids. Mol Microbiol *42*, 215-228.

Galan, J.M., Wiederkehr, A., Seol, J.H., Haguenauer-Tsapis, R., Deshaies, R.J., Riezman, H., and Peter, M. (2001). Skp1p and the F-box protein Rcy1p form a non-SCF complex involved in recycling of the SNARE Snc1p in yeast. Mol Cell Biol *21*, 3105-3117.

Galloway, D.A., Phillips, A.E.M., Owen, D.R.J., and Moore, C.S. (2019). Phagocytosis in the Brain: Homeostasis and Disease. Front Immunol *10*, 790.

Gander, S., Bonenfant, D., Altermatt, P., Martin, D.E., Hauri, S., Moes, S., Hall, M.N., and Jenoe, P. (2008). Identification of the rapamycin-sensitive phosphorylation sites within the Ser/Thr-rich domain of the yeast Npr1 protein kinase. Rapid Commun Mass Spectrom *22*, 3743-3753.

Garcia-Bustos, J.F., Marini, F., Stevenson, I., Frei, C., and Hall, M.N. (1994). PIK1, an essential phosphatidylinositol 4-kinase associated with the yeast nucleus. EMBO J *13*, 2352-2361.

Gey, U., Czupalla, C., Hoflack, B., Krause, U., and Rödel, G. (2014). Proteomic analysis reveals a novel function of the kinase Sat4p in Saccharomyces cerevisiae mitochondria. PLoS One *9*, e103956.

Ghaddar, K., Merhi, A., Saliba, E., Krammer, E.M., Prévost, M., and André, B. (2014). Substrate-induced ubiquitylation and endocytosis of yeast amino acid permeases. Mol Cell Biol *34*, 4447-4463.

Godard, P., Urrestarazu, A., Vissers, S., Kontos, K., Bontempi, G., van Helden, J., and André, B. (2007). Effect of 21 different nitrogen sources on global gene expression in the yeast Saccharomyces cerevisiae. Mol Cell Biol *27*, 3065-3086.

Goh, L.K., Huang, F., Kim, W., Gygi, S., and Sorkin, A. (2010). Multiple mechanisms collectively regulate clathrin-mediated endocytosis of the epidermal growth factor receptor. J Cell Biol *189*, 871-883.

Gong, X., and Chang, A. (2001). A mutant plasma membrane ATPase, Pma1-10, is defective in stability at the yeast cell surface. Proc Natl Acad Sci U S A *98*, 9104-9109.

González, A., and Hall, M.N. (2017). Nutrient sensing and TOR signaling in yeast and mammals. EMBO J *36*, 397-408.

Gournas, C., Gkionis, S., Carquin, M., Twyffels, L., Tyteca, D., and André, B. (2018). Conformation-dependent partitioning of yeast nutrient transporters into starvation-protective membrane domains. Proc Natl Acad Sci U S A *115*, E3145-E3154.

Gournas, C., Saliba, E., Krammer, E.M., Barthelemy, C., Prévost, M., and André, B. (2017). Transition of yeast Can1 transporter to the inward-facing state unveils an α-arrestin target sequence promoting its ubiquitylation and endocytosis. Mol Biol Cell *28*, 2819-2832.

Gowans, G.J., Hawley, S.A., Ross, F.A., and Hardie, D.G. (2013). AMP is a true physiological regulator of AMP-activated protein kinase by both allosteric activation and enhancing net phosphorylation. Cell Metab *18*, 556-566.

Graves, J.D., and Krebs, E.G. (1999). Protein phosphorylation and signal transduction. Pharmacol Ther *82*, 111-121.

Grossmann, G., Malinsky, J., Stahlschmidt, W., Loibl, M., Weig-Meckl, I., Frommer, W.B., Opekarová, M., and Tanner, W. (2008). Plasma membrane microdomains regulate turnover of transport proteins in yeast. J Cell Biol *183*, 1075-1088.

Grossmann, G., Opekarová, M., Malinsky, J., Weig-Meckl, I., and Tanner, W. (2007). Membrane potential governs lateral segregation of plasma membrane proteins and lipids in yeast. EMBO J *26*, 1-8.

Guiney, E.L., Klecker, T., and Emr, S.D. (2016). Identification of the endocytic sorting signal recognized by the Art1-Rsp5 ubiquitin ligase complex. Mol Biol Cell *27*, 4043-4054.

Hanks, S.K., and Hunter, T. (1995). Protein kinases 6. The eukaryotic protein kinase superfamily: kinase (catalytic) domain structure and classification. FASEB J *9*, 576-596.

Hara, K., Yonezawa, K., Weng, Q.P., Kozlowski, M.T., Belham, C., and Avruch, J. (1998). Amino acid sufficiency and mTOR regulate p70 S6 kinase and eIF-4E BP1 through a common effector mechanism. J Biol Chem *273*, 14484-14494.

Harris, S.L., Na, S., Zhu, X., Seto-Young, D., Perlin, D.S., Teem, J.H., and Haber, J.E. (1994). Dominant lethal mutations in the plasma membrane H(+)-ATPase gene of Saccharomyces cerevisiae. Proc Natl Acad Sci U S A *91*, 10531-10535.

Hedbacker, K., and Carlson, M. (2008). SNF1/AMPK pathways in yeast. Front Biosci *13*, 2408-2420.

Hirasaki, M., Horiguchi, M., Numamoto, M., Sugiyama, M., Kaneko, Y., Nogi, Y., and Harashima, S. (2011). Saccharomyces cerevisiae protein phosphatase Ppz1 and

protein kinases Sat4 and Hal5 are involved in the control of subcellular localization of Gln3 by likely regulating its phosphorylation state. J Biosci Bioeng *111*, 249-254.

Holt, L.J., Tuch, B.B., Villén, J., Johnson, A.D., Gygi, S.P., and Morgan, D.O. (2009). Global analysis of Cdk1 substrate phosphorylation sites provides insights into evolution. Science *325*, 1682-1686.

Hong, S.P., Leiper, F.C., Woods, A., Carling, D., and Carlson, M. (2003). Activation of yeast Snf1 and mammalian AMP-activated protein kinase by upstream kinases. Proc Natl Acad Sci U S A *100*, 8839-8843.

Hunter, T. (2012). Why nature chose phosphate to modify proteins. Philos Trans R Soc Lond B Biol Sci *367*, 2513-2516.

Hunter, T., and Plowman, G.D. (1997). The protein kinases of budding yeast: six score and more. Trends Biochem Sci *22*, 18-22.

Jaleel, M., McBride, A., Lizcano, J.M., Deak, M., Toth, R., Morrice, N.A., and Alessi, D.R. (2005). Identification of the sucrose non-fermenting related kinase SNRK, as a novel LKB1 substrate. FEBS Lett *579*, 1417-1423.

Jewell, J.L., Kim, Y.C., Russell, R.C., Yu, F.X., Park, H.W., Plouffe, S.W., Tagliabracci, V.S., and Guan, K.L. (2015). Metabolism. Differential regulation of mTORC1 by leucine and glutamine. Science *347*, 194-198.

Karotki, L., Huiskonen, J.T., Stefan, C.J., Ziółkowska, N.E., Roth, R., Surma, M.A., Krogan, N.J., Emr, S.D., Heuser, J., Grünewald, K., and Walther, T.C. (2011). Eisosome proteins assemble into a membrane scaffold. J Cell Biol *195*, 889-902.

Katzmann, D.J., Babst, M., and Emr, S.D. (2001). Ubiquitin-dependent sorting into the multivesicular body pathway requires the function of a conserved endosomal protein sorting complex, ESCRT-I. Cell *106*, 145-155.

Knight, Z.A., and Shokat, K.M. (2007). Chemical genetics: where genetics and pharmacology meet. Cell *128*, 425-430.

Krupa, A., Abhinandan, K.R., and Srinivasan, N. (2004). KinG: a database of protein kinases in genomes. Nucleic Acids Res *32*, D153-155.

Kung, J.E., and Jura, N. (2016). Structural Basis for the Non-catalytic Functions of Protein Kinases. Structure *24*, 7-24.

Kübler, E., and Riezman, H. (1993). Actin and fimbrin are required for the internalization step of endocytosis in yeast. EMBO J *12*, 2855-2862.

Lauwers, E., Erpapazoglou, Z., Haguenauer-Tsapis, R., and André, B. (2010). The ubiquitin code of yeast permease trafficking. Trends Cell Biol *20*, 196-204.

Lawrence, R.E., Cho, K.F., Rappold, R., Thrun, A., Tofaute, M., Kim, D.J., Moldavski, O., Hurley, J.H., and Zoncu, R. (2018). A nutrient-induced affinity switch controls mTORC1 activation by its Rag GTPase-Ragulator lysosomal scaffold. Nat Cell Biol *20*, 1052-1063.

Lawrence, R.E., and Zoncu, R. (2019). The lysosome as a cellular centre for signalling, metabolism and quality control. Nat Cell Biol.

Lecchi, S., Nelson, C.J., Allen, K.E., Swaney, D.L., Thompson, K.L., Coon, J.J., Sussman, M.R., and Slayman, C.W. (2007). Tandem phosphorylation of Ser-911 and Thr-912 at the C terminus of yeast plasma membrane H+-ATPase leads to glucose-dependent activation. J Biol Chem *282*, 35471-35481.

Lee, S., Ho, H.C., Tumolo, J.M., Hsu, P.C., and MacGurn, J.A. (2019). Methionine triggers Ppz-mediated dephosphorylation of Art1 to promote cargo-specific endocytosis. J Cell Biol.

Lee, S., Tumolo, J.M., Ehlinger, A.C., Jernigan, K.K., Qualls-Histed, S.J., Hsu, P.C., McDonald, W.H., Chazin, W.J., and MacGurn, J.A. (2017). Ubiquitin turnover and endocytic trafficking in yeast are regulated by Ser57 phosphorylation of ubiquitin. Elife *6*.

Leech, A., Nath, N., McCartney, R.R., and Schmidt, M.C. (2003). Isolation of mutations in the catalytic domain of the snf1 kinase that render its activity independent of the snf4 subunit. Eukaryot Cell *2*, 265-273.

Letunic, I., and Bork, P. (2019). Interactive Tree Of Life (iTOL) v4: recent updates and new developments. Nucleic Acids Res.

Lewis, M.J., Nichols, B.J., Prescianotto-Baschong, C., Riezman, H., and Pelham, H.R. (2000). Specific retrieval of the exocytic SNARE Snc1p from early yeast endosomes. Mol Biol Cell *11*, 23-38.

Li, X., Gerber, S.A., Rudner, A.D., Beausoleil, S.A., Haas, W., Villén, J., Elias, J.E., and Gygi, S.P. (2007). Large-scale phosphorylation analysis of alpha-factor-arrested Saccharomyces cerevisiae. J Proteome Res *6*, 1190-1197.

Lin, C.H., MacGurn, J.A., Chu, T., Stefan, C.J., and Emr, S.D. (2008). Arrestin-related ubiquitin-ligase adaptors regulate endocytosis and protein turnover at the cell surface. Cell *135*, 714-725.

Liu, Z., Thornton, J., Spírek, M., and Butow, R.A. (2008). Activation of the SPS amino acid-sensing pathway in Saccharomyces cerevisiae correlates with the phosphorylation state of a sensor component, Ptr3. Mol Cell Biol *28*, 551-563.

Ljungdahl, P.O. (2009). Amino-acid-induced signalling via the SPS-sensing pathway in yeast. Biochem Soc Trans *37*, 242-247.

Ljungdahl, P.O., and Daignan-Fornier, B. (2012). Regulation of amino acid, nucleotide, and phosphate metabolism in Saccharomyces cerevisiae. Genetics *190*, 885-929.

Llopis-Torregrosa, V., Ferri-Blázquez, A., Adam-Artigues, A., Deffontaines, E., van Heusden, G.P., and Yenush, L. (2016). Regulation of the Yeast Hxt6 Hexose Transporter by the Rod1 α-Arrestin, the Snf1 Protein Kinase, and the Bmh2 14-3-3 Protein. J Biol Chem *291*, 14973-14985.

Loewith, R., and Hall, M.N. (2011). Target of rapamycin (TOR) in nutrient signaling and growth control. Genetics *189*, 1177-1201.

Ludin, K., Jiang, R., and Carlson, M. (1998). Glucose-regulated interaction of a regulatory subunit of protein phosphatase 1 with the Snf1 protein kinase in Saccharomyces cerevisiae. Proc Natl Acad Sci U S A *95*, 6245-6250.

Luo, W., and Chang, A. (2000). An endosome-to-plasma membrane pathway involved in trafficking of a mutant plasma membrane ATPase in yeast. Mol Biol Cell *11*, 579-592.

Léon, S., and Haguenauer-Tsapis, R. (2009). Ubiquitin ligase adaptors: regulators of ubiquitylation and endocytosis of plasma membrane proteins. Exp Cell Res *315*, 1574-1583.

MacDonald, C., Payne, J.A., Aboian, M., Smith, W., Katzmann, D.J., and Piper, R.C. (2015). A family of tetraspans organizes cargo for sorting into multivesicular bodies. Dev Cell *33*, 328-342.

MacGurn, J.A., Hsu, P.C., and Emr, S.D. (2012). Ubiquitin and membrane protein turnover: from cradle to grave. Annu Rev Biochem *81*, 231-259.

MacGurn, J.A., Hsu, P.C., Smolka, M.B., and Emr, S.D. (2011). TORC1 regulates endocytosis via Npr1-mediated phosphoinhibition of a ubiquitin ligase adaptor. Cell *147*, 1104-1117.

Madeira, F., Park, Y.M., Lee, J., Buso, N., Gur, T., Madhusoodanan, N., Basutkar, P., Tivey, A.R.N., Potter, S.C., Finn, R.D., and Lopez, R. (2019). The EMBL-EBI search and sequence analysis tools APIs in 2019. Nucleic Acids Res.

Maloy, K.J., and Powrie, F. (2011). Intestinal homeostasis and its breakdown in inflammatory bowel disease. Nature *474*, 298-306.

Manning, G., Plowman, G.D., Hunter, T., and Sudarsanam, S. (2002). Evolution of protein kinase signaling from yeast to man. Trends Biochem Sci *27*, 514-520.

Marchal, C., Haguenauer-Tsapis, R., and Urban-Grimal, D. (2000). Casein kinase I-dependent phosphorylation within a PEST sequence and ubiquitination at nearby lysines signal endocytosis of yeast uracil permease. J Biol Chem *275*, 23608-23614.

Martin, J., Anamika, K., and Srinivasan, N. (2010). Classification of protein kinases on the basis of both kinase and non-kinase regions. PLoS One *5*, e12460.

Mason, A.B., Allen, K.E., and Slayman, C.W. (2014). C-terminal truncations of the Saccharomyces cerevisiae PMA1 H+-ATPase have major impacts on protein conformation, trafficking, quality control, and function. Eukaryot Cell *13*, 43-52.

Mayer, F.V., Heath, R., Underwood, E., Sanders, M.J., Carmena, D., McCartney, R.R., Leiper, F.C., Xiao, B., Jing, C., Walker, P.A., Haire, L.F., Ogrodowicz, R., Martin, S.R., Schmidt, M.C., Gamblin, S.J., and Carling, D. (2011). ADP regulates SNF1, the Saccharomyces cerevisiae homolog of AMP-activated protein kinase. Cell Metab *14*, 707-714.

Mayinger, P. (2012). Phosphoinositides and vesicular membrane traffic. Biochim Biophys Acta *1821*, 1104-1113.

Mazón, M.J., Eraso, P., and Portillo, F. (2015). Specific phosphoantibodies reveal two phosphorylation sites in yeast Pma1 in response to glucose. FEMS Yeast Res *15*, fov030.

McCartney, R.R., Garnar-Wortzel, L., Chandrashekarappa, D.G., and Schmidt, M.C. (2016). Activation and inhibition of Snf1 kinase activity by phosphorylation within the activation loop. Biochim Biophys Acta *1864*, 1518-1528.

Merhi, A., and André, B. (2012). Internal amino acids promote Gap1 permease ubiquitylation via TORC1/Npr1/14-3-3-dependent control of the Bul arrestin-like adaptors. Mol Cell Biol *32*, 4510-4522.

Merhi, A., Gérard, N., Lauwers, E., Prévost, M., and André, B. (2011). Systematic mutational analysis of the intracellular regions of yeast Gap1 permease. PLoS One *6*, e18457.

Modell, H., Cliff, W., Michael, J., McFarland, J., Wenderoth, M.P., and Wright, A. (2015). A physiologist's view of homeostasis. Adv Physiol Educ *39*, 259-266.

Moharir, A., Gay, L., Appadurai, D., Keener, J., and Babst, M. (2018). Eisosomes are metabolically regulated storage compartments for APC-type nutrient transporters. Mol Biol Cell *29*, 2113-2127.

Moravcevic, K., Mendrola, J.M., Schmitz, K.R., Wang, Y.H., Slochower, D., Janmey, P.A., and Lemmon, M.A. (2010). Kinase associated-1 domains drive MARK/PAR1 kinases to membrane targets by binding acidic phospholipids. Cell *143*, 966-977.

Morvan, J., Rinaldi, B., and Friant, S. (2012). Pkh1/2-dependent phosphorylation of Vps27 regulates ESCRT-I recruitment to endosomes. Mol Biol Cell *23*, 4054-4064.

Mulet, J.M., Leube, M.P., Kron, S.J., Rios, G., Fink, G.R., and Serrano, R. (1999). A novel mechanism of ion homeostasis and salt tolerance in yeast: the Hal4 and Hal5 protein kinases modulate the Trk1-Trk2 potassium transporter. Mol Cell Biol *19*, 3328-3337.

Na, S., Hincapie, M., McCusker, J.H., and Haber, J.E. (1995). MOP2 (SLA2) affects the abundance of the plasma membrane H(+)-ATPase of Saccharomyces cerevisiae. J Biol Chem *270*, 6815-6823.

Nayak, V., Zhao, K., Wyce, A., Schwartz, M.F., Lo, W.S., Berger, S.L., and Marmorstein, R. (2006). Structure and dimerization of the kinase domain from yeast Snf1, a member of the Snf1/AMPK protein family. Structure *14*, 477-485.

Nicastro, R., Tripodi, F., Gaggini, M., Castoldi, A., Reghellin, V., Nonnis, S., Tedeschi, G., and Coccetti, P. (2015). Snf1 Phosphorylates Adenylate Cyclase and Negatively Regulates Protein Kinase A-dependent Transcription in Saccharomyces cerevisiae. J Biol Chem *290*, 24715-24726.

Nikko, E., and Pelham, H.R. (2009). Arrestin-mediated endocytosis of yeast plasma membrane transporters. Traffic *10*, 1856-1867.

O'Donnell, A.F., McCartney, R.R., Chandrashekarappa, D.G., Zhang, B.B., Thorner, J., and Schmidt, M.C. (2015). 2-Deoxyglucose impairs Saccharomyces cerevisiae growth by stimulating Snf1-regulated and α-arrestin-mediated trafficking of hexose transporters 1 and 3. Mol Cell Biol *35*, 939-955.

Olivera-Couto, A., Graña, M., Harispe, L., and Aguilar, P.S. (2011). The eisosome core is composed of BAR domain proteins. Mol Biol Cell *22*, 2360-2372.

Omnus, D.J., Pfirrmann, T., Andréasson, C., and Ljungdahl, P.O. (2011). A phosphodegron controls nutrient-induced proteasomal activation of the signaling protease Ssy5. Mol Biol Cell *22*, 2754-2765.

Panieri, E., and Santoro, M.M. (2016). ROS homeostasis and metabolism: a dangerous liason in cancer cells. Cell Death Dis *7*, e2253.

Peng, Y., Grassart, A., Lu, R., Wong, C.C., Yates, J., Barnes, G., and Drubin, D.G. (2015). Casein kinase 1 promotes initiation of clathrin-mediated endocytosis. Dev Cell *32*, 231-240.

Pennings, M., Meurs, I., Ye, D., Out, R., Hoekstra, M., Van Berkel, T.J., and Van Eck, M. (2006). Regulation of cholesterol homeostasis in macrophages and consequences for atherosclerotic lesion development. FEBS Lett *580*, 5588-5596.

Pettersen, E.F., Goddard, T.D., Huang, C.C., Couch, G.S., Greenblatt, D.M., Meng, E.C., and Ferrin, T.E. (2004). UCSF Chimera--a visualization system for exploratory research and analysis. J Comput Chem *25*, 1605-1612.

Pfirrmann, T., Heessen, S., Omnus, D.J., Andréasson, C., and Ljungdahl, P.O. (2010). The prodomain of Ssy5 protease controls receptor-activated proteolysis of transcription factor Stp1. Mol Cell Biol *30*, 3299-3309.

Posas, F., Casamayor, A., and Ariño, J. (1993). The PPZ protein phosphatases are involved in the maintenance of osmotic stability of yeast cells. FEBS Lett *318*, 282-286.

Poulsen, P., Gaber, R.F., and Kielland-Brandt, M.C. (2008). Hyper- and hyporesponsive mutant forms of the Saccharomyces cerevisiae Ssy1 amino acid sensor. Mol Membr Biol *25*, 164-176.

Primo, C., Ferri-Blázquez, A., Loewith, R., and Yenush, L. (2017). Reciprocal Regulation of Target of Rapamycin Complex 1 and Potassium Accumulation. J Biol Chem *292*, 563-574.

Prosser, D.C., Whitworth, K., and Wendland, B. (2010). Quantitative analysis of endocytosis with cytoplasmic pHluorin chimeras. Traffic *11*, 1141-1150.

Prosser, D.C., Wrasman, K., Woodard, T.K., O'Donnell, A.F., and Wendland, B. (2016). Applications of pHluorin for Quantitative, Kinetic and High-throughput Analysis of Endocytosis in Budding Yeast. J Vis Exp.

Pérez-Valle, J., Jenkins, H., Merchan, S., Montiel, V., Ramos, J., Sharma, S., Serrano, R., and Yenush, L. (2007). Key role for intracellular K+ and protein kinases Sat4/Hal4 and Hal5 in the plasma membrane stabilization of yeast nutrient transporters. Mol Cell Biol *27*, 5725-5736.

Pérez-Valle, J., Rothe, J., Primo, C., Martínez Pastor, M., Ariño, J., Pascual-Ahuir, A., Mulet, J.M., Serrano, R., and Yenush, L. (2010). Hal4 and Hal5 protein kinases are required for general control of carbon and nitrogen uptake and metabolism. Eukaryot Cell *9*, 1881-1890.

Robinson, J.S., Klionsky, D.J., Banta, L.M., and Emr, S.D. (1988). Protein sorting in Saccharomyces cerevisiae: isolation of mutants defective in the delivery and processing of multiple vacuolar hydrolases. Mol Cell Biol *8*, 4936-4948.

Robinson, M., Poon, P.P., Schindler, C., Murray, L.E., Kama, R., Gabriely, G., Singer, R.A., Spang, A., Johnston, G.C., and Gerst, J.E. (2006). The Gcs1 Arf-GAP mediates Snc1,2 v-SNARE retrieval to the Golgi in yeast. Mol Biol Cell *17*, 1845-1858.

Roelants, F.M., Leskoske, K.L., Martinez Marshall, M.N., Locke, M.N., and Thorner, J. (2017). The TORC2-Dependent Signaling Network in the Yeast Saccharomyces cerevisiae. Biomolecules *7*.

Romero, M.F. (2004). In the beginning, there was the cell: cellular homeostasis. Adv Physiol Educ *28*, 135-138.

Rossi, G., Salminen, A., Rice, L.M., Brünger, A.T., and Brennwald, P. (1997). Analysis of a yeast SNARE complex reveals remarkable similarity to the neuronal SNARE complex and a novel function for the C terminus of the SNAP-25 homolog, Sec9. J Biol Chem *272*, 16610-16617.

Ruiz, A., del Carmen Ruiz, M., Sánchez-Garrido, M.A., Ariño, J., and Ramos, J. (2004). The Ppz protein phosphatases regulate Trk-independent potassium influx in yeast. FEBS Lett *578*, 58-62.

Röder, P.V., Wu, B., Liu, Y., and Han, W. (2016). Pancreatic regulation of glucose homeostasis. Exp Mol Med *48*, e219.

Sali, A., and Blundell, T.L. (1993). Comparative protein modelling by satisfaction of spatial restraints. J Mol Biol *234*, 779-815.

Sancak, Y., Peterson, T.R., Shaul, Y.D., Lindquist, R.A., Thoreen, C.C., Bar-Peled, L., and Sabatini, D.M. (2008). The Rag GTPases bind raptor and mediate amino acid signaling to mTORC1. Science *320*, 1496-1501.

Sanz, P., Alms, G.R., Haystead, T.A., and Carlson, M. (2000). Regulatory interactions between the Reg1-Glc7 protein phosphatase and the Snf1 protein kinase. Mol Cell Biol *20*, 1321-1328.

Savir, Y., Martynov, A., and Springer, M. (2017). Achieving global perfect homeostasis through transporter regulation. PLoS Comput Biol *13*, e1005458.

Schmid, S.L. (2017). Reciprocal regulation of signaling and endocytosis: Implications for the evolving cancer cell. J Cell Biol *216*, 2623-2632.

Schmidt, A., Beck, T., Koller, A., Kunz, J., and Hall, M.N. (1998). The TOR nutrient signalling pathway phosphorylates NPR1 and inhibits turnover of the tryptophan permease. EMBO J *17*, 6924-6931.

Schmidt, M.C., and McCartney, R.R. (2000). beta-subunits of Snf1 kinase are required for kinase function and substrate definition. EMBO J *19*, 4936-4943.

Schuberth, C., and Wedlich-Söldner, R. (2015). Building a patchwork - The yeast plasma membrane as model to study lateral domain formation. Biochim Biophys Acta *1853*, 767-774.

Scott, B.L., Van Komen, J.S., Irshad, H., Liu, S., Wilson, K.A., and McNew, J.A. (2004). Sec1p directly stimulates SNARE-mediated membrane fusion in vitro. J Cell Biol *167*, 75-85.

Shaner, N.C., Lambert, G.G., Chammas, A., Ni, Y., Cranfill, P.J., Baird, M.A., Sell, B.R., Allen, J.R., Day, R.N., Israelsson, M., Davidson, M.W., and Wang, J. (2013). A bright monomeric green fluorescent protein derived from Branchiostoma lanceolatum. Nat Methods *10*, 407-409.

Shirra, M.K., McCartney, R.R., Zhang, C., Shokat, K.M., Schmidt, M.C., and Arndt, K.M. (2008). A chemical genomics study identifies Snf1 as a repressor of GCN4 translation. J Biol Chem *283*, 35889-35898.

Spormann, D.O., Heim, J., and Wolf, D.H. (1992). Biogenesis of the yeast vacuole (lysosome). The precursor forms of the soluble hydrolase carboxypeptidase yscS are associated with the vacuolar membrane. J Biol Chem *267*, 8021-8029.

Stothard, P. (2000). The sequence manipulation suite: JavaScript programs for analyzing and formatting protein and DNA sequences. Biotechniques *28*, 1102, 1104.

Stracka, D., Jozefczuk, S., Rudroff, F., Sauer, U., and Hall, M.N. (2014). Nitrogen source activates TOR (target of rapamycin) complex 1 via glutamine and independently of Gtr/Rag proteins. J Biol Chem *289*, 25010-25020.

Subramanian, B., Gao, S., Lercher, M.J., Hu, S., and Chen, W.H. (2019). Evolview v3: a webserver for visualization, annotation, and management of phylogenetic trees. Nucleic Acids Res.

Vanoni, S., Scantamburlo, G., Dossena, S., Paulmichl, M., and Nofziger, C. (2019). Interleukin-Mediated Pendrin Transcriptional Regulation in Airway and Esophageal Epithelia. Int J Mol Sci *20*.

Vela, D. (2019). Keeping heart homeostasis in check through the balance of iron metabolism. Acta Physiol (Oxf), e13324.

Velivela, S.D., and Kane, P.M. (2018). Compensatory Internalization of Pma1 in V-ATPase Mutants in. Genetics *208*, 655-672.

Vida, T.A., and Emr, S.D. (1995). A new vital stain for visualizing vacuolar membrane dynamics and endocytosis in yeast. J Cell Biol *128*, 779-792.

Vincent, O., Townley, R., Kuchin, S., and Carlson, M. (2001). Subcellular localization of the Snf1 kinase is regulated by specific beta subunits and a novel glucose signaling mechanism. Genes Dev *15*, 1104-1114.

Waldhart, A.N., Dykstra, H., Peck, A.S., Boguslawski, E.A., Madaj, Z.B., Wen, J., Veldkamp, K., Hollowell, M., Zheng, B., Cantley, L.C., McGraw, T.E., and Wu, N. (2017). Phosphorylation of TXNIP by AKT Mediates Acute Influx of Glucose in Response to Insulin. Cell Rep *19*, 2005-2013.

Wang, Q., and Chang, A. (1999). Eps1, a novel PDI-related protein involved in ER quality control in yeast. EMBO J *18*, 5972-5982.

Waterhouse, A.M., Procter, J.B., Martin, D.M., Clamp, M., and Barton, G.J. (2009). Jalview Version 2--a multiple sequence alignment editor and analysis workbench. Bioinformatics *25*, 1189-1191.

Weinberg, J., and Drubin, D.G. (2012). Clathrin-mediated endocytosis in budding yeast. Trends Cell Biol *22*, 1-13.

Wilson, W.A., and Roach, P.J. (2002). Nutrient-regulated protein kinases in budding yeast. Cell *111*, 155-158.

Wu, B., Ottow, K., Poulsen, P., Gaber, R.F., Albers, E., and Kielland-Brandt, M.C. (2006). Competitive intra- and extracellular nutrient sensing by the transporter homologue Ssy1p. J Cell Biol *173*, 327-331.

Wu, N., Zheng, B., Shaywitz, A., Dagon, Y., Tower, C., Bellinger, G., Shen, C.H., Wen, J., Asara, J., McGraw, T.E., Kahn, B.B., and Cantley, L.C. (2013). AMPK-dependent degradation of TXNIP upon energy stress leads to enhanced glucose uptake via GLUT1. Mol Cell *49*, 1167-1175.

Yenush, L., Mulet, J.M., Ariño, J., and Serrano, R. (2002). The Ppz protein phosphatases are key regulators of K+ and pH homeostasis: implications for salt tolerance, cell wall integrity and cell cycle progression. EMBO J *21*, 920-929.

Young, E.T., Zhang, C., Shokat, K.M., Parua, P.K., and Braun, K.A. (2012). The AMP-activated protein kinase Snf1 regulates transcription factor binding, RNA polymerase II activity, and mRNA stability of glucose-repressed genes in Saccharomyces cerevisiae. J Biol Chem *287*, 29021-29034.

Zhao, Y., Macgurn, J.A., Liu, M., and Emr, S. (2013). The ART-Rsp5 ubiquitin ligase network comprises a plasma membrane quality control system that protects yeast cells from proteotoxic stress. Elife *2*, e00459.

Ziółkowska, N.E., Karotki, L., Rehman, M., Huiskonen, J.T., and Walther, T.C. (2011). Eisosome-driven plasma membrane organization is mediated by BAR domains. Nat Struct Mol Biol *18*, 854-856.

Zoncu, R., Bar-Peled, L., Efeyan, A., Wang, S., Sancak, Y., and Sabatini, D.M. (2011). mTORC1 senses lysosomal amino acids through an inside-out mechanism that requires the vacuolar H(+)-ATPase. Science *334*, 678-683.